VERTICES AND VORTICES IN HIGH T_C SUPERCONDUCTORS

By

Mohammad H. Sharifzadeh Amin

B. Sc. (Electrical Engineering) Shiraz University, Shiraz, Iran.

M. Sc. (Physics) Sharif University of Technology, Tehran, Iran.

A THESIS SUBMITTED IN PARTIAL FULFILLMENT OF

THE REQUIREMENTS FOR THE DEGREE OF

DOCTOR OF PHILOSOPHY

in

THE FACULTY OF GRADUATE STUDIES

PHYSICS

We accept this thesis as conforming

to the required standard

THE UNIVERSITY OF BRITISH COLUMBIA

September 1999

In presenting this thesis in partial fulfilment of the requirements for an advanced degree at the University of British Columbia, I agree that the Library shall make it freely available for reference and study. I further agree that permission for extensive copying of this thesis for scholarly purposes may be granted by the head of my department or by his or her representatives. It is understood that copying or publication of this thesis for financial gain shall not be allowed without my written permission.

Department of Physics

The University of British Columbia
Vancouver, Canada

Date Oct. 14, 1999

DE-6 (2/88)

Abstract

This thesis is organized in two independent parts, in which I study two different aspects of high T_c superconductivity.

The first part begins with an introduction aimed to briefly introduce some relevant experimental and theoretical works performed in recent years, that have helped us to think about cuprates the way we do now. Afterwards, I introduce Landau Fermi liquid theory in a standard text book way. The question of validity of Fermi liquid theory in 2-d is then raised and investigated by searching for singularities in Landau's f-function. I show that the interaction function between two quasiparticles whose momenta approach each other near a curved point of the Fermi surface, contains a 1-d singularity not strong enough to change the Fermi liquid behavior. On the other hand, inflection points provide 2-d singularities that have to be taken seriously in Fermi liquid considerations. I then introduce nearly antiferromagnetic Fermi liquid theory (NAFL), which is a phenomenological theory proposed to describe high T_c systems. I mainly focus on the self-consistency of the theory in calculations. I criticize the theory on the basis of overlooking the vertex corrections in the strong coupling calculations of the transition temperature T_c. I calculate the first vertex correction for an optimally doped system and show that it is of the same order of magnitude as the bare vertex. Migdal's theorem is therefore not valid and Eliashberg formalism is not applicable to this situation. The same conclusion is obtained even after inclusion of the quasiparticle residue Z to the calculation. The sign of the vertex correction is then considered. I show that the positive sign of the vertex correction for the optimally doped system requires a phase transition of some sort as the doping is decreased.

Part II of the thesis is devoted to the vortex lattice properties of high T_c superconductors. I establish a method to study vortex lattice properties of d-wave superconductors based on a generalization of the London model. The method has the advantage of simplicity as well as having very few free parameters (one at most) compared to other methods. The generalized London free energy is obtained from an s-d mixing Ginsburg-Landau free energy and also from the microscopic theory of Gorkov. The generalized London equation is found to be analytic at high temperatures. At very low temperatures however non-analyticities arise as a result of the nodes on the superconducting gap. I then present the results of our calculations of some measurable quantities, such as the vortex lattice geometry and the effective penetration depth (as defined in μSR experiments). Comparison between our results and different experimental data is then performed. Especially our prediction for the magnetic field dependence of the effective penetration depth at $T = 0$, which is recently observed in μSR experiments with excellent agreement, is discussed.

To my parents

Table of Contents

List of Tables

List of Figures

Acknowledgement

First, I would like to give my special thanks to my both supervisors Ian Affleck and Philip Stamp for teaching me the basics of physics and research and also for all their support, encouragement and patience. I especially would like to thank Philip Stamp for directing me to condensed matter physics and teaching me superconductivity and basics of high T_c superconductivity, and also Ian Affleck for teaching me the concepts of condensed matter physics during several magnificent courses and informal discussions, and supporting me whenever I needed. I would like to thank both for being a friend and sometimes like a caring father to me.

I also would like to take the opportunity to thank Victor Barzykin, Alexander Zagoskin and most of all Igor Herbut for very stimulating and encouraging discussions and for explaining difficult materials to me in simple language. I am also grateful to Walter Hardy, and Doug Bonn and Rob Keifl for providing me up to date experimental information, Jeff Sonier for several useful discussions about μSR experiments and providing me his data, Marc Julien for teaching me the basics of NMR experiments and especially Saeid Kamal for helping me understand microwave experiments as well as being a supporting friend for me during these five years.

I also would like to thank all my friends, specially Shahrokh Parvizy and Ali Sheikholeslam for encouraging me to choose physics as my career, all my friends in Canada especially Siavash Jahromi, Mahan Movassaghi, Ali Mirabedini and Nima Ahmadvand for all good times I had with them during my years of Ph.D., and Andrea and Jeff for lending me their laptop with which I wrote most parts of this thesis.

Outside the physics world, I would like to thank my parents and my sister Parvaneh

for their loving support and encouragement and believing in me and providing me all the supports I needed all through the years of my study. I also want to thank my uncle Ali Joukar and his wife Roya Sadeghi for making Vancouver my home by all their love and support.

Finally I would like to give my especial thank to my gorgeous wife Roxana Pardis for her love and support, for always being with me during difficult times of life, giving me lessons of living and making me believe in myself.

Part I

Fermi Liquids, Non-Fermi Liquids and Nearly Antiferromagnetic Fermi Liquids

Chapter 1

Introduction

It has been more than a decade since the discovery of the first high temperature superconductor [1], and still no consensus about the microscopic theory relevant to cuprates exists. New theories have been emerging one after another and disputes about the older theories are still unsettled. A general feature of all cuprates is their strong anisotropy which makes them effectively 2-d electronic systems. Fig. 1.1 shows the crystal structure of the YBCO compound which is one of important high T_c materials. At the center there are two CuO_2 planes separated with Y atoms in between. Between these two planes and another two planes above or below them, there are oxygen chains (that play crucial role in the doping of the system) and also Ba atoms. It is generally agreed that the CuO_2 planes play an important role in determining the characteristics of cuprates at all dopings. Fig. 1.1 shows the crystal structure of YBCO material In the early days of high Tc's, Anderson [2] proposed an effective Hamiltonian which describes a single band 2D Hubbard model with an infinite on site repulsion U. Soon after, Zhang and Rice [3] tried to justify the Anderson's suggested model (known as the t-J model) for cuprates. They proposed that the holes which primarily reside on oxygen sites would delocalize onto four O sites around Cu^{+2} ions. The combination of a delocalized O hole and a Cu^{+2} ion forms a singlet which would hop between Cu^{+2} sites in the same way as a hole does in a simple Cu^{+2} square lattice.

In the absence of doping, CuO_2 planes are half filled and form a quasi-2D antiferromagnet with an insulating Néel ground state. Numerical simulations, experiments, and

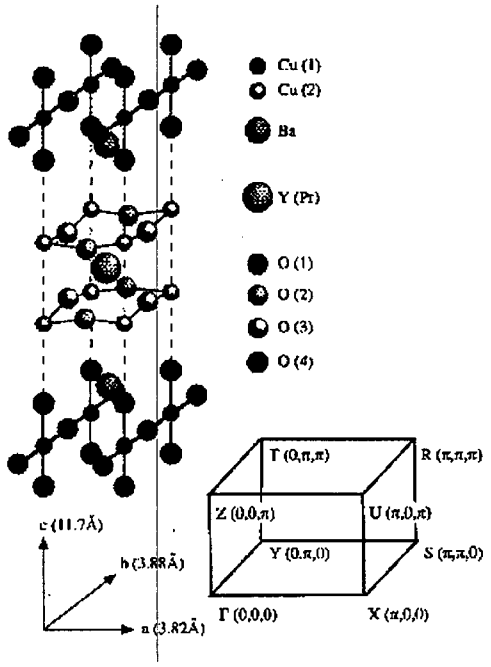

Figure 1.1: Crystal structure of YBCO

scaling theory, all suggest that above the Néel temperature, the antiferromagnetic spin correlations are well described by the isotropic 2D Heisenberg model [4] with exchange coupling $J \simeq 1550K$ between nearest neighbors. However, according to the Hohenberg-Mermin-Wagner theorem [5], classical fluctuations destroy Néel ordering at an arbitrarily small nonzero temperature. The small ($\sim 10^{-5}J$), but finite correlations between the planes are believed to be responsible for the observed long-range order [4]. Chakravarty, Halperin, and Nelson [6] on the other hand, have employed quantum non-linear σ model for the long-wavelength action of the $2D$, $s = 1/2$ Heisenberg model. A scaling analysis of this model describes correctly both experimental and numerical data [4].

Introducing a small amount of holes into the CuO_2 planes, the Néel temperature falls off rapidly from its undoped value. Increasing the doping level even further, the system moves into a state with a metallic normal state and a transition to a superconducting ground state at low temperatures (cf. Fig. 1.2). The superconducting transition temperature increases initially as doping is increased. After reaching its maximum at optimal

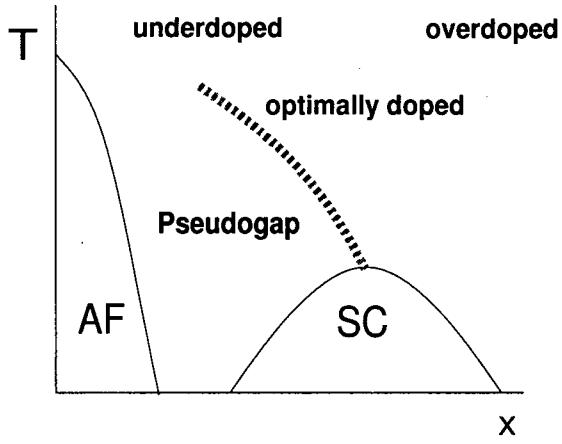

Figure 1.2: Phase diagram of high temperature superconductors. x represents doping, AF antiferromagnetically ordered phase and SC superconducting phase. Upper line is the crossover to pseudogap state. [12]

doping, it starts to decrease and the superconductor enters a so called overdoped regime (Fig. 1.2). All over the metallic phase, the antiferromagnetic correlation is short ranged with ξ between one and (up to) fifteen lattice spacings, depending on the material, doping and temperature.

Experiments evidently indicate that the electronic properties of the underdoped and overdoped materials are different [7, 8, 9, 10, 11]; especially the pseudogap phase which exits only for underdoped compounds [12] (Fig. 1.2). Among experiments, inelastic neutron scattering (INS) and nuclear magnetic resonance (NMR) experiments provide important information about the magnetic properties of the system. INS directly probes the spin response function, $\chi''(\vec{q},\omega)$. In $La_{1.85}Sr_{0.15}CuO_4$ the INS experiments [8] display four sharp magnetic peaks located at $\delta q \simeq \pi/4$ away from the antiferromagnetic wave vector. These incommensurate peaks were also observed recently in $YBa_2Cu_3O_{6.6}$. [13] Like many experiments, INS has some inherent problems. For example it is difficult to determine experimentally the absolute value of intensity. It is also not easy to separate the phonon spectrum from the magnetic excitations.

NMR experiments [14, 15] on the other hand, are much more exact, and can detect

much lower intensities. However, NMR is an indirect probe and its data analysis involves using a theoretical Hamiltonian connecting nuclear and electron spins, the hyperfine Hamiltonian. Moreover, since NMR experiments are done at very low frequencies ($\sim$ nuclear spin Zeeman splitting), no information about ω-dependence of $\chi(\omega, T)$ can be obtained. Early measurements of the Magnetic Hyperfine Shift (Knight shift) at the oxygen sites showed that most of the total spin polarization was carried by the copper sites [16, 17]. Alloul *et al.* [18] reported that in $YBa_2Cu_3O_{6+x}$, the knight shift of Yttrium scales linearly with the macroscopic susceptibility. This was interpreted as a proof of the existence of a single spin fluid in agreement with the t-J model, because yttrium is coupled to the magnetic susceptibility of the CuO_2 planes mainly through the polarization of the oxygen orbitals. Further measurements of knight shift showed the same T-dependence on all nuclear sites [14]. Similar result was obtained for all other cuprates indicating that the single spin fluid nature is a common feature of all these materials. Assuming a single fluid picture, Shastry [19] and also Mila and Rice [20] (SMR) proposed a hyperfine Hamiltonian in which the only source of coupling is the localized electronic spins at the copper sites.

While the magnetic hyperfine shift (Knight shift) gives a measure of the uniform magnetic susceptibility, the Nuclear Spin Lattice Relaxation Rate ($1/T_1$) provides information about the imaginary part of the dynamic spin susceptibility $\chi(\vec{q}, \omega)$. An important experiment by Takigawa [16] on $YBa_2Cu_3O_7$, in the early days, displayed a significant difference between the temperature dependence of $1/T_1$ for the CuO_2 plane copper and oxygen sites. The relaxation rate for oxygen sites (and also ^{89}Y sites) obeys Korringa relation $^{17}T_1T \approx Const.$ while the relaxation rate for copper sites is much shorter than for ^{17}O and ^{89}Y sites and shows non-Korringa behavior. Using SMR Hamiltonian, Moriya

[21] showed that

$$(T_1T)^{-1} \propto \lim_{\omega\to 0} \sum_{\vec{q}} F(\vec{q}) \frac{\chi''(\vec{q},\omega)}{\omega} \tag{1.1}$$

where $\chi''(\vec{q},\omega)$ is the imaginary part of the magnetic susceptibility and $F(\vec{q})$ is a form factor which depends on the site and the direction of the magnetic field. For ^{17}O sites, $F(\vec{q})$ is peaked at $\vec{q}=0$ and vanishes at the antiferromagnetic (AF) wave vector $\vec{Q} = (\pi/a, \pi/a)$. For ^{63}Cu sites on the other hand, it is peaked at $\vec{q}=\vec{Q}$. Thus different nuclei probe different regions of the momentum space of $\chi''(\vec{q},0)$. The significant difference between the ^{63}Cu and ^{17}O relaxation rates could then be understood as a result of an enhanced susceptibility at $\vec{q}=\vec{Q}$.

Another important quantity measured by NMR experiments is the nuclear spin-spin relaxation rate $(1/T_{2G})$ which is the rate of relaxation of the nuclear spins among themselves and is usually much larger than $1/T_1$. In most solids T_{2G} is temperature independent and is related to spin-spin dipolar coupling and therefore doesn't give any information about electron susceptibility. In cuprates however, because of the antiferromagnetic enhancement of the spin susceptibility, indirect coupling of spins via nonlocal spin susceptibility dominates the nuclear spin-spin coupling. Thus T_{2G} can provide important information about the antiferromagnetic exchange between electron spins as was pointed out first by Pennington *et al.* [22]. Measurements of $1/T_{2G}$ in different materials with different dopings have found $1/T_{2G}$ to increase with decreasing temperature, with sometimes a flattening or small decrease close to T_c [14]. This is considered as a proof for the existence of AF correlations in all cuprates.

To have a quantitative description, Millis, Monien and Pines (MMP) [23] proposed a phenomenological form for the magnetic susceptibility $\chi(\vec{q},\omega)$ which has a peak near the Antiferromagnetic (AF) wave vector $\vec{Q} = (\pi/a, \pi/a)$

$$\chi(\vec{q},\omega) = \frac{\chi_Q}{1+\xi^2(\vec{q}-\vec{Q})^2 - i\omega/\omega_{sf}} + \frac{\chi_0}{1-i\omega/\Gamma_0} \tag{1.2}$$

where χ_0 is the measured bulk spin susceptibility which in general is temperature dependent, χ_Q is the staggered susceptibility which is some orders of magnitude greater than the bulk susceptibility and Γ_0 is an energy scale of order of quasiparticle bandwidth or Fermi energy. The first term in Eq.(1.2) produces a peak at AF wave vector $\vec{Q}$ and the second term is the ordinary Fermi liquid susceptibility. For the ^{17}O sites, the effect of the first term is suppressed by the form factor $F(\vec{q})$ (cf. Eq. (1.1)) and the second term (the Fermi liquid term) is the only term that remains. To the lowest order, Eq.(1.2) gives $(^{17}T_1T)^{-1} \propto \chi_0(T)$ which is consistent with the Korringa relation. For copper sites however, the contribution of the first term is dominant near $\vec{Q}$ and one can safely neglect the second term. Assuming large correlation length ξ, the form factor can be treated as a constant and the integration can be simply carried out to get

$$(^{63}T_1T)^{-1} \propto \frac{\chi_Q}{\omega_{sf}\xi^2} = \frac{\alpha}{\omega_{sf}} \tag{1.3}$$

where α is defined by $\chi_Q = \alpha\xi^2$ and assumed to be temperature independent. Thus the spin lattice relaxation rate provides information about the temperature dependence of ω_{sf} in the MMP model

$$^{63}T_1T \propto \omega_{sf}/\alpha \tag{1.4}$$

This is completely different from the ^{17}O case and has non-Korringa behavior.

In the early days of high T_c's, there existed some speculations that antiferromagnetic correlation was responsible for Cooper pairing in high T_c materials [24, 25, 26, 27, 28] (the idea of d-wave pairing already existed in the context of heavy fermions [29, 30]). Inspired by paramagnon theory, Pines and collaborators [31, 32] proposed a (phenomenological) nearly antiferromagnetic Fermi liquid (NAFL) theory to describe pairing process as well as normal state properties of high T_c superconductors. The theory assumes that the low lying excitations of a high T_c system in its normal state, are Fermi liquid quasiparticles interacting with each other via antiferromagnetic spin-fluctuations. The susceptibility

(1.2) can be thought of as the propagator of bosonic particles that describe spin fluctuations. One of the first predictions of NAFL theory was $d_{x^2-y^2}$-wave pairing which was then confirmed by various experiments [33, 34]. Transition temperature was calculated in weak [31] and strong [35, 36] coupling limits and a T_c as high as 90K was obtained using several fitting parameters.

NAFL theory, as we mentioned above, is constructed based on the assumption that the excitations of the system are Fermi liquid quasiparticles. Almost none of the normal state properties of cuprates agree with Fermi liquid theory (at least in low to moderate doping regimes). The proximity to Mott-insulating antiferromagnetic phase might suggest that non-Fermi liquid properties are actually signatures of non-Fermi liquid excitations. NAFL theory on the other hand believes that the anomalous behavior is a result of strong interaction between the Fermi liquid quasiparticles due to antiferromagnetic spin fluctuations.

Orthogonal to the above philosophy was Anderson's proposal in 1990 [37, 38] that 2-dimensional Fermi liquids are unstable to the formation of a 2-d Luttinger liquid. Since Anderson, theorists have been trying to understand if and when "non-Fermi liquid" (NFL) can appear in itinerant Fermi systems. There is strong evidence [39] for NFL behavior in the $\nu = 1/2$ quantum Hall liquid; theoretical understanding of this assumes a singular gauge interaction between the quasiparticles [40]. The high T_c problem is more complex because the lattice introduces an on-site constraint for strong Hubbard repulsion- which means the lattice problem is fundamentally different from a continuum model. Perturbative investigations of the nature and existence of singular interactions in the low-density regime [41, 42, 43] have not shown NFL behavior, even in a finite box [43] (although they do reveal weak singular structure in the quasiparticle interactions [42, 43]). However, these results do not rule out non-perturbative singular behavior in the higher density lattice problem- no consensus yet exists on whether these exist in 2

dimensions. We stress that this question is quite different from that of the existence of instabilities to ordered phases (e.g., Superconducting or SDW instabilities), which can be understood using standard methods [44].

As discussed by various authors [37, 38, 43], NFL behavior is typically expected if the interaction between quasiparticles with momenta $\vec{p}$ and $\vec{p}'$ is singular when $\vec{Q} = \vec{p} - \vec{p}' \to 0$. It is nevertheless essential to satisfy all relevant Ward identities and crossing symmetry in any calculation, given the way singular behavior in one channel can influence that in the others. An approach which reveals the structure in the irreducible interactions as a function of $\vec{Q}$ and which satisfies the above requirements, involves calculating the irreducible 4-point vertex $f_{pp'}^{\sigma\sigma'}$ perturbatively [45], and then using this to determine the full scattering function and quasiparticle dispersion. If $f_{pp'}^{\sigma\sigma'}$ is not singular, then it is nothing but Landau's f-function.

In the next chapter, after an overview on Landau Fermi liquid theory, we perform a calculation of $f_{pp'}^{\sigma\sigma'}$ along the line mentioned above for a regular Fermi surface and also near inflection points of the Fermi surface. Our calculation for a curved Fermi surface reproduces the previous results [43] existing in the literature. Near inflection points however, we find that $f_{pp'}^{\sigma\sigma'}$ is singular in $\vec{Q}$ already at 2nd order in a short-ranged repulsive interaction. We stress that the NFL behavior found previously for Fermi surfaces having finite curvature everywhere appeared only at infinite order, and was too weak to destroy Fermi liquid behavior [42, 43]. Calculating the imaginary part of the self energy to second order in the singular interaction, we find a frequency dependence different from the expected Fermi liquid form.

Besides the controversy about the Fermi liquid starting point, the validity of Eliashberg formalism used in NAFL theory to calculate T_c is under question. Migdal's theorem is an essential ingredient of Eliashberg formalism which states that the vertex corrections to the bare coupling between electrons and the bosonic medium (here spin fluctuations)

are small. In the case of phonons, the small ratio of Debye frequency and Fermi energy (ω_D/E_F) makes the vertex corrections small [46]; despite the large bare coupling. In the case of spin-fermion coupling on the other hand, the only relevant energy scales are E_F and the antiferromagnetic exchange coupling J. The ratio J/E_F however, is of order one [47]. Thus it is not clear why vertex corrections should be small in the spin fermion interaction.

Calculations of the vertex corrections close to the antiferromagnetic ordered state [47, 48, 49] showed that the vertex corrections are actually the same order as the bare vertex and therefore are not small. Schrieffer [47] showed that in the ordered state, the dressed vertex should vanish at the antiferromagnetic wave vector. The vertex corrections therefore should be equal to the bare vertex but with opposite sign. The magnitude of the vertex correction at higher dopings is more important because the superconducting transition is suppressed at low doping.

In chapter 3, we first give a brief introduction to paramagnon theory, which is a theory for Fermi liquid systems near a ferromagnetic instability. We then turn to the nearly antiferromagnetic Fermi liquid theory pointing out the similarities and differences between NAFL and paramagnon theory. The self-consistency of NAFL theory is then discussed. We calculate the first correction to the bare spin-fermion vertex. We find that the vertex correction is actually big and of the same order as the bare vertex. The self-consistency of the calculation including quasiparticle renormalization is discussed afterwards.

The sign of the vertex corrections is another subject of dispute. As we mentioned above, the sign of the vertex corrections is negative near the ordered state. At optimal doping the sign of our vertex correction is also negative in disagreement with some other results [50]. We talk about the sign of the vertex corrections at the end of the 3rd chapter. Our discussion is based on the flow of the renormalized vertex versus change in doping.

We argue that the positive sign of the vertex corrections at the optimal doping requires a phase transition at some intermediate doping. In fact, for other reasons, this phase transition has been suggested by Chubukov to be a Lifshitz transition in the topology of the Fermi surface [51]. However, there is no experimental evidence for this or any other phase transitions at intermediate doping at the time of writing [52].

Chapter 2

Fermi Liquid Theory

2.1 Landau Theory of Fermi Liquids

Systems of strongly interacting electrons are very difficult, if not impossible, to solve. Perturbative methods fail to work as a result of the strong coupling between particles. Non-perturbative methods, also, are not quite well developed for systems of more than one dimension. It was Landau's ingenuity that realized the low energy excitations of a strongly interacting fermion system could still be fermionic quasiparticles similar to non-interacting electrons. Proposed in 1957 [53, 54], Landau's Fermi liquid theory has been extremely successful in describing low temperature properties of liquid ^{3}He [55, 56] as well as interacting electrons in metals [57]. It especially explains the success of non-interacting electron theory for low temperature properties of metals.

In his theory, Landau assumes that if one adiabatically turns on the interaction between electrons, the non-interacting ground state evolves into an interacting ground state with a one to one correspondence between the bare particle states and the quasiparticles in the interacting state. A necessary condition for this to happen is that no bound states should form during this process. A system that possesses this property is called "Normal Fermi Liquid". Superconductors therefore do not belong to this category. In Landau's picture, the number of quasiparticles, N, is the same as the number of bare electrons. They carry the same charge as electrons and obey Fermi statistics. One has to be careful not to go too far with this picture. For example, the ground state energy is not the same

as the sum of the quasiparticles energies. As we will see later, the quasiparticle states are meaningful only near the Fermi surface. A better way, is to define the quasiparticles as excitations of the system above its ground state and also quasiholes as absence of particles in the ground state. More precisely, a quasiparticle state with momentum $\vec{p}$ ($> p_F$, Fermi momentum) is defined by adiabatic evolution of a non-interacting Fermi sea with an extra electron at momentum $\vec{p}$ (and likewise a quasihole state).

Yet another assumption is necessary to establish the Landau Fermi liquid theory. The assumption is that the quasiparticles interact with each other via an interaction function $f^{\sigma\sigma'}_{\vec{p}\vec{p}'}$. (For simplicity from now on we suppress the spin indices and denote the f-function by $f_{pp'}$. We put them back when necessary later.) The scattering of quasiparticles due to this interaction causes the quasiparticles to decay. If the decay rate is large, then the quasiparticle lifetime, τ_p may be too short. The quasiparticle states therefore will be ill-defined. In other words, the quasiparticle states are not exact eigenstates of the interacting Hamiltonian, i.e. the energy levels have finite width ($\sim 1/\tau_p$). In order to have distinguished energy levels, the width should be smaller than the energies, or

$$\frac{1}{\tau_p} \ll (\epsilon_p - E_F) \tag{2.5}$$

The key point here is that the scattering of these quasiparticles occurs at a vanishingly small rate as the quasiparticles get close to the Fermi surface. The reason behind this lies in the Pauli exclusion principle which restricts the phase space available for quasiparticles to scatter to. At $T = 0$ this phase space is proportional to $(p - p_F)^2$ where p is the momentum of the scattered particle [58]. The scattering therefore, is very small when $p \approx p_F$. At higher temperatures, the scattering rate increases like T^2. As a result, the quasiparticle picture is meaningful only at low temperatures and for quasiparticles with momenta close to the Fermi surface. Thus Landau's picture, with N quasiparticles filling up the states up to the Fermi surface, should be considered only as a formal assumption.

Still this picture is useful especially in the context of Luttinger's theorem that allows to state that for a spherical Fermi surface, the value of K_F is the same in the interacting and non-interacting system.

Let us apply a weak perturbation to the system to take it away from its ground state. The effect of this perturbation is to change the occupation number by $\delta n_{\vec{p}}$. Landau postulated that the change in the energy of the system is given by the expansion

$$\delta E = \sum_{\vec{p}} \epsilon^0_{\vec{p}} \delta n^0_{\vec{p}} + \frac{1}{2V} \sum_{\vec{p},\vec{p'}} f_{pp'} \delta n^0_{\vec{p}} \delta n^0_{\vec{p'}} \tag{2.6}$$

where $\epsilon^0_{\vec{p}}$ is the quasiparticle energy and V is the volume of the system. In general, one can expand to higher powers of $\delta n_{\vec{p}}$. However, expansion to the second order is enough for most practical purposes. The quasiparticle energy affected by other quasiparticles is given by

$$\epsilon_{\vec{p}} = \frac{\delta E}{\delta n^0_{\vec{p}}} = \epsilon^0_{\vec{p}} + \frac{1}{V} \sum_{\vec{p'}} f_{pp'} \delta n^0_{\vec{p'}} \tag{2.7}$$

Landau's f-function is therefore the second derivative of the energy with respect to $\delta n_{\vec{p}}$ and $\delta n_{\vec{p'}}$

$$f_{pp'} = \frac{\delta^2 E}{\delta n^0_{\vec{p}} \delta n^0_{\vec{p'}}} \tag{2.8}$$

Since there is a one to one correspondence between quasiparticle states and non-interacting electron states, the quasiparticles should obey Fermi statistics (a more rigorous proof involves maximization of the entropy. [57])

$$n^0_{\vec{p}} = \frac{1}{e^{\beta(\epsilon_{\vec{p}} - \mu)} + 1} \tag{2.9}$$

where μ is the chemical potential; which can be shown to be equal to the Fermi energy E_F at T=0 [59]. For a SU(2) symmetric system, one can write (putting back spin indices again)

$$f^{\sigma\sigma'}_{\vec{p}\vec{p'}} = f_{\vec{p}\vec{p'}} + 4\vec{\sigma} \cdot \vec{\sigma'} \phi_{\vec{p}\vec{p'}} \tag{2.10}$$

These functions are usually expressed in terms of spherical harmonics

$$f_l = \left(\frac{2l+1}{4\pi}\right)\int d\Omega P_l(\cos\theta)\left[f_{\vec{p}\vec{p}'}\right]_{|\vec{p}|=|\vec{p}'|=p_F}$$
$$\phi_l = \left(\frac{2l+1}{4\pi}\right)\int d\Omega P_l(\cos\theta)\left[\phi_{\vec{p}\vec{p}'}\right]_{|\vec{p}|=|\vec{p}'|=p_F} \tag{2.11}$$

f_l and ϕ_l are known as Landau parameters. In terms of these parameters, the quasiparticle's effective mass is given by (for all derivations and proofs see Ref. [60])

$$\frac{1}{m} = \frac{1}{m^*} + \frac{p_F}{3\pi^2}f_1 \tag{2.12}$$

Observable quantities are usually given in terms of dimensionless Landau parameters $F_l = N(0)f_l$ and $Z_l = N(0)\phi_l$, with the density of states at the Fermi surface

$$N(0) = \frac{1}{V}\sum_{\vec{k},\sigma}\delta(\epsilon_k^0 - \mu) = \frac{m^* p_F}{\pi^2} \tag{2.13}$$

In terms of F_l's and Z_l's, we have [60]

Effective Mass :	$\frac{m^*}{m} = \left(1 + \frac{F_1}{3}\right)$
Specific Heat :	$c_V = \frac{1}{3}m^* p_F k_B^2 T$
Compressibility :	$\frac{1}{\kappa} = \frac{n p_F^2}{3m^*}(1+F_0)$
Sound Velocity :	$c_1^2 = \frac{p_F^2}{3mm^*}(1+F_0)$
Magnetic Susceptibility :	$\chi_M = \frac{\gamma^2 p_F m^*}{4\pi^2(1+Z_0)}$

where $n = N/V$ is the density of electrons and $\gamma = e\hbar/mc$ is the electron's gyromagnetic ratio.

2.2 Microscopic Foundation of Fermi Liquid Theory

As emphasized in the previous section, the basic ingredient of Landau's Fermi liquid theory is the function $f_{pp'}$; which describes the interaction of low energy quasiparticles.

The simple form of the interaction term in (2.6), essential in Fermi liquid calculations, is far from obvious. Renormalization group theory [44] provides a plausible derivation for a low energy effective Hamiltonian in agreement with Fermi liquid theory. As we will see later however, renormalization group might miss some essential singularities in the quasiparticle interaction by putting all the momenta on the Fermi surface. Moreover, although renormalization group is a conserving approximation [61, 62], it does not satisfy the Pauli principle [63, 64, 65]. Another way, is to find a relation between $f_{pp'}$ and the dressed two-particle interaction or 4-point vertex function in many-particle theory. What we do in this section is to first derive $f_{pp'}$ for a low density electron gas by variation of the ground state energy using second order perturbation theory. We then discuss the connection between many-particle theory and Fermi liquid theory. In particular, we find a relation between Landau's f-function and 4-point vertex function in many-particle theory.

2.2.1 Calculation of $f_{pp'}$ for a Dilute Fermi Gas

In a dilute Fermi gas, one can calculate $f_{pp'}$ using Abrikosov-Khalatnikov's formalism [45] (for more detailed derivation, see also Ref. [66], or Ref. [43, 67] for derivation in 2-d). In the dilute limit one can assume short range interaction between electrons. The interaction Hamiltonian therefore can be approximated by

$$H_{\text{int}} = \frac{U}{V} \sum_{\vec{q},\vec{p},\vec{p'}} c^{\dagger}_{\vec{p}+\vec{q}\uparrow} c^{\dagger}_{\vec{p'}-\vec{q}\downarrow} c_{\vec{p'}\downarrow} c_{\vec{p}\uparrow} \tag{2.14}$$

where U is the coupling constant and V is the volume of the system. We do our expansion in powers of the s-wave *scattering amplitude*, a, which is given to the first order in U by

$$U = \frac{4\pi a}{m} \tag{2.15}$$

Applying perturbation theory to $H_{\rm int}$, the first order correction to the ground state energy is given by

$$E^{(1)} = \frac{U}{V}\sum_{1,2} n_1 n_2 Q_{12} = \frac{\pi a N^2}{mV} \tag{2.16}$$

Here the index (1) represents both momentum and spin, n_i is the occupation number and Q_{ij} requires spins to be antiparallel

$$Q_{ij} = \frac{1}{4}(1 - \vec{\sigma}_i \cdot \vec{\sigma}_j) \tag{2.17}$$

where σ's are the Pauli matrices. To second order in perturbation theory we have

$$E^{(2)} = \sum_{m\neq 0} \frac{|(H_{\rm int})_{m0}|^2}{E^{(0)} - E_m^{(0)}} = \frac{U^2}{V^2}\sum_{1,2,3,4} \delta_{p_1+p_2,p_3+p_4} \frac{n_1 n_2 (1-n_3)(1-n_4) Q_{12} Q_{34}}{\epsilon_1 + \epsilon_2 - \epsilon_3 - \epsilon_4} \tag{2.18}$$

Eq. (2.18) is divergent at large momenta. To get away from this divergence we have to expand everything in terms of a instead of U. First notice that (2.15) is not exact. To second order in U, (2.15) can be written as

$$\frac{4\pi a}{m} = \bar{U} = U + \frac{U^2}{V}\sum_{1,2,3,4} \delta_{p_1+p_2,p_3+p_4} \frac{Q_{34}}{\epsilon_1 + \epsilon_2 - \epsilon_3 - \epsilon_4} \tag{2.19}$$

Here, $\bar{U}$ is the renormalized coupling. Inverting (2.19), U can be written in terms of a

$$U = \frac{4\pi a}{m} - \frac{(4\pi a)^2}{m^2 V}\sum_{1,2,3,4} \delta_{p_1+p_2,p_3+p_4} \frac{Q_{34}}{\epsilon_1 + \epsilon_2 - \epsilon_3 - \epsilon_4} \tag{2.20}$$

substituting this into (2.16), we get a term second order in a which should be combined with (2.18) to get the second order correction to the ground state energy. Combining all, after some manipulations, we get

$$E^{(2)} = -\frac{32\pi^2 a^2}{m^2 V^2}\sum_{1,2,3,4} \delta_{p_1+p_2,p_3+p_4} \frac{n_1 n_2 n_3 Q_{12} Q_{34}}{\epsilon_1 + \epsilon_2 - \epsilon_3 - \epsilon_4} \tag{2.21}$$

This now converges at large momenta, since all momenta are limited because of the n_i's. Taking the derivatives with respect to $n_{p\sigma}$ and $n_{p'\sigma'}$, we get

$$\begin{aligned} f_{pp'}^{\sigma\sigma'} &= \frac{4\pi a}{m}\delta_{\sigma,-\sigma'} - \frac{(4\pi a)^2}{m^2 V}\sum_{\vec{k}} n_{\vec{k}}\Big[\frac{2\delta_{\sigma,-\sigma'}}{\epsilon_{\vec{p}} + \epsilon_{\vec{p}'} - \epsilon_{\vec{k}} - \epsilon_{\vec{p}+\vec{p}'-\vec{k}}} \\ &\quad + \frac{1}{\epsilon_{\vec{p}} - \epsilon_{\vec{p}'} + \epsilon_{\vec{k}} - \epsilon_{\vec{k}+\vec{p}-\vec{p}'}} + \frac{1}{\epsilon_{\vec{p}'} - \epsilon_{\vec{p}} + \epsilon_{\vec{k}} - \epsilon_{\vec{k}+\vec{p}'-\vec{p}}}\Big] \end{aligned} \tag{2.22}$$

The first term in the bracket is the "Cooper" channel and the last two terms belong to the "crossed" channels. The denominators of the last two terms vanish when $\vec{p} = \vec{p'}$. The singularities however get canceled between the two terms except for special cases (we will return to this point later).

2.2.2 Fermi Liquid Theory and Many-Particle Theory

In many-particle theory [58, 60, 66, 68], the excitations of the system above its ground state are given by the poles of the single particle Green's function $G(\omega, \vec{k})$ [58]. In the absence of any phase transition, $G(\omega, \vec{k})$ has a form very similar to non-interacting Green's function. One can write [58]

$$G(\omega, \vec{k}) = \frac{Z_k}{\omega - \epsilon_k + i\tau_k^{-1}} + \Phi(\omega, \vec{k}) \tag{2.23}$$

where Z_k and τ_k are quasiparticle residue and quasiparticle lifetime respectively. The first term in the right hand side of (2.23) is similar to the non-interacting electron Green's function

$$G^{(0)}(\omega, \vec{k}) = \frac{1}{\omega - \epsilon_k + i\delta_k} \tag{2.24}$$

where $\delta_k = \delta \ \mathrm{sgn}(\epsilon_k - \mu)$ with $0 < \delta \ll 1$. The second term, $\Phi(\omega, \vec{k})$, represents the incoherent part of the Green's function. For most calculations, the first term in (2.23) is sufficient to give correct physical behavior up to the desired accuracy. This explains why Fermi liquid theory, which is very similar to non-interacting electron theory, works so well for complex systems like metals. In any calculation however, one has to make sure that the incoherent part of the Green's function does not make significant contribution.

In terms of quasiparticle self-energy $\Sigma_{\vec{k}}(\omega)$, Z_k and τ_k are give by [68]

$$\tau_k^{-1} = -Z_k \ \mathrm{Im}\Sigma_{\vec{k}}(\epsilon_k) \tag{2.25}$$

$$Z_k = \left(1 - \frac{\partial}{\partial\omega}\mathrm{Re}\Sigma_{\vec{k}}(\omega)\right)^{-1}_{\omega=\epsilon_k} \tag{2.26}$$

We can see from (2.24) that the quasiparticle lifetime in non-interacting systems is infinite ($\tau_k \to \infty$). In interacting systems however, τ_k is finite. In fact, one can show that [58] for a 3-d Fermi liquid $\tau_k^{-1} \propto (\epsilon_k - \mu)^2$, and therefore the lifetime diverges as the particle gets close the Fermi surface. The closer to the Fermi surface, the more stable the quasiparticle state is. For states with momenta far away from the Fermi surface, the quasiparticle concept is not meaningful as emphasized before.

For small ω, the self energy behaves like

$$\mathrm{Im}\Sigma_{p_F}(\omega) \sim \omega^2 \qquad \text{and} \qquad \mathrm{Re}\Sigma_{p_F}(\omega) \sim \omega \tag{2.27}$$

Substituting into (2.26) we find Z ($\equiv Z_{(k=p_F)}$) a nonzero positive constant (always < 1). Z measures the amount of the spectral weight accumulated in the quasiparticle peak [68]. It has other meanings as well. It can be shown [69, 59] that the occupation number n_k is always discontinuous at the Fermi surface with a jump exactly equal to Z. Thus the Fermi surface concept survives even after turning on the interaction. The existence of the Fermi surface, in fact, is equivalent to the validity of Fermi liquid theory. When $Z = 0$, as it is in 1-d Luttinger liquids, the occupation number doesn't have a jump at p_F. Consequently, there is no well defined Fermi surface; although higher order derivatives of n_k still are singular right at the position of the Fermi surface. Fermi liquid theory therefore breaks down in such cases.

The dressed interaction between two quasiparticles is given by 4-point vertex function $\Gamma^{(2)}(P_1, P_2; P_3, P_4)$ which is related to the 2-particle Green's function $G^{(2)}$ by

$$\begin{aligned} G^{(2)}(P_1, P_2; P_3, P_4) &= (2\pi)^8 G(P_1)G(P_2)\left[\delta(P_1 - P_3)\delta(P_2 - P_4) - \delta(P_1 - P_4)\delta(P_2 - P_3)\right] \\ &+ i(2\pi)^4 \delta(P_1 + P_2 - P_3 - P_4)\; G(P_1)G(P_2)G(P_3)G(P_4)\; \Gamma^{(2)}(P_1, P_2; P_3, P_4) \end{aligned} \tag{2.28}$$

with $P = (\nu, \vec{p})$. Since in Fermi liquid theory, interaction between two quasiparticles is described by $f_{pp'}$, it is natural to expect connection between $f_{pp'}$ and $\Gamma^{(2)}$. To see the

connection, let us define $\Gamma(P, P'; K)$ by

$$\Gamma(P, P'; K) = \Gamma^{(2)}(P, P'; P + K, P' - K) \tag{2.29}$$

where $K = (\omega, \vec{k})$. It has been shown that the following integral equation holds under certain assumptions [60]

$$\Gamma(P, P'; K) = \Gamma^{(\omega)}(P, P') + \frac{Z^2 p_F^2}{(2\pi)^3} \int d\Omega \Gamma^{(\omega)}(P, Q) \frac{\hat{q} \cdot \vec{k}}{\omega - \hat{q} \cdot \vec{k}} \Gamma(Q, P'; K) \tag{2.30}$$

where Z is the quasiparticle residue, $Q = (\mu, p_F \hat{q})$, with μ being the chemical potential, and the function $\Gamma^{(\omega)}$ is defined by

$$\Gamma^{(\omega)}(P, P') = \lim_{\omega \to 0} \lim_{\vec{k} \to 0} \Gamma(P, P', K) \tag{2.31}$$

The order of the limits plays important role here (we will see this shortly). The integration in (2.30) is over all directions of $\hat{q}$. The function $\Gamma^{(\omega)}$ is closely related to the Landau's f-function [66]. More precisely, at low energies putting all the momenta on the Fermi surface we have

$$f_{pp'} = Z^2 \Gamma^{(\omega)}(\hat{p}, \hat{p}') \tag{2.32}$$

The notation means that $P = (\mu, p_F \hat{p})$ and $P' = (\mu, p_F \hat{p}')$. $f_{pp'}$ does not have direct physical meaning by itself [66]. However, one can change the order of limits in (2.31) to define

$$\Gamma^{(k)}(P, P') = \lim_{\vec{k} \to 0} \lim_{\omega \to 0} \Gamma(P, P', K) \tag{2.33}$$

$Z^2 \Gamma^{(k)}$ is actually the physical forward scattering interaction between two quasiparticles [66]. Taking the limit $\vec{k} \to 0$ and $\omega / k \to 0$ in (2.30), one can find the relation between $Z^2 \Gamma^{(k)}$ and $f_{pp'}$

$$Z^2 \Gamma^{(k)}(\hat{p}, \hat{p}') = f_{pp'} - \frac{p_F^2}{(2\pi)^3} \int d\Omega \; f_{pq} \; Z^2 \Gamma^{(k)}(\hat{q}, \hat{p}') \tag{2.34}$$

The quantity $Z^2\Gamma^{(k)}$ is usually called scattering amplitude or T-matrix [56, 43]. More precisely the T-matrix $t_{pp'}(\vec{q},\omega)$ is defined by

$$t_{pp'}(\vec{q},\omega) = Z_p Z_{p'} \Gamma(P,P';Q) \tag{2.35}$$

A modified version of (2.30) gives $t_{pp'}(\vec{q},\omega)$ in terms of $f_{pp'}$ [56]

$$t_{pp'}(\vec{q},\omega) = f_{pp'} + \sum_{\vec{k}} f_{pk} \frac{\vec{q}\cdot\vec{v}_k}{\vec{q}\cdot\vec{v}_k - \omega + i\delta} n_{\vec{k}}^{(0)} t_{kp'}(\vec{q},\omega). \tag{2.36}$$

This equation is usually known as Bethe-Salpeter equation. One can again write

$$t_{\vec{p}\vec{p}'}^{\sigma\sigma'} = t_{\vec{p}\vec{p}'}^{s} + 4\vec{\sigma}\cdot\vec{\sigma}' t_{\vec{p}\vec{p}'}^{a} \tag{2.37}$$

In the limit $q \to 0$, $\omega/q \to 0$, and for p and p' on the Fermi surface, Eq. (2.36) gives

$$\begin{aligned} t_l^s &= \frac{F_l}{1 + F_l/(2l+1)} \\ t_l^a &= \frac{Z_l}{1 + Z_l/(2l+1)} \end{aligned} \tag{2.38}$$

where t_l^s and t_l^a are spherical harmonics.

2.3 Fermi Liquid Theory in 2-d

In the last section, we introduced Landau's Fermi liquid theory as a powerful tool to describe fermionic systems in 3-d. It is well known, on the other hand, that 1-d electron systems are not Fermi liquids but Luttinger liquids [70]. The question for 2-d systems is more subtle and has been a subject of controversy for almost a decade. Anderson in 1990 [37, 38] suggested that 2-d interacting electron systems are also Luttinger liquids and not Fermi liquids. He conjectured that Landau's quasiparticle interaction function would become singular in 2-d. The singularity he suggested had the form

$$f_{pp'} \sim \frac{\vec{p}\cdot(\vec{p}-\vec{p}')}{|\vec{p}-\vec{p}'|^2} \tag{2.39}$$

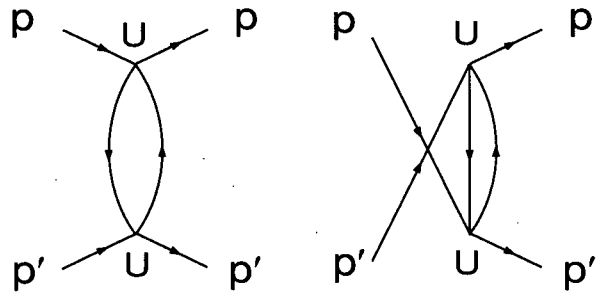

Figure 2.3: Crossed channel diagrams contributing in $I_{pp'}$.

This singular interaction will result in vanishing quasiparticle residue and break down of Fermi liquid theory [43]. One immediately notices that the numerator of (2.39) vanishes (as $p \to p'$) when both particles are located on the Fermi surface. Thus the singularity can be detected only when the particles are away from the Fermi surface. Methods such as Renormalization Group, which put their initial momenta on the Fermi surface, are unable to detect this singularity. Since Anderson, there have been several attempts to prove or disprove Fermi liquid theory in 2-d [43, 41, 71, 42, 72]; all of them in agreement with Fermi liquid theory (at least for systems with isotropic Fermi surface). On the other hand, it is well known that Van Hove singularities [73] or nested Fermi surfaces [74, 44] do not preserve Fermi liquid theory. Therefore the geometry of the Fermi surface plays an important role in the Fermi liquid behavior of the system. In this section, we shall study the effect of local geometry of the Fermi surface on the interaction function $f_{pp'}$. We especially find a singularity at points where the Fermi surface has zero curvature. This singularity is shown, in the next section, to change the Fermi liquid behavior of the quasiparticles near the inflection points.

2.3.1 Calculation of $f_{pp'}$ for a Curved Fermi Surface

Let us start with a 2-d Hubbard Hamiltonian

$$H = \sum_{\vec{p},\sigma} \epsilon_{\vec{p}} c^\dagger_{\vec{p}\sigma} c_{\vec{p}\sigma} + \frac{U}{\Omega} \sum_{\vec{q},\vec{p},\vec{p'}} c^\dagger_{\vec{p}+\vec{q}\uparrow} c^\dagger_{\vec{p'}-\vec{q}\downarrow} c_{\vec{p'}\downarrow} c_{\vec{p}\uparrow} \tag{2.40}$$

where $\epsilon_{\vec{p}}$ defines the "bare" band structure and Ω is the area of the sample. We wish to find $f^{\sigma\sigma'}_{pp'}$ up to second order in small coupling U, or more precisely, the renormalized coupling $\bar{U}$, the same way as we did in Sec. (2.2.1). Note that by small coupling we mean $U/t \ll 1$ (this is not necessarily a low-density limit, but it is a weak-interaction limit). Following the method we described in Sec. (2.2.1), we find

$$f^{\sigma\sigma'}_{pp'} = (\hbar^2 g_{pp'}/m)\delta_{\sigma,-\sigma'} - (\hbar^2 g_{pp'}/m)^2 (I_{pp'} + C^{\sigma\sigma'}_{pp'}) \tag{2.41}$$

where the dimensionless coupling $g_{pp'}$ is given by [45, 43]

$$g_{pp'} = \frac{m\bar{U}}{\hbar^2} = \frac{m}{\hbar^2}\left[U + \frac{U^2}{2}\sum_{\vec{q}} \frac{1}{\epsilon_{\vec{p}} + \epsilon_{p\prime} - \epsilon_{\vec{p'}+\vec{q}} - \epsilon_{\vec{p}-\vec{q}}}\right] \tag{2.42}$$

we also identify the "Cooper" channel and "crossed" channel by (cf. Fig. 2.3)

$$C^{\sigma\sigma'}_{pp'} = \sum_{\vec{k}} \left(\frac{2\delta_{\sigma,-\sigma'}\, n_{\vec{k}}}{\epsilon_{\vec{p}} + \epsilon_{\vec{p'}} - \epsilon_{\vec{k}} - \epsilon_{\vec{p}+\vec{p'}-\vec{k}}}\right) \tag{2.43}$$

$$I_{pp'} = \sum_{\vec{k}} \left(\frac{n_{\vec{k}}}{\epsilon_{\vec{p}} - \epsilon_{\vec{p'}} + \epsilon_{\vec{k}} - \epsilon_{\vec{k}+\vec{Q}}} + (\vec{p} \leftrightarrow \vec{p'})\right) \tag{2.44}$$

The Cooper term, $C^{\sigma\sigma'}_{pp'}$, is singular when $\vec{p} = (\vec{p}+\vec{p'})/2 \to 0$, but regular near $\vec{Q} \equiv \vec{p}-\vec{p'} = 0$ (as is $g_{pp'}$). We thus drop $C^{\sigma\sigma'}_{pp'}$ and approximate $g_{pp'} \approx g_0$. $I_{pp'}$, on the other hand, may become singular when $\vec{Q} \to 0$. This can be seen by the fact that the denominators in (2.44) vanish at $\vec{Q} = 0$. We therefore have to examine $I_{pp'}$ more carefully. Let us define

$$\vec{v}_{\vec{k}} = \frac{\partial \epsilon_{\vec{k}}}{\partial \vec{k}} \qquad \text{and} \qquad (M^{-1}_{\vec{k}})_{ij} = \frac{\partial^2 \epsilon_{\vec{k}}}{\partial k_i \partial k_j} \tag{2.45}$$

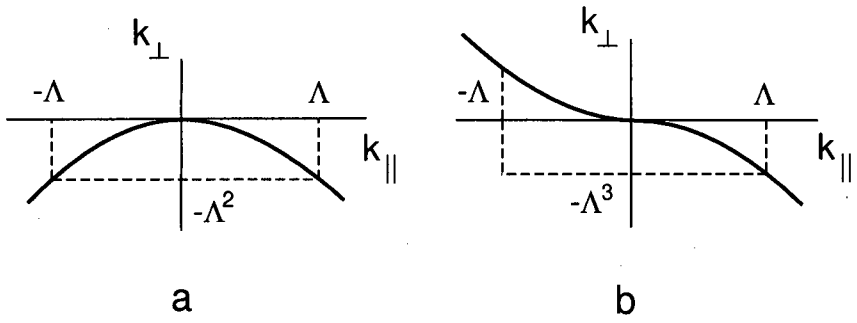

Figure 2.4: The two situations considered in the text. In (a) we assume the Fermi surface has finite curvature at $\vec{k} = \vec{k}_0$; in (b) the curvature is zero when $\vec{k} = \vec{k}_0$ (inflection point). Hatched lines show the integration regions discussed in the text.

Expanding the denominators to second order in $\vec{Q}$, we have

$$\begin{aligned} I_{pp'} &= \int \frac{d^2k}{(2\pi)^2} \left(\frac{n_{\vec{k}}}{(\vec{v}_{\vec{p}} - \vec{v}_k)\cdot\vec{Q} - \frac{1}{2}\vec{Q}\cdot\mathcal{M}_{\vec{k}}^{-1}\cdot\vec{Q}} - \frac{n_{\vec{k}}}{(\vec{v}_{\vec{p}} - \vec{v}_k)\cdot\vec{Q} + \frac{1}{2}\vec{Q}\cdot\mathcal{M}_{\vec{k}}^{-1}\cdot\vec{Q}} \right) \\ &= \frac{1}{(2\pi)^2} \int d^2k \frac{n_{\vec{k}}(2\Delta_{\vec{k},Q}/Q)}{[(\vec{v}_{\vec{p}} - \vec{v}_k)\cdot\hat{Q}]^2 - \Delta_{\vec{k},Q}^2} \propto I_{\vec{p}}(\vec{Q}) \end{aligned} \tag{2.46}$$

where

$$I_{\vec{p}}(\vec{Q}) \equiv \int d^2k \frac{n_{\vec{k}}}{[(\vec{v}_{\vec{p}} - \vec{v}_k)\cdot\hat{Q}]^2 - \Delta_{\vec{k},Q}^2} \tag{2.47}$$

The "gap" $\Delta_{\vec{k},\vec{Q}}$ is defined by

$$\Delta_{\vec{k},\vec{Q}} = \frac{\vec{Q}\cdot\mathcal{M}_{\vec{k}}^{-1}\cdot\vec{Q}}{2|\vec{Q}|} \propto |\vec{Q}| \tag{2.48}$$

and $\hat{Q} \equiv \vec{Q}/|\vec{Q}|$. For a quadratic dispersion relation $\epsilon_{\vec{k}} = k^2/2m$, $\mathcal{M}_{\vec{k}}^{-1}$ $(= 1/m)$ is independent of $\vec{k}$. In more general cases however, it has $\vec{k}$-dependence but this does not affect our calculation (we will consider the $\vec{k}$-dependence of $\mathcal{M}_{\vec{k}}^{-1}$ when appropriate later). Thus for the moment, we can safely neglect the $\vec{k}$-dependence and write $\Delta_{\vec{k},\vec{Q}} = \Delta_{\vec{Q}}$.

Our goal is now to understand the behavior of $I_{\vec{p}}(\vec{Q})$ as $\vec{Q} \to 0$. Infrared singularity occurs when $(\vec{v}_{\vec{p}} - \vec{v}_k)\cdot\hat{Q} = 0$. This condition is usually satisfied on a line in k-space

inside the Fermi surface (corresponding to a straight line in $\vec{v}$-space). Let's confine our integration to a region within a cutoff Λ around this line, where $|\vec{Q}| \ll \Lambda \ll p_F$, and p_F is the Fermi momentum. The integration inside the Fermi surface then has the form

$$\int_{-\Lambda}^{\Lambda} \frac{du}{u^2 - \Delta_{\vec{Q}}^2} = \frac{1}{\Delta_{\vec{Q}}} \ln\left(\frac{|\Lambda - \Delta_{\vec{Q}}|}{|\Lambda + \Delta_{\vec{Q}}|}\right) \sim \frac{1}{\Delta_{\vec{Q}}}\left(-\frac{2\Delta_{\vec{Q}}}{\Lambda}\right) = -\frac{2}{\Lambda} \tag{2.49}$$

Thus the integration inside the Fermi surface contains no singularity as $\Delta_{\vec{Q}} \to 0$. Singularity, if any, should therefore come from the integration near the Fermi surface. Let $\vec{k}_0$ be a point on the Fermi surface, satisfying $(\vec{v}_{\vec{p}} - \vec{v}_{k_0}) \cdot \hat{Q} = 0$. We first consider points where Fermi surface has finite curvature (Fig. 2.4 (a)). Writing $\vec{k} = \vec{k}_0 + k_\perp \hat{e}_\perp + k_{||}\hat{e}_{||}$, where $\hat{e}_{||}$ ($\hat{e}_\perp$) are unit vectors parallel (perpendicular) to the Fermi surface at $\vec{k}_0$, we then define $\epsilon_{\vec{k}}$ by the expansion

$$\epsilon_{\vec{k}} = E_F + v_{k_0} k_\perp + a k_\perp^2 + b k_{||}^2 + c k_\perp k_{||} \tag{2.50}$$

Near $\vec{k}_0$ therefore, $\vec{v}_k$ can be written as

$$\vec{v}_k = v_{k_0}\hat{e}_\perp + \vec{\gamma}_{||} k_{||} + \vec{\gamma}_\perp k_\perp \tag{2.51}$$

where

$$\vec{\gamma}_\perp = 2a\hat{e}_\perp + c\hat{e}_{||} \quad , \quad \vec{\gamma}_{||} = c\hat{e}_\perp + 2b\hat{e}_{||}. \tag{2.52}$$

Fermi surface also is defined by

$$v_{k_0} k_\perp + a k_\perp^2 + b k_{||}^2 + c k_\perp k_{||} = 0 \tag{2.53}$$

Since the Fermi surface has finite curvature at $\vec{k}_0$, $\vec{\gamma}_{||}$ and b are non-zero. Rescaling the integral in (2.46) so that $v_{k_0} = b = 1$, we have a Fermi surface near k_0 obeying $k_{||}^2 \approx -k_\perp$ (cf. (2.53)). It is not difficult to see that singularities in $I_{pp'}$, for $\vec{p}, \vec{p'}$ close to $\vec{k}_0$, arise only when

$$\vec{\gamma}_{||} \cdot \hat{Q} \to 0 \tag{2.54}$$

In that case:

$$I_{pp'} \sim \int_{-\Lambda^2}^{0} dk_\perp \int_{-\sqrt{-k_\perp}}^{\sqrt{-k_\perp}} \frac{dk_{||}}{k_\perp^2 - \Delta^2_{\vec{k},\vec{Q}}} \sim \frac{\pi}{|Q|^{1/2}} \tag{2.55}$$

To get (2.55) we have made use of the following integral

$$\int du \frac{\sqrt{u}}{u^2 - \Delta^2} = \frac{1}{\sqrt{\Delta}} (\frac{1}{2} \ln \frac{|\sqrt{u} - \sqrt{\Delta}|}{|\sqrt{u} + \sqrt{\Delta}|} + \tan^{-1} \sqrt{\frac{u}{\Delta}}) \tag{2.56}$$

This singularity is just that found already for a circular Fermi surface [42, 43]. It only occurs if $\vec{p}$ and $\vec{p'}$ approach each other along the direction orthogonal to $\vec{\gamma}_{||}$. For a circular Fermi surface, this direction is orthogonal to the Fermi surface. For non-circular Fermi surfaces (with no inflection point) on the other hand, $\vec{\gamma}_{||} \cdot \hat{Q} = 0$ for directions which are not necessarily normal to the Fermi surface; but the singularity is still along lines. This case was also studied away from the Fermi surface by Fukuyama and Ogata [72]. A closer look at the singular region in k-space for the case of a circular Fermi surface shows that it is bounded by circular arcs of opposite curvature which touch at the Fermi surface [43].

This singularity does not change the Fermi liquid behavior [43]. A simple way to see this, is to look at the quasiparticle energy

$$\epsilon_{\vec{p}} = \epsilon^0_{\vec{p}} + \sum_{\vec{p'}} f_{\vec{p}\vec{p'}} \delta n_{\vec{p'}} \tag{2.57}$$

Singularity in $f_{pp'}$ is summed over in this equation. In our case here, the $|Q|^{1/2}$ singularity is always along a line. Integration over this term removes the singularity and gives Fermi liquid behavior as one approaches the Fermi surface [42, 43].

2.3.2 Calculation of $f_{pp'}$ near an Inflection Point

At points where the Fermi surface has zero curvature, $\vec{\gamma}_{||} \to 0$ and consequently, condition (2.54) is always satisfied. It is therefore natural to expect a singularity in any direction

of $\hat{Q}$; which may now cause break down of Fermi liquid theory. We wish to study this singularity near an inflection point. We must therefore extend (2.53) to higher order, and also include the k-dependence of $\mathcal{M}_{\vec{k}}^{-1}$ (which now vanishes in certain directions). Expanding about an inflection point at $\vec{k} = \vec{k}_0$, we write

$$\epsilon_{\vec{k}} = v_{k_0} k_\perp + a k_\perp^2 + g k_\parallel^3 \tag{2.58}$$

(cf. Fig.1(b)). Substituting directly into (2.44) we get

$$I_{\bar{p}}(\vec{Q}) = \frac{1}{3gQ_\parallel} \int_{-\Lambda}^{\Lambda} dk_\parallel \int_{-g\Lambda^3/v_{k_0}}^{-gk_\parallel^3/v_{k_0}} \left(\frac{dk_\perp}{c_{\hat{Q}} k_\perp + k_\parallel^2 + Q_\parallel k_\parallel + T(\vec{\kappa}, \vec{Q})} \right) + (\vec{Q} \to -\vec{Q}) \tag{2.59}$$

We have defined $\vec{\kappa} = \vec{p} - \vec{k}_0$ (i.e., the center of mass momentum relative to $\vec{k}_0$), $c_Q = 2aQ_\perp/3gQ_\parallel$ and

$$T(\vec{\kappa}, \vec{Q}) = \kappa_\parallel^2 - \frac{Q_\parallel^2}{4} + c_Q(\kappa_\perp + \frac{Q_\perp}{2}) \tag{2.60}$$

Integration over $\kappa_\perp$ is straightforward. One finds

$$I_{\bar{p}}(\vec{Q}) = \frac{1}{2aQ_\perp} \int_{-\Lambda}^{\Lambda} dk_\parallel \ln \left| \frac{k_\parallel^2 + Q_\parallel k_\parallel - (c_Q g/v_{k_0}) k_\parallel^3 + T(\vec{\kappa}, \vec{Q})}{k_\parallel^2 + Q_\parallel k_\parallel - (c_Q g/v_{k_0})\Lambda^3 + T(\vec{\kappa}, \vec{Q})} \right| + (\vec{Q} \to -\vec{Q}) \tag{2.61}$$

The $k_\parallel^3$ term in the numerator is small compared to the other terms unless if $Q_\parallel \to 0$ (or $c_Q \to \infty$). We therefore neglect this term except when $Q_\parallel \ll Q_\perp$ (we will come back to this case later). To calculate the above integrals we should use

$$\begin{aligned} &\int du \ln|u^2 + \beta u + \gamma| = (u + \beta/2) \ln|u^2 + \beta u + \gamma| - 2u \\ &+2\sqrt{|W|} \left[\theta(-W) \frac{1}{2} \ln \left(\frac{u + \beta/2 + \sqrt{|W|}}{u + \beta/2 - \sqrt{|W|}} \right) + \theta(W) \tan^{-1} \left(\frac{u + \beta/2}{\sqrt{|W|}} \right) \right] \end{aligned} \tag{2.62}$$

where $W = \gamma - \beta^2/4$. However , it turns out that all the terms in the above integral are regular as $\vec{Q} \to 0$ except for the "$\tan^{-1}$" term. Keeping only the singular terms we find

$$I_{\bar{p}}(\vec{Q}) \sim \theta(W_{\vec{\kappa},\vec{Q}}) \left(\frac{\sqrt{W_{\vec{\kappa},\vec{Q}}}}{2Q_\perp} \right) \left[\tan^{-1} \left(\frac{\Lambda + Q_\parallel/2}{\sqrt{W_{\vec{\kappa},\vec{Q}}}} \right) + \tan^{-1} \left(\frac{\Lambda - Q_\parallel/2}{\sqrt{W_{\vec{\kappa},\vec{Q}}}} \right) \right] + (\vec{Q} \to -\vec{Q}) \tag{2.63}$$

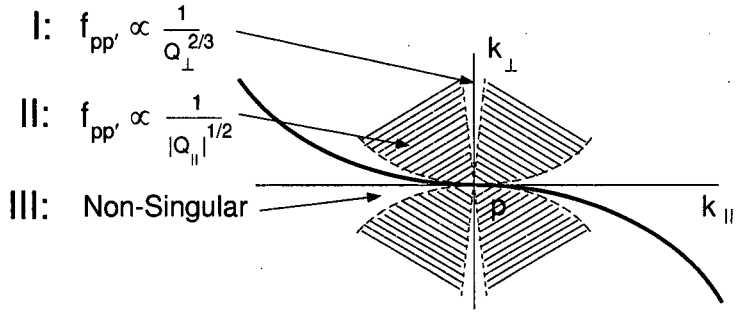

Figure 2.5: Three different regions in k-space around the inflection points with different singular behavior. We have put $\vec{p} = \vec{k}_0$ therefore the regions shown are actually the regions where $\vec{p}'$ can be. Between I and II, there is a crossover whereas between II and III there is a sharp edge.

where

$$W_{\vec{\kappa},\vec{Q}} = T(\vec{\kappa},\vec{Q}) + \frac{Q_\parallel^2}{4} = -\kappa_\parallel^2 - c_Q(\kappa_\perp + Q_\perp/2) \tag{2.64}$$

In the limit where $\kappa, Q \ll \Lambda$ we approximately get

$$I_{\vec{p}}(\vec{Q}) = \frac{\pi}{aQ_\perp}[|W_+|^{1/2}\theta(W_+) - |W_-|^{1/2}\theta(W_-)] + ... \tag{2.65}$$

where (...) represents non-singular terms and $W_\pm \equiv W_{\vec{\kappa},\pm\vec{Q}}$.

This behavior of $I_{pp'}$ is rather complicated. We can get some feeling for it if we first take the case where $\vec{p} = \vec{k}_0$, i.e., where one quasiparticle is at the inflection point (see Fig. 2.5). Then for most regions in k-space, (2.65) gives

$$I_{\vec{k}_0,\vec{k}_0+\vec{Q}} \sim \frac{\theta(4cQ_\perp^2 - Q_\parallel^3)\theta(Q_\parallel)}{|Q_\parallel|^{1/2}} \tag{2.66}$$

This is the same inverse square root as found for the circular Fermi surface (cf. (2.55)), but now extending over large "butterfly wing" regions in k-space.) Fig. 2.5 shows different regions in k-space with different singular behavior. The singularity in the left wing of the butterfly region comes from switching $\vec{p}$ and $\vec{p}'$, i.e. putting $\vec{p}'$ at the inflection point.

When $Q_{\|} \to 0$, the above approximation does not hold anymore. In that case (2.59) becomes

$$\begin{aligned} I_{\bar{p}}(\vec{Q}) &= \frac{1}{2aQ_{\perp}} \int_{-\Lambda}^{\Lambda} dk_{\perp} \int_{-(v_{k_0} k_{\perp}/g)^{1/3}}^{(v_{k_0}\Lambda/g)^{1/3}} dk_{\|} \left[\frac{1}{k_{\perp} - p_{\perp} + k_{0\perp}} + (\vec{p} \leftrightarrow \vec{p'}) \right] \\ &= \frac{\zeta (v_{k_0}/g)^{1/3}}{2aQ_{\perp}} \left[(\kappa_{\perp} + Q_{\perp}/2)^{1/3} - (\kappa_{\perp} - Q_{\perp}/2)^{1/3} \right] + \ldots \end{aligned} \tag{2.67}$$

where $\zeta \approx \int_{-\infty}^{\infty} dz/(z^3 - 1) = -\pi/\sqrt{3}$. If we again put $\vec{p} = \vec{k}_0$, we get

$$I_{\bar{p}}(\vec{Q}) \sim Q_{\perp}^{-2/3} \qquad (Q_{\|} \ll Q_{\perp}) \tag{2.68}$$

The singularity here is stronger than what we found before ($\sim Q_{\|}^{-1/2}$). There is a crossover between these two different behaviors (cf. Fig. 2.5).

It is very important to note also the non-singular region (region III in Fig. 2.5) which lies close to the Fermi surface as Q approaches the origin. There is no singularity in the interaction between 2 quasiparticles if they are both on the Fermi surface. Thus any calculation (perturbative or renormalization group) of the scattering between quasiparticles confined to the Fermi surface will miss all the singular behavior in (2.66).

In the more general case where neither particle is at k_0, the behavior of $I_{pp'}$ is not so easily displayed. As the quasiparticles approach each other one finds the simple behavior

$$I_{\vec{k}_0, \vec{k}_0 + \vec{Q}} \propto \frac{\theta(-\kappa_{\|}^2 - c_Q \kappa_{\perp})}{[-\kappa_{\|}^2 - c_Q \kappa_{\perp}]^{1/2}} \qquad (Q \ll \kappa) \tag{2.69}$$

2.4 Calculation of Self Energy

Fermi or non-Fermi liquid nature of the system can be checked by calculating the self energy $\Sigma_{\vec{p}}(\omega)$. We already have seen how the quasiparticle lifetime and quasiparticle residue are related to the real and imaginery parts of the self energy (cf. (2.25) and (2.26)). The imaginary part of $\Sigma_{\vec{p}}(\omega)$ is specially important because it can be calculated

easily using the Fermi golden rule. We saw that in a 3-d Fermi liquid, at low energies, we have

$$\mathrm{Im}\Sigma_{p_F}(\omega) \sim \omega^2 \tag{2.70}$$

In this section we first see how this relation is different for a 2-d Fermi liquid with non-singular interaction. We then find the effect of our singularities on $\mathrm{Im}\Sigma_{p_F}(\omega)$ and show the deviation from Fermi liquid behavior.

2.4.1 Non-Singular Interaction

Let us first consider the non-singular case. Landau's f-function is therefore regular and given by the cylindrical harmonics f_l the same way as before. For the present calculation, it is enough to consider the isotropic harmonic and write

$$f_{pp'} = f_0 \tag{2.71}$$

Having Landau's f-function, we can calculate the quasiparticle T-matrix using the Bethe-Salpeter equation (2.36). In the isotropic channel, which we consider here, the T-matrix is simply given by [56]

$$t_{pp'}(\vec{q},\omega) = t_0(\eta) = \frac{f_0}{1 + f_0\chi^0(\vec{q},\omega)} \tag{2.72}$$

where $\chi^0(\vec{q},\omega)$ is the 2-dimensional Lindhard function [43]

$$\chi^0(\vec{q},\omega) = N(0)\left[1 - \eta\left(\frac{\theta(\eta^2-1)}{\sqrt{\eta^2-1}} + i\frac{\theta(1-\eta^2)}{\sqrt{1-\eta^2}}\right)\right], \tag{2.73}$$

$\eta = \omega/qv_F$ and density of states at the Fermi surface $N(0) = p_F/2\pi v_F$. All the physical quantities can then be found from the T-matrix. What we wish to do here however, is to calculate the quasiparticle self energy and compare it with the 3-d case discussed before (calculation we present here is based on Ref. [43]).

It is always easier to calculate the imaginary part of the self energy which is equivalent to the scattering rate and is given by Fermi golden rule [56]

$$\mathrm{Im}\Sigma_p(\omega) = \pi \sum_{\vec{p}',\vec{q}} |t_{pp'}(\vec{q},\omega)|^2 n^0_{\vec{p}'}(1-n^0_{\vec{p}-\vec{q}})(1-n^0_{\vec{p}'+\vec{q}})\delta(\omega+\epsilon_{\vec{p}'}-\epsilon_{\vec{p}-\vec{q}}-\epsilon_{\vec{p}'+\vec{q}}) \tag{2.74}$$

We calculate the energy on shell (i.e. $\omega = \epsilon_{\vec{p}}$). Assuming $q \ll p_F$ we have

$$\epsilon_{\vec{p}-\vec{q}} = \epsilon_{\vec{p}} - v_F q\mu = \omega - v_F q\mu \tag{2.75}$$

where $\mu = \hat{p}\cdot\hat{q}$. The δ-function in (2.74) can be written as

$$\begin{aligned}\delta(\omega+\epsilon_{\vec{p}'}-\epsilon_{\vec{p}-\vec{q}}-\epsilon_{\vec{p}'+\vec{q}}) &= \int_{-\infty}^{\infty} d\nu\delta(\nu-\omega+\epsilon_{\vec{p}-\vec{q}})\delta(\nu-\epsilon_{\vec{p}'}-\epsilon_{\vec{p}'+\vec{q}})) \\ &= \int_{-\infty}^{\infty} d\nu\delta(\nu-qv_F\mu)\delta(\nu-qv_F\mu')\end{aligned} \tag{2.76}$$

with $\mu' = \hat{p}'\cdot\hat{q} = \cos\theta'$. On the other hand (at $T=0$)

$$n^0_{\vec{p}'}(1-n^0_{\vec{p}'+\vec{q}}) = \theta(p_F-p')\theta(p'+q\mu'-p_F) \tag{2.77}$$

Eq. (2.77) requires $p' < p_F$ and $\mu' > 0$. Therefore

$$\sum_{vecp'} n^0_{\vec{p}'}(1-n^0_{\vec{p}'+\vec{q}}) = \int_{-\pi/2}^{\pi/2}\frac{d\theta'}{2\pi}\int_{p_F-q\mu'}^{p_F}\frac{p'dp'}{2\pi} = \frac{p_F q}{(2\pi)^2}\int_{-\pi/2}^{\pi/2}\mu' d\theta' \tag{2.78}$$

Substituting all back into (2.74) we find

$$\mathrm{Im}\Sigma_p(\omega) = \frac{p_F}{2\pi v_F}\sum_{\vec{q}}\int\frac{\nu d\nu}{\sqrt{v_F^2q^2-\nu^2}}|t(q,\nu)|^2\theta(\omega-qv_F\mu)\theta(qv_F-\nu)\delta(\nu-qv_F\mu) \tag{2.79}$$

One can write

$$\sum_{\vec{q}} = \int\frac{d^2q}{(2\pi)^2} = \int\frac{qdq}{(2\pi)^2}\int\frac{d\mu}{\sqrt{1-\mu^2}} \tag{2.80}$$

Because of the δ-function, the μ-integral will require $\mu = \nu/qv_F \equiv \eta$. As a result

$$\mathrm{Im}\Sigma_p(\omega) = \frac{p_F}{(2\pi)^3 v_F}\int qdq\int\nu d\nu\frac{|t(\vec{q},\nu)|^2_{\mu=\eta}}{q^2v_F^2-\nu^2}\theta(\omega-\nu)\theta(qv_F-\nu) \tag{2.81}$$

In the isotropic case, $t(\vec{q},\nu)$ is only a function of η (cf. (2.72)). For $\eta < 1$, which is actually the case here, we have

$$t(\eta) = \frac{f_0}{1 + f_0(1 - i\eta/\sqrt{1-\eta^2})N(0)} = \frac{1}{N(0)}\frac{A_0}{1 + iA_0\eta/\sqrt{1-\eta^2}} \tag{2.82}$$

where $A_0 = F_0/(1+F_0)$ with $F_0 = N(0)f_0$ dimensionless Landau parameter. In this case (2.81) becomes

$$\begin{aligned} \mathrm{Im}\Sigma_p(\omega) &= \frac{p_{_F}}{(2\pi v_{_F})^3}\int_0^\Lambda \frac{dq}{q}\int \nu d\nu \frac{|t(\eta)|^2}{1-\eta^2}\theta(\omega-\nu)\theta(qv_{_F}-\nu) \\ &= \frac{p_{_F}}{(2\pi v_{_F})^3}\int_0^\omega \nu d\nu \int_{\nu/\omega_c}^1 \frac{d\eta}{\eta}\frac{|t(\eta)|^2}{1-\eta^2} \end{aligned} \tag{2.83}$$

where $\omega_c = \Lambda v_{_F}$ is the energy cutoff. Substituting $t(\eta)$ from (2.82) we get

$$\mathrm{Im}\Sigma_p(\omega) = K\int_0^\omega \nu d\nu \int_{\nu/\omega_c}^1 \frac{d\eta}{\eta}\frac{1}{1+(A_0-1)\eta^2} \approx K\int_0^\omega \nu d\nu \int_{\nu/\omega_c}^1 \frac{d\eta}{\eta} \tag{2.84}$$

where $K = A_0^2/2\pi v_{_F} p_{_F}$. In the last step we have dropped the η^2 term in the denominator. We therefore simply get

$$\mathrm{Im}\Sigma_p(\omega) \sim \int_0^\omega d\nu\nu \ln|\frac{\omega_c}{\nu}| \sim \omega^2(1 + 2\ln|\frac{\omega_c}{\omega}|) \tag{2.85}$$

The leading ω dependence is therefore

$$\mathrm{Im}\Sigma_p(\omega) \sim \omega^2 \ln\omega \tag{2.86}$$

Although this is different from the 3-d case (2.70), it does not change Fermi liquid behavior [43]. Now let us see how our singular interaction will change this result.

2.4.2 Singular Interaction

We now calculate the self energy for the singular interaction we found near inflection points. As in some previous studies of various kinds of singular interaction [43, 42, 40,

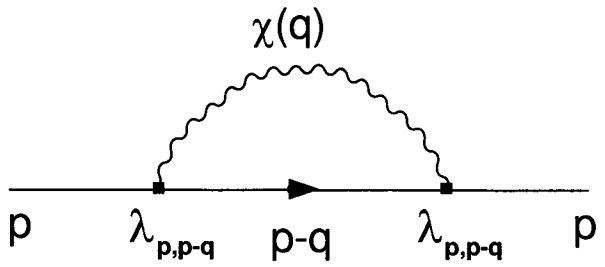

Figure 2.6: Self energy to second order in $\lambda_{p,p-q}$.

75, 76], it is convenient to begin with that part of $\Sigma_{\vec{p}}(\omega)$ which is 2nd-order in the singular interaction. Let us write

$$f_{pp'} = f_{pp'}^{FLT} + \lambda_{pp'} \tag{2.87}$$

where $f_{pp'}^{FLT}$ is the non-singular part of $f_{pp'}$ and $\lambda_{pp'}$ is the singular part. We calculate $\Sigma_{\vec{p}}(\omega)$ to second order in $\lambda_{pp'}$, but to all orders in $f_{pp'}^{FLT}$. Since we are not particularly interested in the angular dependence of the regular Fermi liquid contribution, we will simply let $f_{pp'}^{FLT} \to f_0$, a constant as before. We do our calculation for $\vec{p} = \vec{k}_0$, i.e. at the inflection point. The singular term $\lambda_{pp'}$ therefore is given by (2.66) and (2.68). Since (2.68) is only valid in a region very close to the normal axis, we take $\lambda_{pp'}$ everywere to be

$$\lambda_{pp'} \sim \frac{1}{\sqrt{|Q_{\|}|}} \tag{2.88}$$

We again use (2.74) as our starting point (note that (2.74) is valid for $\omega > 0$, as can be immidiately seen by the form of the occupation numbers. A full version is given in Ref. [56]). In order to calculate to 2nd order in $\lambda_{pp'}$, $|t_{pp'}|^2$ in (2.74) should be replaced by [43]

$$|t_{pp'}(\vec{q},\omega)|^2 \sim \frac{\lambda_{pp'}^2}{|1 + f_0\chi^0(\vec{q},\omega)|^2} \tag{2.89}$$

where $\chi^0(\vec{q},\omega)$ is the generalization of (2.73) for a non-circular Fermi surface. This is equivalent to calculating the diagram presented in Fig. 2.6 [43], where $\chi(\vec{q},\nu)$ is the usual fluctuation propagator

$$\chi(\vec{q},\nu) = \frac{\chi^0(\vec{q},\nu)}{1+f_0\chi^0(\vec{q},\nu)} \tag{2.90}$$

Since we are going to calculate everything near the inflection point, we can assume that $\chi^0(\vec{q},\omega)$ behaves regularly at the inflection point and treat it as a constant. At $T=0$ we have

$$\mathrm{Im}\Sigma_{k_0}(\omega) \sim \sum_{\vec{p}',\vec{q}} \frac{1}{Q_{\|}}\theta(-\epsilon_{\vec{p}'})\theta(\epsilon_{\vec{p}-\vec{q}})\theta(\epsilon_{\vec{p}'+\vec{q}})\delta(\omega+\epsilon_{\vec{p}'}-\epsilon_{\vec{p}-\vec{q}}-\epsilon_{\vec{p}'+\vec{q}}) \tag{2.91}$$

We expand $\epsilon_{\vec{k}}$ near the inflection point $\vec{k}_0$ by

$$\epsilon_{\vec{k}} = v_{k_0}\kappa_{\perp} + g\kappa_{\|}^3 \tag{2.92}$$

where $\vec{\kappa} = \vec{k} - \vec{k}_0$. From now on, for simplisity, we take $v_{k_0} = g = 1$.Thus

$$\begin{aligned}
\epsilon_{\vec{p}'} &= -Q_{\perp} - Q_{\|}^3 \\
\epsilon_{\vec{p}-\vec{q}} &= -q_{\perp} - q_{\|}^3 \\
\epsilon_{\vec{p}'+\vec{q}} &= q_{\perp} - Q_{\perp} + (q_{\|} - Q_{\|})^3
\end{aligned} \tag{2.93}$$

The self energy now becomes

$$\begin{aligned}
\mathrm{Im}\Sigma_{k_0}(\omega) \sim & \int \frac{dQ_{\|}}{Q_{\|}} \int dq_{\|} \int_{-Q_{\|}^3}^{\Lambda} dQ_{\perp} \int_{-\Lambda}^{-q_{\|}^3} dq_{\perp}\theta(\omega - Q_{\perp} - Q_{\|}^3 + q_{\perp} + q_{\|}^3) \\
& \times\delta(\omega - 3Q_{\|}^2 q_{\|} + 3Q_{\|}q_{\|}^2)
\end{aligned} \tag{2.94}$$

Performing the $q_{\perp}$ integral, we get

$$\begin{aligned}
\mathrm{Im}\Sigma_{k_0}(\omega) \sim & \int \frac{dQ_{\|}}{Q_{\|}} \int dq_{\|} \int_{-Q_{\|}^3}^{\Lambda} dQ_{\perp}(\omega - Q_{\perp} - Q_{\|}^3)\theta(\omega - Q_{\perp} - Q_{\|}^3) \\
& \times\delta(\omega - 3Q_{\|}^2 q_{\|} + 3Q_{\|}q_{\|}^2)
\end{aligned} \tag{2.95}$$

Integrating over $Q_\perp$ is also trivial

$$\mathrm{Im}\Sigma_{k_0}(\omega) \sim \frac{1}{2}\omega^2 \int_{-\Lambda}^{\Lambda} \frac{dQ_\parallel}{Q_\parallel} \int_{-\Lambda}^{\Lambda} dq_\parallel \delta(\omega - 3Q_\parallel^2 q_\parallel + 3Q_\parallel q_\parallel^2) \tag{2.96}$$

We now change the variables to $Q_\parallel \to \omega^{1/3}x$ and $q_\parallel \to \omega^{1/3}y$. Integration limits also change to $\pm\Lambda/\omega^{1/3}$. For small ω ($\ll \Lambda^3$, or more precisely $\ll g\Lambda^3$), the integration limits can be replaced by $\pm\infty$. However, one has to make sure that the integral does not diverge as the limits go to infinity. We finally get

$$\mathrm{Im}\Sigma_{k_0}(\omega) \sim \omega^{4/3} \int_{-\infty}^{\infty} \frac{dx}{x} \int_{-\infty}^{\infty} dy \delta(1 - 3x^2 y + 3xy^2) \tag{2.97}$$

The integral is regular at integration limits and also at $x = 0$. Therefore we can confidently write

$$\mathrm{Im}\Sigma_{k_0}(\omega) \sim \omega^{4/3} \tag{2.98}$$

This is clearly different from the Fermi liquid form (2.70) or the 2-d version of it (2.86). This is also different from the result obtianed by Fukuyama and Ogata [72] which they find the power to be (5/3) instead of (4/3) for inflection points. The reason for this descripency is that they miss the singular interaction in their calculation. Notice that if we drop the $1/Q_\parallel$ factor (which comes from the singular interaction) in the integrand of (2.96), we get $\mathrm{Im}\Sigma \sim \omega^{5/3}$ in agreement with Ref. [72].

We can repeat this calculation for a curved Fermi surface using

$$\epsilon_k = \kappa_\perp + \kappa_\parallel^2 \tag{2.99}$$

instead of (2.92). Eq. (2.96) then becomes

$$\begin{aligned} \mathrm{Im}\Sigma_{k_0}(\omega) &\sim \omega^2 \int_{-\Lambda}^{\Lambda} dQ_\parallel \int_{-\Lambda}^{\Lambda} dq_\parallel \delta(\omega + 2Q_\parallel q_\parallel - 2q_\parallel^2) \\ &\sim \omega^2 \int_{-\Lambda}^{\Lambda} \frac{dQ_\parallel}{|Q_\parallel|} \\ &\sim \omega^2 \ln \omega \end{aligned} \tag{2.100}$$

which agrees with (2.86). Although (2.98) is different from (2.100), the difference is not enough to break down Fermi liquid theory (in the sense that $Z \neq 0$ and Fermi surface exists) [72]. On the other hand, higher order calculations can change this result significantly. For example simple estimate indicates that the 4th order calculation gives *marginal* Fermi liquid behavior $\mathrm{Im}\Sigma \sim \omega$. Systematic higher order calculation therefore is necessary to acheive the final conclusion [77].

2.5 Summary

Our calculation of $f_{pp'}$ for a 2-d electron system reveals a 1-d singularity near curved points of the Fermi surface as $\vec{p} \to \vec{p'}$. This is in agreement with previous results and is shown to preserve Fermi liquid behavior [43]. Near inflection points of the Fermi surface, on the other hand, we find a 2-d singularity again with $|\vec{p} - \vec{p'}|^{-1/2}$ behavior. To second order in the singular term, the imaginary part of the self energy shows an $\omega^{4/3}$-dependence in disagreement with the ordinary Fermi liquid result (i.e. $\omega^2 \ln \omega$). This however does not invalidate Fermi liquid theory [72]. Inclusion of Higher order diagrams is necessary for any rigorous conclusion.

We should point out that our result is different from Ref. [72] in a sense that they do not incorporate singular interaction at the inflection points in their calculation of the self energy. They report $\omega^{5/3}$-dependence for the imaginary self energy near an inflection point, different from what we find ($\omega^{4/3}$). Ref. [78] has also investigated the effect of the inflection points. They however consider the scattering between two quasiparticles located on two inflection points opposite to each other with respect to the center of the Brillouin zone. This is clearly different from our calculation. Employing renormalization group technique they find that inflection points would increase the lower critical dimension for instability from Fermi liquid fixed point from d=1 to d=3/2. Thus

2-d systems will still be stable under such an effect.

Chapter 3

Nearly Antiferromagnetic Fermi Liquid Theory

At zero doping, all cuprates are Mott insulators with antiferromagnetically ordered spins. On the other hand, the physical behavior of overdoped samples is well described by Fermi liquid theory. However, the most interesting region in the phase space of high T_c's is none of the above phases, but the intermediate doping regime. One can think about the intermediate doping as a continuation of the metallic phase or the extension of the insulating phase. Depending on which way to choose, one may end up with two different schools of thought based on Fermi liquid or non-Fermi liquid theories. At this time not only no consensus about the older theories of high T_c has been achieved, but also different new theories such as, SO(5) theory [79], theory of stripes [80], and more recently theory of nodal liquids [81], etc. have emerged. In this chapter we shall focus on one of the older theories which is based on the Fermi liquid assumption, and because of its simplicity in calculations, has attracted considerable attention especially among experimentalists.

Nearly antiferromagnetic Fermi liquid theory (NAFL) is a phenomenological theory motivated by nearly ferromagnetic spin fluctuation theory or paramagnon theory, proposed in 1960's to describe metals near their ferromagnetic instability as well as liquid ^{3}He. Both theories are based on the assumption that the excitations of the electronic system are Fermi liquid quasiparticles, interacting among each other via the damped spin waves. Besides the similarities, there are fundamental differences between these two theories which have made NAFL not as widely accepted as paramagnon theory. In this chapter, after a brief review of paramagnon theory, we introduce NAFL emphasising on

the similarities and differences between the two theories.

3.1 Paramagnon Theory

Fermi liquid theory is primarily constructed to describe properties of low energy electron-hole excitations [68]. There also exist other excitations in a Fermi liquid, which are inherently different from electron-hole excitations (although they can be views as collective resonances of them [68]), such as density oscillations and damped spin waves. These excitations are usually known as *plasmons* and *paramagnons* respectively. On the other hand, although thermodynamic and static measurements such as specific heat and spin susceptibility can be expressed in terms of the Fermi liquid parameters, the information contained in Landau parameters is not enough to describe some other measurements, e.g. transport properties and superconductivity (or superfluidity in ^{3}He). In particular, the interaction between the quasiparticles plays important role for these properties. We saw in the last chapter that the effective interaction between quasiparticles can be obtained from the Landau interaction function via Bethe-Salpeter equation (2.36). This is however, not always the easiest route to take. The other way is to assume a model Hamiltonian for interaction between quasiparticles and apply field theory techniques to calculate the physical properties. The reliability of these calculations should then be judged by experiments. One of the theories that follow this path is paramagnon theory which we describe briefly here.

Magnetic susceptibility of a Fermi liquid is given by [60]

$$\chi_M = \frac{\gamma^2 p_F m^*}{4\pi^2(1+Z_0)} \tag{3.101}$$

If the Landau parameter $Z_0 \to -1$, the denominator of (3.101) vanishes and therefore magnetic susceptibility diverges. The system in that case undergoes a phase transition to a ferromagnetically ordered state. When the denominator in (3.101) is not zero but

very small, the magnetic susceptibility is still large and the neighboring spins still have the tendency to align, although the long range order no longer exists. On the other hand, the interaction between the quasiparticles is given by the T-matrix which can be found by Bethe-Salpeter equation (2.36). In particular (2.38) gives

$$t_0^a = Z_0/(1+Z_0) \tag{3.102}$$

which also diverges as $Z_0 \to -1$. Thus strong magnetic susceptibility results in strong interaction between quasiparticles; which tends to align the neighboring spins. The dynamic susceptibility of a Fermi liquid was suggested by Leggett [55] to be

$$\chi(\vec{q},\omega) = \frac{\chi^{(0)}(\vec{q},\omega)}{1+Z_0\chi^{(0)}(\vec{q},\omega)/N(0)} \tag{3.103}$$

where $\chi^{(0)}$ is the susceptibility of the non-interacting electron system (particle-hole bubble). In 3-d isotropic systems, $\chi^{(0)}$ is given by Lindhard function [68].

Eq. (3.103) was proposed by Leggett using deductive reasoning. An attempt to derive it was first made by paramagnon theory [82]. The theory assumes that the (effective) interaction occurs only between quasiparticles with the opposite spins. The model Hamiltonian for this interaction was first proposed by Berk and Schrieffer [83] as

$$H_{\text{int}} = I\int d^3r\; n_\uparrow(\vec{r})n_\downarrow(\vec{r}) = \frac{I}{V}\sum_{\vec{k},\vec{k}',\vec{q}} c^\dagger_{\vec{k}+\vec{q}}c_{\vec{k}}c^\dagger_{\vec{k}'-\vec{q}}c_{\vec{k}'} \tag{3.104}$$

where $c^\dagger_{\vec{k}}$ ($c_{\vec{k}}$) is an operator that creates (annihilates) a quasiparticle with momentum $\vec{k}$ and $I > 0$ is the coupling constant. Performing Eliashberg type calculations, Berk and Schrieffer showed that in nearly ferromagnetic metals, such as Pd, superconductivity is suppressed as a result of ferromagnetically enhenced coupling between the quasiparticles. This model was then adopted by Doniach and Engelsberg [82] and Rice [84] for liquid ^{3}He.

Spin susceptibility can be calculated from (3.104) using Kubo formula [68] and RPA approximation [82]

$$\chi(\vec{q},\omega) = \frac{\chi^{(0)}(\vec{q},\omega)}{1 - I\chi^{(0)}(\vec{q},\omega)} \tag{3.105}$$

Comparing (3.103) and (3.105) we find

$$Z_0 = -N(0)I \tag{3.106}$$

Thus the interaction I is closely related to Fermi liquid interaction function $f_{pp'}$. In low energy and momentum, one can expand (3.105) to get

$$\chi(\vec{q},\omega) = \frac{N(0)}{1 - \bar{I} + (\bar{I}/12)\bar{q}^2 - i(\pi/4)\bar{I}\omega/\bar{q}} \tag{3.107}$$

where $\bar{I} = IN(0)$ and $\bar{q} = q/p_F$. The susceptibility $\chi(\vec{q},\omega)$ in (3.107) is peaked at $q = 0$, reflecting the proximity to ferromagnetism. Near the antiferromagnetic instability, one expects the susceptibility to be peaked near $\vec{q} = (\pm\pi/a, \pm\pi/a, \pm\pi/a)$ where a is the lattice spacing.

$\chi(\vec{q},\omega)$ can be viewed as the propagator of a bosonic field that mediates the interaction between the fermionic quasiparticles. The corresponding bosons are called paramagnons which are critically damped spin waves. Eq. (3.107) can be written as

$$\chi(\vec{q},\omega) = \frac{\chi_0}{1 + \xi^2 q^2 - i\omega/\omega_q} \tag{3.108}$$

where $\chi_0 = SN(0)$ is the enhanced static susceptibility, $\xi = \sqrt{S\bar{I}/12p_F^2}$ is the ferromagnetic correlation length and $\omega_q = 4q/\pi\bar{I}p_F$ is an energy scale that characterizes the damping of the bosonic particles. Here, $S = 1/(1 - \bar{I})$ is the Stoner enhancement factor which measures the proximity to the ferromagnetic instability.

Although paramagnon theory gives the right form for the spin susceptibility, it has some internal inconsistencies [63]. For example if we calculate the density-density correlation, instead of (3.106) we get [68]

$$F_0 = N(0)I \tag{3.109}$$

(3.106) and (3.109) can be satisfied simultaneously only if $F_0 = -Z_0$. This is obviously not always the case. For example for liquid ^{3}He [68], $F_0 = 10$ but $Z_0 = -0.67$. Thus paramagnon theory cannot be the right quantitative theory for the bare quasiparticles in liquid ^{3}He. Even without comparison with experiments the theory has internal inconsistencies. For example RPA approximation does not satisfy Pauli principle [64]. Another problem is the absence of Migdal's theorem in the electron-spin fluctuation interaction, first raised by Hertz *et al.* [85]. Vertex corrections was shown to be of the same order as the bare interaction. This invalidates the Migdals theorem and therefore any Eliashberg type calculation. We will study this point in the context of NAFL theory later. Besides quantitative inconsistency, paramagnon theory gives some qualitatively right results. We will not discuss the applications of paramagnon theory in this thesis. Instead, we proceed to the antiferromagnetic version of the theory which is relevant to high T_c superconductivity. Interested reader should refer to Ref. [63] for more information about paramagnon theory.

3.2 Antiferromagnetic Spin Fluctuations

It is more or less well established that high T_c materials are effectively 2-dimensional electron systems close to the antiferromagnetic instability. As we showed in the last chapter, a two-dimensional electron system with a smoothly curved Fermi surface can be a Fermi liquid (at least in weak interaction regime). On the other hand, NMR experiments [14] and inelastic neutron scattering (INS) [86] indicate enhanced staggered susceptibility, even at optimal doping. One therefore might be tempted to generalize paramagnon theory to antiferromagnetic systems to describe high T_c superconductors. It is well known that for a nested Fermi surface, the RPA susceptibility (3.105) diverges at the wave vector $\vec{q} = \vec{Q} = (\pm\pi/2a, \pm\pi/2a)$ resulting in spin density wave instability [44]. For a general

Fermi surface however, microscopic derivation of the spin susceptibility fails to succeed because the incoherent parts of the quasiparticle spectral function play important role in the calculation of the real part of the particle-hole bubble [87]. The low frequency part of the imaginary part of the particle-hole bubble, on the other hand, is given merely by the coherent parts and can be easily calculated. We will discuss this issue when we talk about vertex corrections later. Based on NMR and NIS results, a phenomenological susceptibility analogous to (3.108) was suggested by Millis, Monien and Pines [23] for high T_c systems

$$\chi(\vec{q},\omega) = \frac{\chi_Q}{1+\xi^2(\vec{q}-\vec{Q})^2 - i\omega/\omega_{sf}} \tag{3.110}$$

where $\chi_Q \gg \chi_0$ is now the static staggered susceptibility, ξ is the antiferromagnetic correlation length and ω_{sf} specifies low frequency relaxation behavior. As in paramagnon theory, quasiparticles are again assumed to interact with each other via the spin fluctuations. The Hamiltonian that describes this interaction was written as [31]

$$\mathcal{H} = \sum_{\vec{p},\sigma} \epsilon_{\vec{p}} \psi^\dagger_{\vec{p}\sigma}\psi_{\vec{p}\sigma} + \frac{\bar{g}}{2} \sum_{\vec{q},\vec{k},\alpha,\beta} \psi^\dagger_{\vec{k}+\vec{q},\alpha}\psi_{\vec{k},\beta}\, \sigma_{\alpha\beta}\cdot\vec{S}(-\vec{q}) \tag{3.111}$$

where $\bar{g}$ is spin-fermion coupling constant and

$$\epsilon_{\vec{p}} = -2t[\cos(p_x a)+\cos(p_y a)] - 4t'\cos(p_x a)\cos(p_y a) - \mu \tag{3.112}$$

is the quasiparticle dispersion relation [35, 88], with $t = 0.25$eV and $t' = -0.45t$. $\vec{S}(\vec{r})$ is the spin fluctuation density operator with a bosonic propagator given by (3.110).

The presence of t' allows "hot spots" [89] on the Fermi surface (Fig. 3.7) which are points that can be connected by $\vec{Q}$; this leads to singular behavior when ξ in (3.110) diverges [49, 89]. Quasiparticles near the hot spots are highly scattered and play important role in NAFL calculations. Full analysis of the scattering rate [89, 90] indicates linear T dependence at the hot spots, while T or T^2 dependence at other points, depending on the temperature and the distance from the hot spots. This is used to explain the linear T

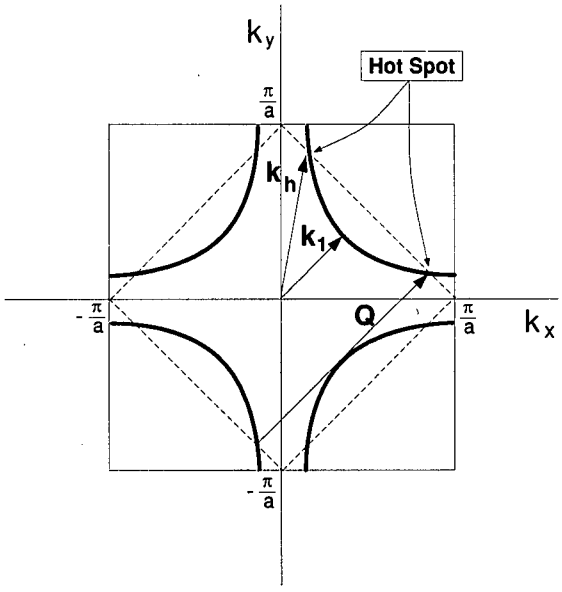

Figure 3.7: Fermi surface in the first Brillouin zone, with the value for t and t' given in the text; and we assume n=0.75. Calculations are presented here for the wave vectors k_1 and k_h.

dependence of the normal state resistivity of cuprates and the crossover between linear T behavior to T^2 behavior [89, 90]. Some other properties of the cuprates such as superconducting T_c [31, 35, 36], Hall conductivity [90], magnetic and scaling properties [91, 92], evolution of Fermi surface [93, 51], Raman scattering [94], etc., have been calculated using NAFL theory. It is not our intention in this thesis to describe these calculations in detail. Instead, we would like to study the self-consistency of the theory. We proceed by briefly discussing how d-wave superconductivity naturally arises from NAFL theory. We then discuss the self-consistency of NAFL and calculations made by this theory.

3.3 d-wave Superconductivity

In NAFL theory, antiferromagnetic spin fluctuations play the same role in the pairing process as phonons do in conventional superconductors. One can therefore apply BCS theory, replacing phonons with magnons. There is however a principle difference here,

that is the effective interaction potential

$$V_{\text{eff}} = g^2\chi(\vec{q}) \tag{3.113}$$

is always positive (repulsive). Here $g = \sqrt{3/4}\bar{g}$ (the factor comes from the consideration of the Pauli matrices). BCS gap equation for this interaction is

$$\Delta_k = -g^2 \int d^2k' \Delta_{k'} \chi(k-k') \frac{\tanh(\epsilon_{k'}/2T)}{2\epsilon_{k'}} \tag{3.114}$$

Since χ is positive, for an s-wave gap Δ_k, both sides of (3.114) appear with different signs and therefore s-wave paring is not possible. However, since $\chi(\vec{q})$ is peaked at $\vec{q} = \vec{Q}$, $d_{x^2-y^2}$ pairing is possible because in that case $\Delta_{k+Q} = -\Delta_k$ and this changes the negative sign in (3.114) to positive. Therefore $d_{x^2-y^2}$ pairing is a natural consequence of NAFL theory. Experimental observation of d-wave pairing is considered as one of the triumphs of NAFL theory.

In order to get high T_c, spin fermion coupling should be strong. At the beginning it was thought that short quasiparticle lifetime due to the strong scattering would reduce T_c dramatically [32]. Weak coupling [31] and also strong coupling (Eliashberg) [35, 36] calculations of Urbana group however, have found a T_c as high as 90K, even including the lifetime effect [36]. Weak coupling calculation in Ref. [31] gives a T_c which is well approximated by

$$T_c = \alpha \left(\frac{\Gamma}{\pi^2}\right) e^{-1/\lambda} \tag{3.115}$$

where $\Gamma \approx 0.04eV$ is an energy scale,

$$\lambda = \eta g^2 \chi_0 N(0) \tag{3.116}$$

is the dimensionless coupling constant, and α and η are dimensionless constants of $O(1)$. Strong coupling calculation of T_c was also done by Monthoux and Pines (MP) [35, 36]

using Eliashberg formalism. For $t' = 0$, a relation similar to (3.115) was again obtained

$$T_c = 0.636 \left(\frac{\Gamma}{\pi^2}\right) e^{-1/0.402N(0)g} \tag{3.117}$$

where

$$N(0) = -\frac{2}{\pi} \sum_{p} \mathrm{Im} G_{R}(\vec{p}, 0) \tag{3.118}$$

is the tunneling density of state calculated from one particle retarded Green's function at T_c [35]. It is interesting that T_c is only sensitive to g and not other parameters. Fitting to the measured value for T_c, one can determine g. For $T_c = 90K$, one gets $g \approx 0.8$ [35].

3.4 Self-Consistency of NAFL

Besides the similarities, there is one fundamental difference between NAFL theory and paramagnon theory: charge properties of ferromagnets are still metallic while antiferromagnets are insulators. The reason behind this difference as pointed out by Anderson [95, 96] is that ferromagnetism is a natural consequence of Hund's rule: exchange interaction favors spins to be parallel in order to keep electrons as far as possible and make the repulsion energy minimum. Antiferromagnetism on the other hand, is a result of superexchange interaction which is inherently a non-perturbative effect and is a property of Mott insulators. Going out of the antiferromagnetically ordered state involves a metal-insulator transition which does not have a counterpart in ferromagnetic case (there is a slight difference between strong coupling and weak coupling here. In weak coupling the Néel ordering and metal-insulator transition - which is not of the Mott type - happen at the same time whereas in strong coupling the system is already an insulator above the Néel temperature). It therefore completely makes sense to talk about a nearly ferromagnetic Fermi liquid but one should be very careful to talk about a nearly antiferromagnetic Fermi liquid. On the other hand, almost none of the properties of high

T_c superconductors resembles of a Fermi liquid, even outside the antiferromagnetically ordered (insulating) region of the phase diagram (except for very high dopings). Thus it is hard to believe that the electron system turns into a Fermi liquid state from a highly non-Fermi liquid insulating state by slightly adding doping.

Another problem, which is more computational than fundamental, is consideration of the vertex corrections (note that in pseudogap problem the strong frequency dependence of the vertex correction may make a difference between having or not having a pseudogap [64]. I that sense vertex correction is a fundamental problem). In order to calculate T_c in strong coupling limit, Eliashberg formalism [68] is commonly used. A necessary condition for the applicability of Eliashberg formalism is Migdal's theorem [46]; which states that the corrections to the bare spin-fermion vertex are negligible compared to the bare vertex. In case of electron-phonon interaction, the vertex corrections are of order of $(\omega_D/E_F) \sim \sqrt{m/M} \ll 1$, where m and M are the masses of electron and nucleus respectively. Spin fluctuations however are different from phonons in three aspects. First, phonons are external excitations while spin fluctuations are excitations of the electronic system itself. Secondly, unlike phonons, spin fluctuations are not propagating modes. Thirdly, the ratio J/E_F, with J being the exchange coupling responsible for antiferromagnetism, is of order of one, so there is no small parameter like (ω_D/E_F) in spin-fluctuation interaction [47].

Early estimates reported small vertex corrections [97]. Calculations of Ref. [48] and [49] on the other hand, indicated that close to the antiferromagnetic instability point, the first vertex correction contains a logarithmically divergent term. However, sum of a series of divergent diagrams results in a power law behavior for the dressed coupling [49, 50]

$$g_{\text{tot}} \sim g(\frac{\xi}{a})^{\beta} \tag{3.119}$$

where β is a small positive number (we should mention that in the original publication

[49], β was reported to be negative but in later publications β was claimed to be positive [50]). Thus near the antiferromagnetic instability ($\xi \to \infty$), $g_{\rm tot}$ become very large. In other words, vertex corrections tend to increase the spin-fermion coupling.

On the other hand, a work by Schrieffer [47] showed that right outside the antiferromagnetically ordered phase, the dressed spin-fermion vertex is given by

$$\frac{\Lambda_{\vec{q}}}{\Lambda_{\circ}} \propto [(\vec{q}-\vec{Q})^2 + \xi^{-2}]^{1/2} \tag{3.120}$$

Thus very close to the antiferromagnetic instability ($\xi \to \infty$), the full vertex vanishes as $\vec{q} \to \vec{Q}$. The vanishing of the dressed vertex is a consequence of Adler principle: in the ordered state, magnons are Goldstone modes and their interaction with other degrees of freedom should vanish at the ordering momentum to preserve the Goldstone modes to all orders in perturbation theory [93]. The above statement means that the vertex corrections should be equal and opposite sign to the bare vertex to make the dressed vertex vanish. Consequently, Migdal's theorem can not exist near the antiferromagnetic instability. However, superconductivity does not happen at very low dopings either. The relevant question therefore is the validity of Migdal's theorem at higher dopings, outside the ordered state where superconducting transition occurs at high temperatures.

The first attempt to calculate vertex corrections at optimal doping was made by us [98]. Using the same parameters as used in NAFL theory, we showed that the first correction to the bare vertex is actually the same order as the bare vertex [98]. The sign of the correction is also controversial because it determines whether vertex corrections increase or suppress the effect of the spin fluctuation coupling. Our finding had a sign opposite to the bare vertex. The effect of the correction is therefore to reduce the spin-fermion coupling, in agreement with Schrieffer's result (3.120). In the next section we describe our calculation in detail. We then discuss the effect of inclusion of the quasiparticle renormalization in our calculation.

To conclude this section we mention one experimental consideration. The susceptibility (3.110) is adopted by NAFL theory only on phenomenological basis and by fitting to experiments. Consequently, NAFL theory is incapable of explaining the incommensurate peaks observed in inelastic neutron scattering (INS) experiments on $La_{2-x}Sr_xCuO_4$ [99] and recently on $YBa_2Cu_3O_{6+x}$ [13]. The peaks are observed in the magnetic response $\chi''(\vec{q},\omega)$ at $\vec{Q}_i = (1\pm\delta,1)\pi$ and $\vec{Q}_i = (1,1\pm\delta)\pi$. It should be pointed out that some other theories such as the theory of stripes have natural explanations for the incommensurate peaks [80, 100].

3.5 Calculation of Vertex Correction

Let us first assume that the quasiparticle residue is $Z \approx 1$. We will discuss the effect of the quasiparticle renormalization later. The first vertex correction is shown in Fig. 3.8 and can be written as

$$\delta\Lambda(3) = \frac{\bar{g}^2}{4}\int \Pi(1-2)\; G(1-3)\; G(3-2) \tag{3.121}$$

where numbers are representing the coordinates and Π is defined by

$$\begin{aligned}\Pi &= \frac{\bar{g}}{2}\sum_{j=1}^{3}\sigma^j\sigma^i\sigma^j < S_1^j S_2^j > = \frac{\bar{g}}{2}\sum_{j=1}^{3}(2\delta^{ij}-\sigma^i\sigma^j)\sigma^j < S_1^j S_2^j > \\ &= \frac{\bar{g}}{2}\sigma^i\left(2 < S_1^i S_2^i > - \sum_{j=1}^{3} < S_1^j S_2^j >\right) = -\Lambda_\circ\;\chi(1-2)\end{aligned} \tag{3.122}$$

where $\Lambda_\circ = (\bar{g}/2)\sigma^i$ is the bare vertex. In the last step we assumed three equivalent modes of spin fluctuation, reflecting the rotational symmetry of the system. In momentum representation the first vertex correction can be calculated for general external momenta. Here we concentrate on the interaction between a Fermi surface electron and a spin fluctuation with $\vec{q} = \vec{Q}$. We have

$$\frac{\delta\Lambda_{\vec{k}}}{\Lambda_\circ} = -\frac{\bar{g}^2}{4}V\sum_{\vec{Q}'}\int\frac{d^2q}{(2\pi)^2}\frac{d\tilde{\omega}}{2\pi}\chi(\vec{Q}'+q,\tilde{\omega})G(\vec{k}+\vec{Q}'+\vec{q},\tilde{\omega})G(\vec{k}+\vec{Q}''+\vec{q},\tilde{\omega}) \tag{3.123}$$

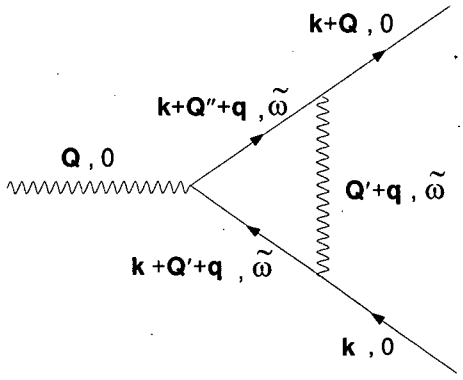

Figure 3.8: First correction $\delta\Lambda_{\vec{k}}$ to the bare vertex, for an incoming fermion with momentum $\vec{k}$ and energy 0 (relative to the Fermi energy), interacting with a fluctuation of wave-vector $\vec{Q}$ and zero energy.

where $\delta\Lambda_{\vec{k}} = \delta\Lambda(\vec{k}, \epsilon = 0; \vec{q} = \vec{Q}, \Omega = 0)$ and $\vec{Q}'' = \vec{Q} + \vec{Q}'$; the sum over $\vec{Q}'$ takes care of Umklapp processes. In the reduced Brillouin zone $\vec{Q}'' = (0, 0)$. Note that the overall sign of the graph in Fig. 3.8 is *negative*, i.e., Eq. (3.123) is negative.

We concentrate on $\delta\Lambda_{\vec{k}}$, with $\vec{k}$ being a point on the Fermi surface, since it gives an indication of the size of vertex corrections. This is because in general $|\delta\Lambda(\vec{k}, \epsilon; q, \Omega)|$ exceeds $|\delta\Lambda_{\vec{k}}|$ (in fact it diverges along a surface in k-space, for given values of $\vec{q}, \Omega$ and ϵ); thus one cannot argue, even after integrating over one or more of its arguments, that $|\delta\Lambda(\vec{k}, \epsilon; \vec{q}, \Omega)|$ will lead to corrections smaller than one would get from just using $\delta\Lambda_{\vec{k}}$ (our argument here parallels Migdal's [46]). More generally one finds that if $\Omega \ll \mathrm{q}v_{\mathrm{F}}, \Delta$, where Δ is the spin gap, then $\delta\Lambda_{\vec{k}}$ is a good approximation to $\delta\Lambda(\vec{k}, \epsilon; \vec{q}, \Omega)$. Writing (3.123) as

$$\frac{\delta\Lambda_{\vec{k}}}{\Lambda_{\circ}} = -\frac{\bar{g}^2}{4} V \sum_{\vec{Q}'} \int \frac{d^2q}{(2\pi)^2} \frac{d\omega}{\pi} \frac{\chi''(\vec{Q}' + \vec{q}, \omega)}{\epsilon_{\vec{k}+\vec{Q}'+\vec{q}} - \epsilon_{\vec{k}+\vec{Q}''+\vec{q}}}$$

$$\times \left(\frac{f_{\vec{k}+\vec{Q}'+\vec{q}}}{\epsilon_{\vec{k}+\vec{Q}'+\vec{q}} - \omega} + \frac{1 - f_{\vec{k}+\vec{Q}'+\vec{q}}}{\epsilon_{\vec{k}+\vec{Q}'+\vec{q}} + \omega} - \frac{f_{\vec{k}+\vec{Q}''+\vec{q}}}{\epsilon_{\vec{k}+\vec{Q}''+\vec{q}} - \omega} - \frac{1 - f_{\vec{k}+\vec{Q}'+\vec{q}}}{\epsilon_{\vec{k}+\vec{Q}'+\vec{q}} + \omega} \right)$$

$$= -g^2 \frac{\chi_Q}{12\pi^3 \omega_{sf}} (\frac{\omega_{sf}}{\mu})^2 \mathcal{I}_{\vec{k}} \tag{3.124}$$

where $g^2 = \frac{3}{4}\bar{g}^2$ and $\mathcal{I}_{\vec{k}}$ is dimensionless; we define g to correspond directly with the coupling constant g used in Monthoux and Pines [35, 36]. At zero temperature one has

$$\mathcal{I}_{\vec{k}} = \int_{-2\pi}^{2\pi} d\bar{q}_x \int_{-2\pi}^{2\pi} d\bar{q}_y \frac{1}{\bar{\epsilon}_1 - \bar{\epsilon}_2} [\mathrm{Sgn}(\bar{\epsilon}_1) G_1(\vec{\bar{q}}, \bar{\epsilon}_1) - \mathrm{Sgn}(\bar{\epsilon}_2) G_1(\vec{\bar{q}}, \bar{\epsilon}_2) - G_2(\vec{\bar{q}}, \bar{\epsilon}_1) + G_2(\vec{\bar{q}}, \bar{\epsilon}_2)] \tag{3.125}$$

where $\bar{q}_x = q_x a$, etc., $\bar{\epsilon}_1$ and $\bar{\epsilon}_2$ are

$$\bar{\epsilon}_1 = \frac{\epsilon_{\vec{k}+\vec{Q}'+\vec{q}}}{\mu} \quad , \quad \bar{\epsilon}_2 = \frac{\epsilon_{\vec{k}+Q''+\vec{q}}}{\mu} = \frac{\epsilon_{\vec{k}+\vec{q}}}{\mu} \tag{3.126}$$

and G_1 and G_2 are defined by

$$G_1(\vec{q}, \bar{\epsilon}) = \frac{\pi X}{2(\bar{\epsilon}^2 + X^2)} \quad , \quad G_2(\vec{q}, \bar{\epsilon}) = \frac{\bar{\epsilon} \ln(X/|\bar{\epsilon}|)}{\bar{\epsilon}^2 + X^2} \tag{3.127}$$

with $X = [1 + (\frac{\xi}{a})^2(\bar{q}_x^2 + \bar{q}_y^2)](\omega_{sf}/|\mu|)$.

$\mathcal{I}_{\vec{k}}$ can be investigated both analytically and numerically. Here we calculate it for two different points in k-space, both on the Fermi surface (see Fig. 3.7); $\vec{k}_1$ makes a 45^o angle with k_x, and $\vec{k}_h$ is a "hot spot" wave vector.

In order to obtain a value for $\delta\Lambda_{\vec{k}}$, we need values for the spin fluctuation energy ω_{sf}, the correlation length ξ, the susceptibility χ_Q, the coupling constant g, and the chemical potential μ (which is determined by the electron filling factor n). There are different values reported in the references [23, 31, 32]. We have evaluated $\delta\Lambda_{\vec{k}}$ for $\vec{k} = \vec{k}_1, \vec{k}_h$, in two ways, viz. (a) by assuming various published values for the different parameters, and (b) by making the simple assumption that one is very close to an AFM instability, and then, in the spirit of RPA, imposing the condition $|(\bar{g}/2)\chi^{(0)}(\vec{Q}, 0)| \approx 1$ where $\chi^{(0)}(\vec{q}, \omega)$ is the electron-hole bubble. Numerical calculation gives $|\chi^{(0)}(\vec{Q}, 0)| = 2.6(\mathrm{eV})^{-1}$ and thereby

	g (eV)	ω_{sf} (meV)	$\mathcal{I}_{\vec{k}_1}$	$\delta\Lambda_{\vec{k}_1}/\Lambda_\circ$	$\mathcal{I}_{\vec{k}_h}$	$\delta\Lambda_{\vec{k}_h}/\Lambda_\circ$
MPI	1.36	7.7	78.6	-1.81	105.6	-2.43
MPII	0.64	14	49.6	-0.46	73.4	-0.68
"RPA"	0.67	7.7	78.6	-0.44	105.6	-0.59
		14	49.6	-0.50	73.4	-0.74

Table 3.1: Calculated values of the vertex correction $\delta\Lambda_{\vec{k}}$ for two different wave-vectors $\vec{k}_1$ and $\vec{k}_h$ on the Fermi surface (columns 4 and 6 in the table). Ref. [35] and [36] give different values for g, and different values for ω_{sf}. From the values for these two models one calculates $\mathcal{I}_{\vec{k}}$ in equation (3.125), and thence $\delta\Lambda_{\vec{k}}/\Lambda_\circ$. The third model is the naive "RPA" model described in the text, for which g is determined; we have calculated $\mathcal{I}_{\vec{k}}$ and $\delta\Lambda_{\vec{k}}/\Lambda_\circ$ for two values of ω_{sf} given in MPI and MPII respectively.

$g = 0.67$ eV, assuming n=0.75 and the band structure in (3.112). Since $\omega_{sf}/|\mu| \ll 1$, this value of g should be a very good guess, within a naive RPA scheme.

The results are summarized in Table 3.1. We use two different values for ω_{sf} ; these are the two different values quoted by Monthoux and Pines *et al.* [35, 36]. We also use two different values for the coupling constant g, quoted from Ref. [35] and [36]. We use values of $\xi = 2.5a$, $\chi_Q = 80$ states/eV (from [35, 36]) and $n = 0.75$, appropriate to $YBa_2Cu_3O_7$ (again quoted from [35, 36]). This value of n corresponds, with the band structure in (3.111), to a value of $|\mu| \sim 1.46t \equiv 0.365$ eV.

We see that even the values for the vertex correction calculated from the simple RPA model (b) are not small; as in the standard discussion of Migdal's theorem, the importance of vertex corrections appears in the ratio $|\delta\Lambda_{\vec{k}}|/\Lambda_\circ$. If one takes values of g from the literature [35, 36], this ratio is quite unreasonably large (as large as 2.43 for the hot spots in the model used by Ref. [35]). Thus vertex corrections are clearly very important. The values we quote for $|\delta\Lambda_{\vec{k}}|/\Lambda_\circ$ are considerably larger than previous estimates [23, 97, 101]. The reason for this difference with previous work can be tracked back to the factor $\mathcal{I}_{\vec{k}}$, which is impossible to guess from purely dimensional arguments.

In fact if we drop the factor $\mathcal{I}_{\vec{k}}$ from $\delta\Lambda_{\vec{k}}$, we get an order of magnitude estimate for $\delta\Lambda_{\vec{k}}$ given by

$$\frac{|\delta\Lambda_{\vec{k}}|}{\Lambda_\circ} \sim O[g^2 \frac{\chi_Q}{4\pi^3|\mu|} \frac{\omega_{sf}}{|\mu|}] \ll 1 \tag{3.128}$$

which is broadly in agreement with previous estimates (see e.g. Millis [97]) ; χ_Q, ω_{sf} and g must be redefined to conform with the parametrizations in this paper).

In fact however $\mathcal{I}_{\vec{k}}$ is surprisingly large, and also shows a significant variation around the Fermi surface, with a maximum at the hot spots, and a minimum at intermediate wave-vector like $\vec{k}_1$. We should emphasize here that analytic calculations of $\delta\Lambda_{\vec{k}}$ have to be approximated rather carefully in order to give reasonable agreement with the numerical results in Table 3.1. Approximations such as those of Hertz *et al.* [85] (see also [101]), which try to separate off a rapidly-varying (in $\vec{q}$-space) contribution from $\chi''(\vec{q},\omega)$, give quantitatively incorrect results (including a completely unphysical $\ln[(\vec{k}-\vec{k}_h)a]$ divergence as one approaches the hot spot).

One might suppose that $\mathcal{I}_{\vec{k}}$ is large simply because of the band structure (i.e., because of van Hove singularities, or the hot spots). If this were true one could argue that the quasiparticle weight ought to be renormalized down near these singular points in the Brillouin zone, and that this would considerably reduce the vertex correction. In fact however we find this is not the case; this can be checked analytically by suppressing the regions immediately around the hot spots in the integral for $\mathcal{I}_{\vec{k}}$, or by simply redoing the numerical calculation for a slightly different band structure. We find that suppressing the hot spots entirely, reduces the vertex correction by a factor which is everywhere less than 2 (and which differs very little from unity when $\vec{k}$ is far from a hot spot).

3.5.1 The Effect of Quasiparticle Renormalization Z

Our calculation of the vertex correction was criticized by Chubukov, Monthoux and Morr (CMM) [50] on the basis of inappropriate quasiparticle renormalization factor Z. As we mentioned earlier the value we used was $Z \approx 1$ which is the value used in NAFL calculations of T_c [31, 35, 36]. CMM's criticism was based on the fact that self consistent consideration of spin fluctuation damping gives spin fluctuation frequency ω_{sf} in terms of other parameters. More precisely, one can write [93] $\omega_{sf} = c_{sw}^2/2\xi^2\gamma$, where c_{sw} is the spin wave velocity, ξ is the correlation rate and γ is the spin damping rate. In fact two points of views can be taken here. One can assume the spin environment as independent degrees of freedom. In that case ω_{sf} will be an independent parameter. On the other hand if one considers a one band model then assuming that the damping of the spin excitations is dominantly due to the spin-fermion interaction (and not other sources such as spin-spin exchange, impurity, etc.), the damping rate γ can be obtained from the imaginary part of the particle-hole bubble at transfer momentum $\vec{Q}$. The result of the calculation given in [50] is

$$\omega_{sf} = \frac{\pi}{4}|\sin\phi_0|\frac{v^2}{g^2Z^2\chi_Q} \tag{3.129}$$

where v is the Fermi velocity at the hot spots and ϕ_0 is the angle between normals to the Fermi surface at the hot spots. CMM claim that if one uses the parameters reported in [36] and at the same time requires $Z = 1$, one finds $\omega_{sf} \approx 1.06meV$ which is one order of magnitude smaller than $\omega_{sf} = 14meV$ used in Ref. [36] and our calculations. CMM then conclude that this is a sign of inconsistency in our calculations. Using the same parameters and solving (3.129) for Z, with $\omega_{sf} = 14meV$ one finds $Z = 0.28$. Substituting this value of Z in the calculations, the vertex correction will be reduced by a factor of $Z^2 = 0.08$. This way the magnitude of the correction will be one order of magnitude smaller than what we obtained, and therefore the vertex corrections will be

small.

We do not dispute the fact that all the calculations should be self-consistent. What we argue actually is that the self-consistency should be considered everywhere throughout the calculation. We also agree that the Hamiltonian (3.111) is valid for renormalized quasiparticles and therefore it is necessary to include the renormalization factor Z in all calculations. All the parameters we used in our calculation (including Z) were based on the reported values by Monthoux and Pines [35, 36]. We emphasize again that the coupling constant g in Ref. [35, 36] is obtained by fitting the calculated T_c to the measured value ($\approx$ 90K). If Z, as claimed in Ref. [50] is much smaller than one, then this value should be also considered in T_c calculations and would affect the magnitude of g which gives a reasonable T_c.

In a strong coupling calculation, this means that all the fermionic lines have to be replaced by renormalized Green's functions. This multiplies the coupling constant g by a factor Z which exactly compensates the reduction of the vertex correction discussed in [50]. This is more clear by looking at (3.118). One realizes that a renormalized G_R is going to reduce $N(0)$ by a factor of Z. This factor multiplies g in the exponent in (3.117). Keeping all the other parameters fixed the coupling constant should be increased to preserve the value of T_c. The new coupling constant is now given by

$$g_z = \frac{g}{Z} \tag{3.130}$$

where g is the (old) coupling obtained using $Z = 1$ (i.e. the values reported in Ref. [35] and [36]). The same statement holds for weak coupling calculation (3.115) keeping in mind that $\lambda \propto g^2 N(0)^2$. Substituting Z and g_z into the calculation of the vertex correction we get

$$\left(\frac{|\delta\Lambda_{\vec{k}}|}{\Lambda_\circ}\right)_{Z=1} \propto g^2 \quad \longrightarrow \quad \left(\frac{|\delta\Lambda_{\vec{k}}|}{\Lambda_\circ}\right)_{Z} \propto Z^2 g_z = Z^2 \frac{g^2}{Z^2} = g^2 \tag{3.131}$$

The factor $1/Z$ in (3.130) therefore exactly cancels the effect of Z^2 in vertex correction calculations and our calculated value remains unchanged. Looking back at (3.129) but now remembering that gZ is actually what one obtains from fitting to T_c, we find $\omega_{sf} = 1.06meV$ even after the inclusion of the renormalization factor Z. The mismatch of this value with the reported value of Ref. [36] reflects the inconsistency of the theory rather than a mistake in our calculations.

3.5.2 Sign of the Vertex Corrections

The sign of the vertex correction is important because if it is positive, the vertex corrections tend to increase the effect of the spin fluctuations on the electron system resulting in a higher T_c. On the other hand if it is negative, it decreases the spin-fermion coupling and reduces the T_c. We saw that at the optimal doping, our calculation indicates a negative sign for the first vertex correction. On the other hand, Ref. [93, 50] report a positive sign at the optimal doping but negative sign near the antiferromagnetic instability. In this section we discuss what a change in the sign of the vertex correction between strong and weak doping would entail physically - essentially it implies a phase transition of some sort for which there is no experimental evidence that we know of. We give our argument based on a fact with which everyone agrees: near the antiferromagnetic instability the sign of the vertex correction has to be negative to suppress the effect of spin-fermion coupling [47].

If the sign of the vertex corrections at the optimal doping is negative, as we found, then the vertex corrections tend to decrease the dressed coupling. Decreasing doping, increases the effect of spin fluctuations and therefore increases the magnitude of the vertex corrections. This can be checked by Eq. (3.124). Decreasing doping would increase χ_Q ($\propto \xi^2$) and thereby the vertex correction. Consequently, the dressed coupling would be decreased even further. This trend continues until the total vertex vanishes completely

at the edge of the ordered phase. Thus the flow of the renormalized coupling when changing the doping is continuous. On the other hand if the vertex corrections have positive sign at the optimal doping, decreasing the doping would increase the dressed vertex. Continuation of this trend towards zero doping would give a very large dressed coupling which is unphysical.

Interestingly it was speculated by Chubukov et al [51, 93] that perhaps a weak phase transition (a Lifshitz transition) might exist in the intermediate doping regime. The transition would change the big Fermi surface, compatible with Luttinger's theorem, to small hole pockets centered at $(\pi/2a, \pi/2a)$ and symmetry related points. If this were really true, and moreover followed from the Hubbard model, it might save the consistency of the NAFL approach, in that it would make it possible for a sign change of the vertex corrections, at some critical $g = g_c$. To our knowledge, no experimental justification exists yet [52] and the evolution of the Fermi surface is not widely believed. Without this evolution, the positive sign of the vertex correction at optimal doping is not physical. At the end we point out that the suppression of the spin-fermion coupling due to the vertex corrections, also gives a natural way to explain why T_c reduces at low dopings in spite of the increase in the spin susceptibility [93] (although other reasons can also be thought of, e.g. reduction of charged carriers, etc.).

3.6 Concluding Remarks

We re-emphasize here that these results do not necessarily invalidate the internal consistency of the Fermi liquid starting point, in NAFL theory. However they do show that the theory cannot be trusted quantitatively, at least in the usual RPA form. As is well known the RPA is not a "conserving approximation", and for spin fluctuation theories this makes it unreliable (cf. ref.[63], especially section 3). It is useful to compare the

case of nearly ferromagnetic ^{3}He liquid, where vertex corrections are also quite large, and where use of the paramagnon model yields values for m^*/m which are off by a large factor [102]. Thus if we use melting curve Landau parameters, $Z_0 \sim 0.75$ and $F_1 \sim 15$, we infer a value for the Stoner factor $S \sim 24$ which yields $m^*/m = \frac{9}{2} \ln S \sim 15$, in the paramagnon model. This is roughly 2.5 times the correct value of ~ 6 (note that the first vertex correction is $\delta\Lambda/\bar{I} \sim \ln S \sim 3$ in this model), and no amount of self-consistent summing of diagrams can cure this numerical problem.

Similar problems can clearly occur in the present NAFL model. We believe this is the main reason for the difficulty one encounters in the MP models, in determining a value for g that (a) gives the correct superconducting T_c, and (b) is consistent with the observed spin susceptibility.

To check the structure at higher order, we have also estimated the contributions from the graphs containing 2 spin fluctuation lines (there are actually 7 distinct graphs at this level), and found that some of them are also large for the values of g used above. Thus, just as for the case of nearly ferromagnetic ^{3}He, we see no reason to believe, *for the values of the parameters given in the table*, that performing infinite graphical sums will lead to results which are numerically more reliable, even if they do converge to some smaller renormalized vertex-there will always be other diagrams with large values, which will in general give uncontrolled contributions.

It is interesting to compare our results with some other investigations. As we mentioned briefly, in the weak-coupling limit, Chubukov [49, 93] has calculated the leading vertex corrections to g, concentrating on the gapless case; in the case where there is a gap, he finds that the renormalized coupling is large (for a large Fermi surface considered in our investigation). On the other hand Schrieffer [47] has argued that a correct formulation of the theory, even in the weak-coupling limit, must take account of the short-range local antiferromagnetic order even in the normal state-if this done, he finds

that a weak-coupling calculation shows very strong *suppression* of the vertex when one is close to the antiferromagnetic transition. This theory seems rather interesting-note that a related calculation by Vilk and Tremblay [64, 103]finds that the existence of such a short-range antiferromagnetic order in 2-d will cause a breakdown of the Fermi-liquid starting point itself when the correlation length becomes larger than the single particle de Broglie wavelength! Thus the question of what is the correct theory itself is rather confused, even in the weak-coupling regime. It is certainly not clear how any of these arguments will work in the regime discussed in this paper, when g is not small enough to control the magnitude of the vertex corrections.

It is of course crucial that these higher-order corrections also be included in any version of this theory that tries to reconcile different experiments - as emphasized by Pines [32], the justification of the theory stands or falls on its ability to do this *quantitatively.* It is possible that such a program might succeed if one can show that the actual parameters g, ω_{sf}, and χ_Q are such that $|\delta\Lambda_{\vec{k}}|/\Lambda_\circ$ is considerably less than one (i.e., if one is genuinely in the weak-coupling regime). This would also be true of versions of the theory in which ω_{sf} depends on g, whilst the spin gap becomes an independent parameter [49]; or of the theory of Schrieffer cited above [47]. On the other hand if $|\delta\Lambda_{\vec{k}}|/\Lambda_\circ > O(1)$, we see no hope that such a scheme could succeed quantitatively (in, e.g., the calculation of T_c), since the vertex corrections become large.

Part II

Vortices in d-wave Superconductors

Chapter 4

Introduction

Although at a microscopic level, theories of high T_c superconductors, especially for normal state properties, are not well established, superconducting properties of cuprates are better understood. Almost everybody now agrees that the symmetry of the order parameter is $d_{x^2-y^2}$-wave, and the existence of nodes in the superconducting gap is well established [33, 34]. A highly anisotropic $d_{x^2-y^2}$-wave order parameter, with four nodes in the superconducting gap is a unique property of cuprates ans also some organic superconductors, with no analog in conventional superconductors. The effect of this anomalous symmetry on different observable quantities has been a subject of investigation in recent years.

An early theoretical investigation of the weak-field response of a $d_{x^2-y^2}$ superconductor by Yip and Sauls [104] predicted a direction dependent non-linear Meissner effect, associated with the quasiclassical shift of the excitation spectrum due to the superflow created by the screening currents. Maeda *et al.* [105] reported experimental evidence for such an effect in $Bi_2Sr_2CaCu_2O_y$, but subsequent experiments [106] failed to confirm their findings and the situation remains controversial. A similar effect was also studied independently by Volovik [107]. In the mixed state, he predicted a contribution to the residual density of states (DOS) proportional to the inter-vortex distance $\sim \sqrt{H}$. Such a contribution was identified in the specific heat measurements on $YBa_2Cu_3O_{7-\delta}$ (YBCO) by Moler *et al.*[108] but later this interpretation was disputed by Ramirez [109] who found evidence for a similar effect in a conventional superconductor V_3Si and by others[110].

Kosztin and Leggett [111] predicted that the nonlocal response at very low temperatures will lead to a T^2 dependence of the penetration depth in clean samples in contrast to the linear T-dependence obtained from the local theory for d-wave materials.

Another important characteristic of high T_c compounds is their short coherence length ξ_0; responsible for strong fluctuation effects near T_c [112]. The large ratio $\kappa = \lambda_0/\xi_0 \gg 1$ (λ_0 is the magnetic penetration depth) also makes them extremely type-II superconductors. Existence of a mixed state, characterized by a regular array of magnetic flux lines penetrating the material, is perhaps one of the most striking properties of type-II superconductors. The original pioneering work of Abrikosov [113], based on the solution of Ginsburg-Landau (GL) equations [114] near the upper critical field H_{c2}, predicted a triangular flux lattice. This prediction was subsequently verified by low field magnetic decoration experiments on a variety of conventional superconductors. In stronger fields neutron scattering experiments revealed significant deviations from perfect triangular lattices [115] which where attributed to anisotropies in the electronic band structure and other effects. These were modeled by GL theories containing additional higher order derivative terms reflecting the material anisotropies [115].

Based on the experience with conventional superconductors one would expect even richer behavior of flux lattices in the copper-oxide superconductors. In high-T_c cuprates much of the experimental and theoretical effort has been focused on the sizable region of the phase diagram just below $T_c(H)$ in which the vortex lattice properties are completely dominated by thermal fluctuations [116]. While understanding the physics of this fluctuation dominated regime poses a very difficult statistical mechanics problem, investigation of the equilibrium vortex lattice structures at low temperatures may provide clues about the microscopic mechanism in these materials.

Neutron scattering [117] and STM [118] experiments on $YBa_2Cu_3O_{7-\delta}$ compound, revealed vortex lattices with centered rectangular symmetry and different orientations

with respect to the ionic lattice. These have been modeled by phenomenological GL theories appropriate for anisotropic superconductors, containing additional quartic derivative terms [119] or a mixed gradient coupling to an order parameter with different symmetry [120, 121, 122, 123]. These works found structures in qualitative agreement with experiment, but their inherent shortcoming is a large number of unknown phenomenological parameters and subsequent lack of predictive power. Also, the GL theory is only solvable for a vortex lattice near H_{c2}, which is experimentally inaccessible in cuprates away from T_c. The observed behavior of the vortex lattice may also be understood by incorporating penetration depth anisotropy and twin-boundary pinning without involving any effects associated with mixing symmetries or gap anisotropy [124].

Muon-spin-rotation (μSR) experiments [125, 126, 127, 128], on the other hand, show an unusual magnetic field dependence in their line-shapes for the magnetic field distribution. This has been attributed to a field dependent penetration depth - which is expected in the Meissner state because of quasiparticle accumulation at gap nodes [104]. It was also modeled using an approach based on the Bogoliubov- de Gennes (BdG) equations in a square lattice tight-binding model [129].

At intermediate fields $H_{c1} < H \ll H_{c2}$, properties of the flux lattice are determined primarily by the superfluid response of the condensate, i.e. by the relation between the supercurrent $\vec{j}$ and the superfluid velocity $\vec{v}_s$. In conventional isotropic strongly type-II superconductors this relation is to a good approximation that of simple proportionality,

$$\vec{j} = -e\rho_s\vec{v}_s, \tag{4.132}$$

where ρ_s is a superfluid density. More generally, however, this relation can be both *nonlocal* and *nonlinear*. The concept of nonlocal response dates back to the ideas of Pippard [130] and is related to the fact that the current response must be averaged over the finite size of the Cooper pair given by the coherence length ξ_0. In strongly type-II

materials the magnetic field varies on a length scale given by the London penetration depth λ_0, which is much larger than ξ_0 and therefore nonlocality is typically unimportant unless there exist strong anisotropies in the electronic band structure [131]. Nonlinear corrections arise from the change of quasiparticle population due to superflow which, to leading order, modifies the excitation spectrum by a quasiclassical shift [130]

$$\mathcal{E}_k = E_k + \vec{v}_f \cdot \vec{v}_s, \tag{4.133}$$

where $E_k = \sqrt{\epsilon_k^2 + \Delta_k^2}$ is the BCS energy. Again, in clean, fully gapped conventional superconductors this effect is typically negligible except when the current approaches the pair breaking value. In the mixed state this happens only in the close vicinity of the vortex cores which occupy a small fraction of the total sample volume at fields well below H_{c2}. The situation changes dramatically when the order parameter has nodes, such as in $d_{x^2-y^2}$ superconductors. Nonlocal corrections to (4.132) become important for the response of electrons with momenta on the Fermi surface close to the gap nodes even for strongly type-II materials. This can be understood by realizing that the coherence length, being inversely proportional to the gap [130], becomes very large close to the node and formally diverges at the nodal point. Thus, quite generally, there exists a locus of points on the Fermi surface where $\xi \gg \lambda_0$ and the response becomes highly nonlocal. This effect was first discussed by Kosztin and Leggett [111] for the Meissner state and by us [132] in the mixed state. Similarly, the nonlinear corrections become important in a d-wave superconductor. Eq. (4.133) indicates that finite areas of gapless excitations appear near the node for arbitrarily small v_s.

One of the simplest theories to study the magnetic behavior of the type-II superconductors is the London model [133]. In London theory the Free energy is written only in terms of magnetic field and is therefore very easy for calculation. Unlike in GL theory, the order parameter does not appear explicitly in London free energy. The effect of the

symmetry of the order parameter or other Fermi surface anisotropies, is therefore not contained in the London model. Simple generalization of the model however can incorporate these effects. The generalized model contains anisotropic higher order and higher derivative terms reflecting the symmetries of the order parameter and the anisotropic Fermi surface.

In the next chapter, we first briefly introduce Ginsburg-Landau (GL) theory, and London theory emphasizing the solutions for a vortex lattice. Starting from a GL model, we then derive the leading fourfold anisotropic corrections to the London equation making the usual assumption that the free energy was an analytic functional of the order parameter and field. The number of new parameters in this model is far smaller than in the GL approach (a reasonable model contains only one new parameter which controls the strength of the symmetry breaking term) and numerical simulations are considerably easier. This provides a useful tool to study vortex lattice structure, pinning by twin boundaries and the magnetic field distribution measured in μSR experiments. The model is suitable to study the intermediate field region $H_{c1} \ll H \ll H_{c2}$ which is experimentally most relevant but traditionally difficult to handle within the GL theory. Furthermore, this approach can be extended to $T = 0$ where GL theory breaks down and the supercurrent becomes singular. With increasing magnetic field this model predicts a transition from triangular to centered rectangular and eventually a square vortex lattice. While no direct experimental evidence exists in cuprates at present to confirm such a prediction, a similar transition has been recently observed in a boro-carbide material $ErNi_2B_2C$ [134] and has been described by a similar London model [131].

In the last chapter of this thesis, we again derive a generalized London free energy, but this time completely from a weak coupling microscopic model, including the nonlinear and nonlocal effects mentioned above. We show that the dominant effect that determines the vortex lattice geometry and the effective penetration depth as defined in μSR experiments

is the nonlocal corrections, while the nonlinear corrections play a secondary role at low T. At high temperatures we obtain a nonlocal correction similar to the one suggested in chapter 5. At low temperatures however, we find a novel singular behavior directly related to the nodal structure of the gap which completely changes the form of the London equation. This singular behavior has profound implications for the structure of the vortex lattice which, as a function of decreasing temperature, undergoes a series of sharp structural transitions and attains a universal limit at $T = 0$. Our theory is now completely *parameter free.* The London free energy at low T is non-analytic and its long wavelength part is fully determined by the nodal structure of the gap function. Such behavior is caused by the low-lying quasiparticle excitations within the nodes and thus could never occur in conventional superconductors with anisotropic band structures.

Finally, in the last section of chapter 6, we talk about the experimental justification of our low temperature nonlinear nonlocal theory. We especially emphasize μSR experiments. Recent μSR data at high fields have justified our prediction for the Field dependence of the penetration depth in vortex state.

Chapter 5

Phenomenological Model

5.1 Ginsburg-Landau Theory

In 1950 Ginsburg and Landau [114] proposed a phenomenological theory to describe the behavior of superconductors near their transition temperature. At a mean field level, the phase transition of superconductors is second order (gauge field fluctuations however are believed to change the order of the transition to a weak first order [135]). A free energy density that can describe such a transition was proposed to be

$$f = \frac{1}{2m^*}|(-i\hbar\nabla - \frac{e^*}{c}\vec{A})\Psi|^2 + \alpha|\Psi|^2 + \frac{\beta}{2}|\Psi|^4 + \frac{H^2}{8\pi} \tag{5.134}$$

where e^* $(= 2e)$ and m^* $(= 2m)$ are the charge and effective mass of a Cooper pair, $\vec{H}$ and $\vec{A}$ are magnetic field and vector potential respectively. Superfluid density n_s is related to the order parameter by $|\Psi|^2 = n_s/n$, where n is the total density of electrons. Ginsburg-Landau (GL) equations can be obtained by minimizing f with respect to Ψ and $\vec{A}$

$$\alpha\Psi + \beta|\Psi|^2\Psi + \frac{1}{2m}|(-i\hbar\nabla - \frac{e^*}{c}\vec{A})^2\Psi = 0 \tag{5.135}$$

$$\vec{j} = \frac{c}{4\pi}\nabla \times \vec{B} = \frac{e^*\hbar}{2im^*}(\Psi^*\nabla\Psi - \Psi\nabla\Psi^*) - \frac{e^{*2}}{m^*c}\Psi^*\Psi\vec{A} \tag{5.136}$$

where $\vec{j}$ is the current density. In the absence of magnetic field (i.e. $\vec{H} = \vec{A} = 0$) and for uniform Ψ, the minimum of f occurs at $|\Psi| = 0$ when $\alpha > 0$, but at $|\Psi| = \sqrt{-\alpha/\beta}$ when $\alpha < 0$. A continuous transition therefore happens as α goes from positive to negative values. Taking $\alpha \propto (T - T_c)$, one can study the critical behavior of the superconductor

and calculate all the critical exponents near T_c. GL theory has been studied extensively in the literature in both Meissner and vortex states of superconductors. It is not our attempt in this thesis to discuss the solutions of GL equations for different problems. Instead, we shall focus on deriving a London theory from GL theory, especially in the vortex state. Interested readers should refer to Ref. [136, 130] or any other standard text books in the subject, for more detailed information.

5.2 London Theory in Vortex State

Although we will use GL equations to derive the London equation, London theory was proposed long before GL, by F. and H. London in 1935 [133]. The basic assumption in their theory is a local proportionality relation between supercurrent $\vec{j}$ and vector potential $\vec{A}$

$$\vec{j} = -\frac{n_s e^2}{mc}\vec{A}. \tag{5.137}$$

This equation is usually taken as the definition of superfluid density n_s. Eq. (5.137) is not a gauge invariant equation. However, to satisfy current conservation, one has to fix the gauge to the London gauge

$$\nabla \cdot \vec{A} = 0. \tag{5.138}$$

This way (5.137) and all the results following from it are gauge independent and therefore physical. Eq. (5.137) plays a very important role in our theory for the vortex lattice. Generalization of this equation will be used in this chapter and also in the next chapter to develop a generalized London theory to describe the vortex lattice properties of d-wave superconductors.

Taking the curl of the both sides of (5.137) and using the Maxwell's equation $\nabla \times \vec{B} = (4\pi/c)\vec{j}$ we get

$$\lambda^2 \nabla \times \nabla \times \vec{B} + \vec{B} = 0 \tag{5.139}$$

which is the famous London equation. λ is called the *London penetration depth* and is given by

$$\lambda = \sqrt{\frac{mc^2}{4\pi n_s e^2}} \tag{5.140}$$

A free energy density that gives rise to (5.139) via minimization with respect to the magnetic field $\vec{B}$, is called the *London free energy density*

$$f_L = \frac{1}{8\pi}\left(\vec{B}^2 + \lambda^2 |\nabla \times \vec{B}|^2\right) \tag{5.141}$$

We now obtain London equations (5.139) from GL equations (5.135) and (5.136).

5.2.1 Derivation of the London Equation from GL Theory

Let us begin our derivation of the London equation by writing the order parameter as $\Psi = \psi e^{i\phi}$, with ψ and ϕ being real functions of position $\vec{x}$. Substituting Ψ into (5.136) we get

$$\lambda^2 \nabla \times \vec{B} + \vec{A} = \frac{\Phi_0}{2\pi}\nabla\phi \tag{5.142}$$

where $\lambda = \sqrt{m^* c^2/4\pi e^{*2}\psi^2}$ is the London penetration depth and $\Phi_0 = (hc/e^*)$ is the flux quantum. In type II superconductors ψ varies over a length scale ξ much smaller than the penetration depth λ. ξ is usually called the coherence length and is of the order of the extent of a cooper pair. In the Meissner state therefore, ψ (and consequently λ) stays constant in the bulk of the superconductor away from the boundaries. The London equation (5.139) can therefore be derived easily by taking the curl of Eq. (5.142) and keeping in mind that $\nabla \times \nabla\phi = 0$.

In the vortex state on the other hand, ψ is not a constant and actually vanishes at the center of each vortex. Taking this into account gives rise to the effect of the vortex core which is the subject of the next subsection. Furthermore, in the derivation of (5.139), we used $\nabla \times \nabla\phi = 0$ which is not true in the vortex state. The reason is that around a

vortex, ϕ has a topological winding number equal to 1. In other words, ϕ increases by 2π in every turn around a vortex core. Integrating $(\nabla \times \nabla\phi) \cdot d\vec{S}$ over a small region around the vortex center we get

$$\int (\nabla \times \nabla\phi) \cdot d\vec{S} = \oint \nabla\phi \cdot d\vec{l} = \phi_f - \phi_i = 2\pi n \tag{5.143}$$

where n is the topological winding number; which is one in our case. This equation is satisfied for every infinitesimal region around the center of the vortex $\vec{r}_0$, only if $\nabla \times \nabla\phi = 2\pi\delta^{(2)}(\vec{r} - \vec{r}_0)$. The London equation in the presence of a vortex will therefore become (assuming constant ψ again)

$$\lambda^2 \nabla \times \nabla \times \vec{B} + \vec{B} = \Phi_0 \delta^{(2)}(\vec{r} - \vec{r}_0) \tag{5.144}$$

To find a solution for a single vortex, it is easy to take the magnetic field in z-direction and write $\vec{B} = B(r)\hat{z}$. Eq. (5.144) then becomes

$$-\frac{\lambda^2}{r}\frac{d}{dr}(r\frac{dB}{dr}) + B = \Phi_0 \delta^{(2)}(\vec{r} - \vec{r}_0) \tag{5.145}$$

which is actually a Bessel's differential equation. The solution to this equation is

$$B(r) = \frac{\Phi_0}{2\pi\lambda^2} K_0(\frac{r}{\lambda}) \tag{5.146}$$

where K_0 is the zero-order modified Bessel function. Important to notice here is that K_0 diverges logarithmically as $r \to 0$; which is apparently non-physical. The reason behind this non-physical behavior lies in the fact that we did not incorporate the effect of the vortex core properly. In other words, the order parameter ψ always vanishes at the center of the vortex. Therefore, it is not a good approximation to consider it to be homogeneous everywhere in the lattice. We shall take into account this effect in more detail in the next subsection.

5.2.2 The Effect of the Vortex Core

Let us start from eq. (5.136) again by writing it as

$$\vec{j}(\vec{r}) = e^* n_s(\vec{r}) \vec{v}_s(\vec{r}) \tag{5.147}$$

where $n_s = \psi^2$ is the superfluid density and $\vec{v}_s$ is the superfluid velocity defined by

$$\vec{v}_s = \frac{\hbar}{m^*}(\nabla\phi - \frac{e^*}{\hbar c}\vec{A}) \tag{5.148}$$

At the center of a vortex, n_s vanishes. We can therefore write

$$n_s(\vec{r}) = n_0 \eta(\vec{r}) \tag{5.149}$$

where $\eta(\vec{r})$ is a function with the property

$$\begin{aligned} \eta(\vec{r}) &= 0 \qquad \text{at} \quad r = 0 \\ \eta(\vec{r}) &\to 1 \qquad \text{for} \quad r/\xi \gg 1 \end{aligned} \tag{5.150}$$

and ξ is the coherence length of the superconductor. The exact form of η should come from a microscopic theory or a complete solution of GL equation. Here, we do not derive η. Instead, we find the source function for a few assumed forms for η. Before that, let us take the curl of both sides of (5.147), keeping in mind that

$$\nabla \times (\eta \vec{v}_s) = \frac{2\pi\hbar}{m^*}\eta(\delta^{(2)}(\vec{r}) - \frac{1}{\Phi_0}\vec{B}) + \nabla\eta \times \vec{v}_s = \frac{2\pi\hbar}{m^*\Phi_0}\vec{B} + \nabla\eta \times \vec{v}_s \tag{5.151}$$

and also from (5.147)

$$\vec{v}_s = -\left(\frac{1}{e^* n_0 \eta}\right)\vec{j} = -\left(\frac{c}{4\pi e^* n_0 \eta}\right)\nabla \times \vec{B} \tag{5.152}$$

The generalized London equation therefore becomes

$$\lambda^2 \nabla \times \nabla \times \vec{B} + \vec{B} = \vec{\rho}(\vec{r}) \tag{5.153}$$

with a source term $\vec{\rho}(\vec{r})$ defined by

$$\vec{\rho}(\vec{r}) = (1-\eta)\vec{B} + \lambda^2 \frac{\nabla\eta}{\eta} \times \nabla \times \vec{B} \tag{5.154}$$

Equations (5.153) and (5.154) can be viewed as a set of self-consistent equations to be solved for $\vec{B}$ and $\vec{\rho}$. However, $\vec{\rho}(\vec{r})$ can be simplified significantly in extremely type II superconductors which have large $\kappa = \lambda/\xi$. First notice that $\vec{\rho}$ is non-zero only in a region of size ξ around the center of the vortex. In this region, both $\vec{B}$ and η scale with ξ. Therefore the first term in the left hand side of (5.153) and the second term on the right hand side of (5.154) are both $O(\lambda^2/\xi^2)B$ and therefore are the dominant terms in (5.153). Ignoring the subdominant terms, (5.153) can be written as

$$\nabla \times \vec{u} = \frac{\nabla\eta}{\eta} \times \vec{u} \qquad \Longrightarrow \qquad \nabla \times \left(\frac{\vec{u}}{\eta}\right) = 0 \tag{5.155}$$

where $\vec{u} = \nabla \times \vec{B}$. If we assume rotational symmetry and let $\vec{B} = B(r)\hat{z}$ and therefore $\vec{u} = u(r)\hat{\theta}$ where θ is the azimuthal angle, then (5.155) leads to

$$\frac{1}{r}\frac{d}{dr}\left(r\frac{u}{\eta}\right) = 0 \qquad \Longrightarrow \qquad u = C\frac{\eta}{r} \tag{5.156}$$

C is a constant that can be found, using the fact that $\int \vec{\rho}\cdot d\vec{S} = \Phi_0$, to be $C = (\Phi_0/2\pi\lambda^2)$. Substituting all into (5.154), the source function now can be written as $\vec{\rho}(r) = \rho(r)\hat{z}$, with

$$\rho(r) = \frac{\Phi_0}{2\pi r}\frac{d\eta}{dr} \tag{5.157}$$

Now let's calculate ρ for different choices of η.

Example 1: Clem's Ansatz

Let's assume that

$$\eta(r) = \frac{r^2}{R^2} \qquad \text{with} \qquad R^2 = r^2 + \xi_v^2 \tag{5.158}$$

where ξ_v is some parameter of the order of the coherence length ξ. Substituting into (5.157), we find the source term to be

$$\rho(r) = \frac{\Phi_0}{\pi}\frac{\xi_v^2}{R^4} \tag{5.159}$$

In order to calculate the magnetic field, it is easier to find the source term in terms of the magnetic field, using (5.154). Ignoring the first term we get

$$\rho(r) = -\frac{2\xi_v^2}{R^3}\frac{dB(r)}{dR}. \tag{5.160}$$

Substituting back into (5.153), with a little algebra, we get

$$-\frac{\lambda^2}{R}\frac{d}{dR}\left(R\frac{dB}{dR}\right) + B = 0 \tag{5.161}$$

Comparing (5.161) with (5.145), the solution would be

$$B(r) = \frac{\Phi_0}{2\pi\lambda^2}K_0\left(\frac{R}{\lambda}\right) \tag{5.162}$$

This result was first obtained by Clem [137], directly by solving GL equation. It was later shown by Brandt [138] that the magnetic field obtained this way in a vortex lattice is consistent with the exact solution of the GL equations. In Clem's approach, ξ_v is a variational parameter to be determined by minimizing the free energy. It turns out that in extremely type II superconductors $\xi_v = \sqrt{2}\xi$. As is clear from (5.162), $B(r)$ is not divergent as $r \to 0$. In fact, $B(0) = (\Phi_0/2\pi\lambda^2)K_0(\xi/\lambda)$.

Another way to find the magnetic field is by Fourier transforming (5.153) to get

$$\lambda^2 k^2 B(k) + B(k) = F(k) \qquad \text{or} \qquad B(r) = \int \frac{d^2k}{(2\pi)^2}\frac{F(k)e^{i\vec{k}\cdot\vec{r}}}{1+\lambda^2k^2} \tag{5.163}$$

where

$$F(k) = \int d^2r e^{-i\vec{k}\cdot\vec{r}}\rho(r) \tag{5.164}$$

is the Fourier transform of the source function which sets an ultraviolet cutoff in momentum integrations. In the present case, it is not difficult to show that

$$F(k) = \Phi_0 \xi_v k K_1(\xi_v k) \tag{5.165}$$

where K_1 is the first order modified Bessel function. Substituting (5.165) into (5.163), we get back to (5.162).

Example 2: Gaussian Source Function

Now let us assume that

$$\eta(r) = 1 - e^{-r^2/2\xi^2} \tag{5.166}$$

The resulting source function will then be

$$\rho(r) = \frac{\Phi_0}{2\pi r}\frac{d\eta}{dr} = \frac{\Phi_0}{2\pi\xi^2} e^{-r^2/2\xi^2} \tag{5.167}$$

The corresponding cutoff function will also have a Gaussian form

$$F(k) = \Phi_0 e^{-\xi^2 k^2/2} \tag{5.168}$$

This form of momentum cutoff was first proposed by Brandt [139]. This is actually the form of cutoff we are going to use in our calculations throughout the rest of this thesis. We will talk about the sensitivity of our solutions to this particular choice of cutoff function, when appropriate later.

5.2.3 Solution for a Vortex Lattice

In a vortex lattice, taking the magnetic field in z-direction ($\vec{B} = B\hat{z}$), equation (5.153) becomes

$$-\lambda^2 \nabla^2 B + B = \sum_i \rho(\vec{r} - \vec{r}_i) \tag{5.169}$$

where $\vec{r}_i$ are lattice vectors indicating the position of vortices. Taking the Fourier transform of both sides of (5.169), we get

$$B_k = \frac{F(k)}{1+\lambda^2 k^2} \qquad \Longrightarrow \qquad B(\vec{r}) = \bar{B}\sum_{\vec{k}} \frac{e^{i\vec{k}\cdot\vec{r}}F(k)}{1+\lambda^2 k^2} \tag{5.170}$$

where $\vec{k}$ are now reciprocal lattice wave vectors, $\bar{B}$ is the average magnetic field given by $\bar{B} = \Phi_0/\Omega$, with Ω being the area of a unit cell. Unlike GL, the London approach does not automatically determine the form of the lattice for us. Instead, one has to calculate the free energy for different configurations of the lattice and find the one that minimizes the free energy. Although this sounds a formidable job, symmetries of the free energy help us in our initial guess. In other words, the lattice that satisfies the symmetries of the free energy the most, is the most likely lattice for the vortices to exist on.

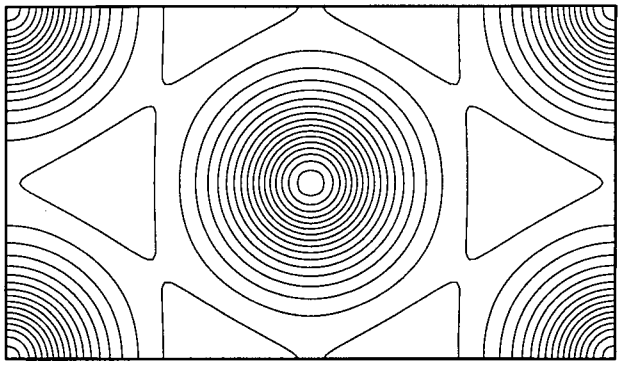

Figure 5.9: Magnetic field distribution in a triangular lattice, using the ordinary London equation with Gaussian cut off.

Using (5.141), the free energy per unit cell is given by

$$f_L = \int_{UC} d^2r[B^2 + (\nabla B)^2] = \sum_{\vec{k}}(1+\lambda^2 k^2)B_k^2 = \bar{B}^2\sum_{\vec{k}}\frac{F(k)^2}{1+\lambda^2 k^2} \tag{5.171}$$

Substituting the Gaussian cutoff function (5.168), we find

$$B(\vec{r}) \;=\; \bar{B}\sum_{\vec{k}}\frac{e^{i\vec{k}\cdot\vec{r}}e^{-\xi^2k^2/2}}{1+\lambda^2 k^2} \tag{5.172}$$

$$f_L = \bar{B}^2 \sum_{\vec{k}} \frac{e^{-\xi^2 k^2}}{1+\lambda^2 k^2} \tag{5.173}$$

These sums can be performed numerically quite easily. The lattice configuration that minimizes the free energy (5.173) is a triangular lattice. The contour plot of the magnetic field in this lattice is shown in Fig 5.9.

An important thing to notice is that the free energy (5.173) is isotropic and therefore does not determine the orientation of the lattice. In other words, there is an infinite degeneracy in the orientation of the lattice. This degeneracy will be removed as soon as symmetry breaking terms are added to the London equation. We will discuss this issue in more detail in the next two sections.

5.3 Mixing of d-wave with s-wave

So far we have established a London theory derived from GL theory, but we didn't mention anything about the symmetry of the order parameter. Since an s-wave order parameter is isotropic, whatever we discussed in the previous sections is expected to hold for an s-wave superconductor. A d-wave order parameter on the other hand, is not isotropic. Instead, it has fourfold anisotropy, and consequently, it is natural to expect this anisotropy to influence the structure of the vortex lattice. Surprisingly, the GL equations, as written in (5.135) and (5.136), have exactly the same form for a d-wave order parameter as s-wave. All the statements in the previous sections should therefore hold for a d-wave superconductor as well. A way out of this dilemma, is to notice the fact that the GL free energy written in (5.134), is an approximation and contains only the lowest order contributions. In other words, we have ignored all higher order derivative terms. We have also overlooked the possibility of existence of a second order parameter that in general can couple to the main (d-wave) order parameter. It is conceivable that including these effects will introduce some fourfold anisotropic terms to the GL equations, reflecting the

d-wave nature of the superconductor. In this section, we shall first consider the second possibility, namely including an s-wave order parameter coupled to the original d-wave order parameter. We shall see that the effect of this inclusion is to introduce higher order derivative terms in the effective GL free energy written only in terms of the d-wave order parameter. We shall then show how this additional high-derivative term will change the London free energy. This way we actually cover both possibilities mentioned above. The material discussed in this section has been published in Ref. [140].

A GL free energy density to describe mixing of d-wave and s-wave order parameters was first proposed by Joynt [141] as

$$\begin{aligned} f &= \alpha_s|s|^2 + \alpha_d|d|^2 + \gamma_s|\vec{\Pi}s|^2 + \gamma_d|\vec{\Pi}d|^2 + f_4 + H^2/8\pi \\ &\quad +\gamma_v[(\Pi_y s)^*(\Pi_y d) - (\Pi_x s)^*(\Pi_x d) + \text{c.c.}]. \end{aligned} \tag{5.174}$$

where $\vec{\Pi} \equiv -i\nabla - e^*\vec{A}/\hbar c$ and f_4 contains the quartic terms. d and s represent d-wave and s-wave order parameters respectively. In the bulk of the superconductor and in the absence of magnetic field, we want only a d-wave order parameter to exist. Therefore below T_c, we expect to have $\alpha_d < 0$, but $\alpha_s > 0$. In finite field ($H > H_{c1}$) on the other hand, a small s-component with a highly anisotropic spatial distribution is nucleated in the vicinity of a vortex [120, 121]. This free energy has been extensively studied in the literature [120, 121, 122, 123, 142]. It is well known that it gives rise to non-triangular equilibrium lattice structures [120, 121]. Our objective here, is not to discuss the solution to the GL equations resulting from this free energy, but to focus on deriving the corrections to the London equation that result from this free energy. Our strategy will be to simplify the free energy (5.174) by integrating out the s-component in favor of higher order derivative terms in d. In this process, some short length-scale information on the order parameter is lost but the magnetic field distribution is described accurately.

Using its Euler-Lagrange equation, s can be expressed to the leading order in $(1 -$

T/T_c) as

$$s = (\gamma_v/\alpha_s)(\Pi_x^2 - \Pi_y^2)d. \tag{5.175}$$

Substituting this into f gives the leading derivative terms in d of the form:

$$f = \gamma_d[|\vec{\Pi}d|^2 - (\gamma_v^2/\gamma_d\alpha_s)|(\Pi_x^2 - \Pi_y^2)d|^2] + \ldots \tag{5.176}$$

Various additional corrections to the free energy are obtained from integrating out s more accurately, taking into account the $\gamma_s|\vec{\Pi}s|^2$ term and quartic terms. However these all involve higher powers of $\vec{\Pi}$ or other terms that will not concern us. The coefficient of the second term has dimensions of (length)^2. For future convenience, we will write it in the form $\epsilon\xi^2/3$, where $\epsilon \equiv 3(\alpha_d\gamma_v^2/\alpha_s\gamma_d^2)$ is a dimensionless parameter which controls the strength of the s-d coupling and $\xi \equiv \sqrt{\gamma_d/|\alpha_d|}$ is the GL coherence length. We henceforth assume $\epsilon \ll 1$. As we will discuss in the next section, neutron scattering and STM experiments probably support this assumption. As mentioned before, a term of the form $|(\Pi_x^2 - \Pi_y^2)d|^2$ could arise without invoking s-d mixing. It can result from a systematic derivation of higher order terms in the GL free energy starting with a BCS-like model and taking into account the square symmetry of the Fermi surface [143, 119, 144, 145].

The free energy (5.176) is not bounded below, exhibiting runaway behavior for rapidly varying d-fields. This is in fact cured by keeping additional higher derivative terms that also arise from integrating out s. In fact, the approximation of Eq. (5.176) will be sufficient for our purposes, yielding a local minimum which we expect would become a global minimum upon including the additional terms.

In the case of extremely type II superconductors - which we are considering here - the penetration depth $\lambda \gg \xi$. We may therefore assume that $|d(\vec{r})| \approx d_0$, the zero field equilibrium value, almost everywhere in the vortex lattice, except within a distance of $O(\xi)$ of the cores. This gives the London free energy,

$$f_L = (1/8\pi)(\vec{B})^2 + \gamma_d d_0^2\{\vec{v}^2 - (\epsilon\xi^2/3)[(v_x^2 - v_y^2)^2 + (\partial_y v_y - \partial_x v_x)^2]\}, \tag{5.177}$$

written in terms of the superfluid velocity (we set $\hbar = m^* = 1$),

$$\vec{v} \equiv \nabla\theta - (e^*/c)\vec{A}, \tag{5.178}$$

where θ is the phase of d.

The corresponding London equation, obtained by varying f_L with respect to $\vec{A}$, is:

$$\frac{c}{4\pi}\nabla\times\vec{B} = \left(\frac{2e^*}{\hbar c}\right)\gamma_d d_0^2\{\vec{v} - \frac{2}{3}\epsilon\xi^2[(\hat{y}v_y - \hat{x}v_x)(v_y^2 - v_x^2) - (\hat{y}\partial_y - \hat{x}\partial_x)(\partial_y v_y - \partial_x v_x)]\}. \tag{5.179}$$

For many purposes it is very convenient to express $\vec{v}$ in terms of $\vec{B}$ and its derivatives, and then substitute this expression for $\vec{v}$ back into f_L, giving an explicit expression for f_L as a functional of $\vec{B}$ only. For $\epsilon = 0$ this gives

$$\vec{v}^{(0)} = \nabla \times \vec{B}/B_0, \tag{5.180}$$

where $B_0 \equiv \Phi_0/2\pi\lambda_0^2$ is a characteristic field of order H_{c1}, and

$$f_L^0 = (1/8\pi)[\vec{B}^2 + \lambda_0^2(\nabla \times \vec{B})^2]. \tag{5.181}$$

which is actually the ordinary London free energy (i.e. Eq. (5.141)). Here the penetration depth, for $\epsilon = 0$ is $\lambda_0^{-2} = 8\pi\gamma_d(e^* d_0/\hbar c)^2$. It is presumably not possible to solve Eq. (5.179) in closed form for $\vec{v}$ as a function of $\vec{B}$ for $\epsilon \neq 0$. However, this can be done readily in a perturbative expansion in ϵ. The first order correction is:

$$\vec{v}^{(1)} = (2\epsilon\xi^2/3)\{(\hat{y}v_y^{(0)} - \hat{x}v_x^{(0)})[(v_y^{(0)})^2 - (v_x^{(0)})^2] - (\hat{y}\partial_y - \hat{x}\partial_x)(\partial_y v_y^{(0)} - \partial_x v_x^{(0)})\} \tag{5.182}$$

with $\vec{v}^{(0)}$ given by Eq. (5.180). The London free energy density, up to $O(\epsilon)$ is then:

$$f_L = f_L^0 + \frac{\epsilon\lambda_0^2\xi^2}{8\pi}[4(\partial_x\partial_y B)^2 + ((\partial_x B)^2 - (\partial_y B)^2)^2/B_0^2]. \tag{5.183}$$

Note that we could have arrived at a similar conclusion by simply writing down all terms allowed by symmetry in f_L, expanding in number of derivatives and powers of B. Square

anisotropy is first possible in the fourth derivative terms. In principle, we should also include all isotropic terms to order B^4 and ∇^4. However, assuming that these have small coefficients, they will not be important. As we shall see in the next chapter, similar results can also be obtained from nonlocal effects due to the divergence of the coherence length along the node directions [132] and also from considering generation of quasi-particles near gap nodes [104, 146], in a range of temperature and field where the supercurrent can be Taylor expanded in the superfluid velocity. More generally, the quadratic and quartic terms in (5.183) have independent coefficients.

The corresponding London equation is obtained by varying f_L with respect to $\vec{B}(\vec{r})$. For B along the z direction, one obtains

$$[1 - \lambda_0^2\nabla^2 + 4\epsilon\lambda_0^2\xi^2(\partial_x\partial_y)^2]B - \epsilon Q[B] = 0, \tag{5.184}$$

where

$$Q[B] = 2\lambda_0^2\xi^2 B_0^{-2}[(\partial_x^2 - \partial_y^2)B + \partial_x B\partial_x - \partial_y B\partial_y][(\partial_x B)^2 - (\partial_y B)^2] \tag{5.185}$$

is the non-linear term arising from the last term in Eq. (5.183).

Our numerical calculation (next section) shows that, the effect of the non-linear term is negligible (Contrary to naive expectation, it doesn't become more important with increasing applied field because the field becomes nearly constant in the vortex lattice when the applied field is large.) Thus to an excellent approximation one may neglect $Q[B]$ in the London equation (5.184). To get a feeling for the effect of the extra nonlocal (four derivative) term, consider a semi-infinite superconductor in its Meissner state with an interface parallel to the yz plane. The magnetic field in this case depends only on x; all the y-derivatives and thereby the extra term vanish. The penetration depth will then remain unchanged and equal to λ_0. On the other hand, if the interface is 45^o rotated with respect to x and y axis (a and b directions), the magnetic field will be a function

of $(x+y)$. Substituting $B = B_0 e^{-(x+y)/\sqrt{2}\lambda}$ into (5.184), we get (neglecting the nonlinear part)

$$\lambda = \lambda_0 \left[\frac{1}{2} + \sqrt{\frac{1}{4} - \frac{\epsilon\xi^2}{\lambda_0^2}}\right]^{1/2}, \tag{5.186}$$

Here we keep only the larger solution because it is the one that determines the decay rate of the field and therefore can be identified as the penetration depth. The penetration depth is now longer along the crystal axes as is clear from (5.186).

To determine vortex lattice structure, we insert source terms $\sum_j \rho(\vec{r}-\vec{r}_j)$ at the vortex core positions, $\vec{r}_j$, on the right hand side of Eq. (5.184). The source term we use is the Gaussian source term introduced in eq. (5.167). Taking Fourier transform, the magnetic field may be written explicitly as:

$$B(\vec{r}) = \bar{B} \sum_{\vec{k}} \frac{e^{i\vec{k}\cdot\vec{r}} e^{-k^2\xi^2/2}}{1 + \lambda_0^2 k^2 + 4\epsilon\lambda_0^2\xi^2(k_x k_y)^2}. \tag{5.187}$$

Here the sum is over all wave-vectors in the reciprocal lattice and $\bar{B}$ is the average field. The lattice constant is determined by the condition that $\bar{B}\Omega = \Phi_0$, where Ω is the area of the unit cell. The lattice symmetry is then determined by minimizing the Gibbs free energy $\mathcal{G}_L = \mathcal{F}_L - H\bar{B}/4\pi$, where

$$\mathcal{F}_L = \bar{B}^2 \sum_{\vec{k}} \frac{e^{-k^2\xi^2}}{1 + \lambda_0^2 k^2 + 4\epsilon\lambda_0^2\xi^2(k_x k_y)^2} \tag{5.188}$$

5.4 Numerical Results and Experimental Realizations

Ignoring the nonlinear term, one can perform the sums in (5.187) and (5.188) numerically to find the magnetic field and lattice structure. The correction due to the nonlinear term can then be found iteratively. To do so, we start by writing (5.184) in Fourier transformed form (with Gaussian source) as

$$B_k^n = \frac{e^{-k^2\xi^2/2} + \epsilon\tilde{Q}[B_k^{n-1}]}{1 + \lambda_0^2 k^2 + 4\epsilon\lambda_0^2\xi^2(k_x k_y)^2} \tag{5.189}$$

where $\widetilde{Q}[B_k]$ is the Fourier transform of $Q[B]$ and the superscript n represents the stage of iteration. The initial B_k^0 is found by neglecting the nonlinear term. At each following step we calculate $\widetilde{Q}[B_k]$ using the known value for B_k, substitute it into (5.189) to find the new B_k. We continue this iteration until we get the desired accuracy. Having B, we then can calculate the Gibbs free energy $\mathcal{G}_L = \mathcal{F}_L - H\bar{B}/4\pi$ using (5.183). We calculate the Free energy this way for different configurations of the vortex lattice. We find that a centered rectangular flux lattice, with principal axes aligned with the ionic crystal lattice minimizes the free energy. An angle β between unit vectors (Fig. 5.10) characterizes the dependence of the lattice on ϵ and the magnetic field. An example of such a centered rectangular lattice is shown in Fig. 5.10.

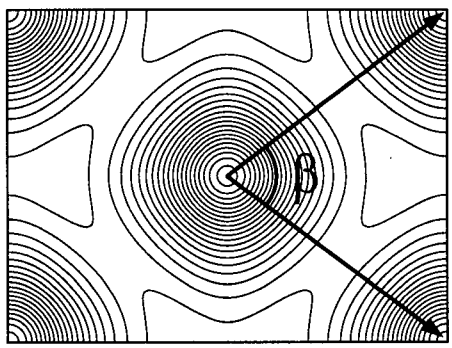

Figure 5.10: Distribution of magnetic field in a vortex lattice for $\epsilon = 0.3$ and $H = 6.8$T, leading to an angle of $\beta \simeq 74°$. We use $\lambda_0 = 1400$Å and $\kappa \equiv \lambda_0/\xi = 68$.

In agreement with earlier results within GL [121] and Eilenberger [147] formalisms, individual vortices are elongated along the crystalline axes. Figure 5.11(a) shows the dependence of Gibbs free energy on β for various values of ϵ at fixed applied field $H = 400B_0 \simeq 6.8$T. For $\epsilon = 0$ minimum occurs for $\beta_{\text{MIN}} = 60°$, corresponding to a hexagonal lattice. As ϵ increases, β_{MIN} continuously increases and for sufficiently large ϵ, the flux

lattice becomes tetragonal with $\beta_{\rm MIN} = 90°$. For $\beta_{\rm MIN} \neq 90^0$, there are always two solutions, related by a 90° rotation, in which the long axis of the centered rectangle is aligned with either the x or y axis. The degeneracy is much larger for $\epsilon = 0$, when the flux lattice may have an arbitrary orientation relative to the ionic crystal lattice.

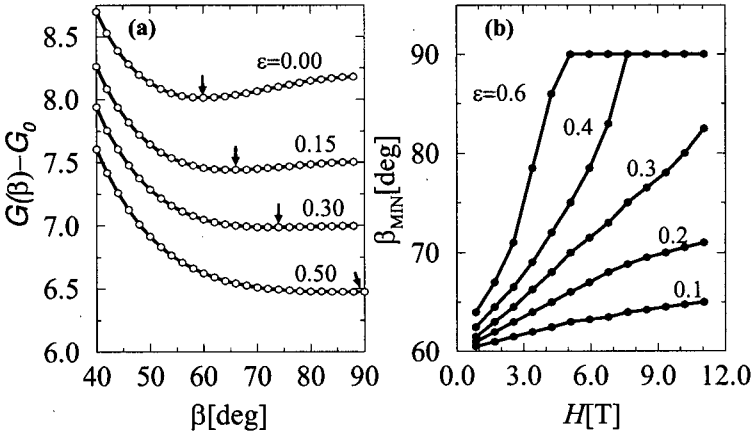

Figure 5.11: a) Gibbs free energy as a function of β for the same parameters as Fig. 5.10 and various values of ϵ. Arrows indicate positions $\beta_{\rm MIN}$ of the minima and $G_0 \equiv -H^2/8\pi$. b) Equilibrium angle $\beta_{\rm MIN}$ as a function of H for several values of ϵ.

The dependence of $\beta_{\rm MIN}$ on the applied field for various values of ϵ is displayed in Fig. 5.11(b). Clearly the anisotropic term becomes more important at larger fields. Our perturbative elimination of $\vec{v}$ in favor of B breaks down when ϵ and H are sufficiently large that $\beta_{\rm MIN}$ differs significantly from 60°. Furthermore, we might expect higher order corrections to (5.177) to be important in this regime. By fitting Fig. 5.11(b) to experimental data on tetragonal materials such as $Tl_2Ba_2CuO_{6+d}$ (once such data become available) one can directly assess the magnitude of ϵ, the only unknown parameter in the model.

The analysis presented here, can be easily extended to take into account effective mass (i.e. penetration depth) anisotropy. In a simple one-component GL model, the derivative term is generalized to:

$$f = \sum_{i=x,y,z} \gamma_i |\Pi_i d|^2. \tag{5.190}$$

We restrict our attention to fields along the z-axis. The anisotropy then can be removed by a rescaling of the x-coordinate and a corresponding rescaling of the magnetic field. The coherence length and penetration depth anisotropies are considered the same: $\xi_y/\xi_x = \lambda_x/\lambda_y$. Making a simplifying assumption that the higher derivative and mixed derivative terms in $\mathcal{F}$ are also simply modified by a rescaling by a common factor, it then follows that the flux lattice shape is obtained by stretching along the x-axis by the factor λ_x/λ_y. We now obtain two possible vortex lattices, both of centered rectangular symmetry, aligned with the ionic lattice, with different angles, β. (Relaxing our simplifying assumption may split the degeneracy between these two lattices.) On the other hand, when $\epsilon = 0$, we may rotate the hexagonal lattice by an arbitrary angle before stretching. This gives an infinite set of oblique lattices with arbitrary orientation.

To compare theory with YBCO we should take into account twin boundaries; which are the boundaries between different orientations of crystal lattice. They may also tend to align the vortex lattice by pinning vortices to the twin boundaries, at $\pm 45^0$ to the x-axis. This effect competes with alignment to the ionic lattice which we have been discussing. Only in the special case of a square vortex lattice does a line of vortices occur at $\pm 45^0$. If this is not the case, and if pinning by twin boundaries is significant, then we should expect that the vortex lattice will align with the ionic lattice far from twin boundaries but will be deformed in the vicinity of a twin boundary in an effort to align itself with the twin boundary. On the other hand, for $\epsilon = 0$, the vortex lattice would remain aligned with the twin boundaries everywhere except within vortex lattice domain

boundaries which necessarily exist roughly midway between the twin boundaries.

Neutron scattering experiments on YBCO [117] suggest that the vortex lattice is well-aligned with the twin boundaries and is close to being centered rectangular (the ratio of lattice constants is about 1.04) with $\beta \approx 73^0$, with weak dependence on H. This corresponds to a rotation away from alignment with the ionic lattice by 9°. Four different orientational domains, related by reflection in the $(1,1,0)$ axis and 90^0 rotation were reported. These results can be rather well fitted [124] by the basic London model ($\epsilon = 0$) with mass anisotropy. For $\lambda_x/\lambda_y = 1.5$, a value roughly consistent with infrared experiments, this lattice has about the right shape. Taking into account the two crystallographic domains (related by interchanging λ_x and λ_y) there are altogether four vortex lattice domains, as seen experimentally. The experimental fact that the vortex lattice appears to be well aligned with the twin boundaries suggests that the tendency to align with the ionic lattice is small. No evidence for a bending of the vortex lattice (by 9^0) into alignment with the ionic lattice far from the twin boundaries has so far been found.

STM imaging of the YBCO vortex lattice [118] also suggests that the (highly disordered) lattice has approximately centered rectangular symmetry with $\beta \approx 77°$. However, no evidence for the 9° tilt into alignment with the twin boundaries was reported. Considering the observed anisotropy of the vortex cores it has been concluded that the mass anisotropy alone cannot account for the measured 77° angle of the vortex lattice. It has been suggested that a mechanism related to the internal symmetry of the order parameter (such as the one discussed in the present thesis) needs to be invoked in order to reconcile these observations.

Low field Bitter decoration data on YBCO [148] show vortex lattice geometry with a very small distortion from hexagonal, consistent with a much smaller anisotropy $\lambda_x/\lambda_y = 1.11 - 1.15$. One may be tempted to attribute this apparent field dependence of β to the effects discussed above in connection with Fig. 5.11(b). An alternative explanation

is a poor quality of samples used in the Bitter decoration experiments that may have resulted in partial washing out of the a-b plane anisotropy [149].

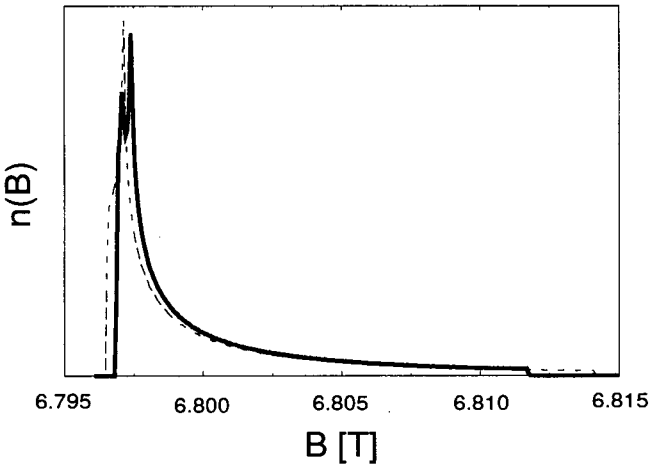

Figure 5.12: Magnetic field distribution function; **Solid line:** using the same parameters as in Fig. 5.10. **Dashed line:** the same parameters except for $\epsilon = 0$.

μSR experiments measure the field distribution $n(B) = (1/\Omega) \int \delta[B - B(\vec{r})] dxdy$. Our calculation of this quantity is shown in Fig. 5.12. For comparison we show our results with (solid line) and without (dashed line) the extra nonlocal term. For $\beta \neq 60°$, $B(\vec{r})$ has two inequivalent saddle points leading to two peaks in $n(B)$. $n(B)$ is unaffected by effective mass anisotropy, as can be shown by the rescaling transformation, mentioned above. Existing μSR experiments show only a single peak [150] but this might be due to the large broadening as a result of finite muon lifetime.

The weak field dependence of β, the alignment with twin boundaries in the neutron scattering experiments, and the single peak in $n(B)$ suggest that ϵ is small in YBCO and that the normal London model, together with twin boundary pinning, provides a good fit to the data. STM and Bitter decoration data on the other hand, seem to favor

finite ϵ and weak pining to twin boundaries. Further experimental work, preferably on untwinned YBCO or other tetragonal superconductors, will probably be necessary to clarify the importance of square lattice anisotropy in high-T_c superconductors.

Most of the experiments mentioned above are done at temperatures far below T_c, i.e. beyond the validity range of GL theory. Thus our derivation of the generalized London model from GL theory is not valid for most experimental situations. However, as we emphasized, the corrections we introduce to the London free energy are the most general analytic corrections possible by symmetry to the order of our concern. It is therefore reasonable that even at lower temperatures all the lowest order analytic corrections come with these forms. We will see in the next chapter that at very low temperatures, the lowest order corrections are actually non-analytic. This is because of the existence of the gap nodes; a unique feature of d-wave superconductors. Even those effects turn into the analytic forms discussed here at higher temperatures.

Chapter 6

Microscopic Model

6.1 Gorkov Theory and Quasi-Classical Approximation

Ginsburg Landau theory, discussed in the last chapter, is a theory that is valid only near the transition temperature T_c. Most of the experiments however, are done at temperatures far below T_c. Also, one of the most essential characteristics of d-wave superconductors, i.e. the existence of nodes in the superconducting gap, does not show a direct effect on the GL equations. Thus a more sophisticated microscopic approach is necessary to describe the vortex lattice properties of high T_c superconductors. The microscopic theory we present here is based on the theory developed by Gorkov [151] in 1959. In his paper, Gorkov showed how GL theory results from pairing theory at temperatures close to T_c. Here, we don't give the detailed derivation of Gorkov's equations from the first principles. Our goal instead, is to derive relations between supercurrent $\vec{j}$ and superfluid velocity $\vec{v}_s$ (or vector potential $\vec{A}$) starting from these equations. This relation is then used to obtain a generalized London equation. For a detailed derivation of the Gorkov equations, interested reader should refer to ref. [136, 152].

Let us start from an interaction Hamiltonian of the form

$$H_{int} = \int d^3r d^3r' \psi_\uparrow^\dagger(\vec{r}')\psi_\uparrow(\vec{r}')\psi_\downarrow^\dagger(\vec{r})\psi_\downarrow(\vec{r})V(\vec{r}-\vec{r}') \tag{6.191}$$

The Gorkov equations for this Hamiltonian are

$$\{-\frac{\partial}{\partial\tau} + \frac{1}{2}[\nabla - \frac{ie}{c}\vec{A}(\vec{r})]^2 + \mu\}\mathcal{G}(\vec{r}\tau, \vec{r}'\tau')$$

$$+\int \Delta(\vec{r},\vec{r}'')\mathcal{F}^{\dagger}(\vec{r}''\tau,\vec{r}'\tau')d^3r'' = \delta^{(3)}(\vec{r}-\vec{r}')\delta(\tau-\tau') \quad (6.192)$$

$$\{\frac{\partial}{\partial\tau}+\frac{1}{2}[\nabla+\frac{ie}{c}\vec{A}(\vec{r})]^2+\mu\}\mathcal{F}^{\dagger}(\vec{r}\tau,\vec{r}'\tau') - \int \Delta^*(\vec{r},\vec{r}'')\mathcal{G}(\vec{r}''\tau,\vec{r}'\tau')d^3r'' = 0 \quad (6.193)$$

where $\mathcal{G}$ and $\mathcal{F}$ are regular and anomalous parts of the Nambu-Gorkov Green function respectively,

$$\mathcal{G}(\vec{r}\tau,\vec{r}'\tau')\delta_{\sigma\sigma'} = -<\mathrm{T}_\tau\psi_\sigma(\vec{r}\tau)\psi^{\dagger}_{\sigma'}(\vec{r}'\tau')> \quad (6.194)$$

$$\mathcal{F}^{\dagger}(\vec{r}\tau,\vec{r}'\tau') = -<\mathrm{T}_\tau\psi^{\dagger}_{\uparrow}(\vec{r}\tau)\psi^{\dagger}_{\downarrow}(\vec{r}'\tau')> \quad (6.195)$$

Here, and also throughout the rest of this chapter, we choose $\hbar = m = 1$. The order parameter Δ is related to the interaction potential V by

$$\Delta(\vec{r}-\vec{r}') = V(\vec{r}-\vec{r}')<\psi_{\uparrow}(\vec{r})\psi_{\downarrow}(\vec{r}')>. \quad (6.196)$$

Equations (6.192) and (6.193) have to be solved for $\mathcal{G}$ and $\mathcal{F}$ self-consistently with Δ. The self-consistency equation follows from (6.195) and (6.196) to be

$$\Delta^*(\vec{r}-\vec{r}') = V(\vec{r}-\vec{r}')\mathcal{F}^{\dagger}(\vec{r}0^+,\vec{r}'0) \quad (6.197)$$

Solving these equations self-consistently, in a general case at the presence of Magnetic field is tedious if not impossible. However, substantial simplification can be achieved using local approximation or gradient expansion. The method we use here (with some minor differences), is a generalization of the gradient expansion method discussed in Ref. [152]. The generalization is necessary to study d-wave superconductivity.

6.1.1 Local Approximation

Gorkov equations (6.192) and (6.193) take much simpler forms in Fourier space. If the system is translationally invariant in time, $\mathcal{G}$ and $\mathcal{F}$ are only functions of $(\tau-\tau')$. We

can therefore take their Fourier transform with respect to $(\tau - \tau')$ and define

$$\mathcal{G}_\omega(\vec{r},\vec{r}') = \int \mathcal{G}(\vec{r}\tau,\vec{r}'0)e^{-i\omega_n\tau}d\tau$$
$$\mathcal{F}^\dagger_\omega(\vec{r},\vec{r}') = \int \mathcal{F}^\dagger(\vec{r}\tau,\vec{r}'0)e^{-i\omega_n\tau}d\tau \qquad (6.198)$$

where $\omega_n = \pi T(2n-1)$ are fermionic Matsubara frequencies. We also change the coordinates to $\vec{R} = r'$ and $\vec{\rho} = r - r'$ and take the Fourier transform with respect to $\vec{\rho}$ to get

$$\mathcal{G}_\omega(\vec{R},\vec{k}) = \int \mathcal{G}_\omega(\vec{R}+\vec{\rho},\vec{R})e^{-i\vec{k}\cdot\vec{\rho}}d^3\rho \qquad (6.199)$$
$$\mathcal{F}^\dagger_\omega(\vec{R},\vec{k}) = \int \mathcal{F}^\dagger_\omega(\vec{R}+\vec{\rho},\vec{R})e^{-i\vec{k}\cdot\vec{\rho}}d^3\rho \qquad (6.200)$$
$$\Delta(\vec{R},\vec{k}) = \int \Delta(\vec{R}+\frac{\vec{\rho}}{2},\vec{R}-\frac{\vec{\rho}}{2})e^{-i\vec{k}\cdot\vec{\rho}}d^3\rho \qquad (6.201)$$

(6.192) therefore becomes

$$\{i\omega_n+\frac{1}{2}[i\vec{k}-\frac{ie}{c}\vec{A}(R+i\frac{\partial}{\partial\vec{k}})]^2+\mu\}\mathcal{G}_\omega(\vec{R},\vec{k})+\int d^3\rho\int d^3r''e^{-i\vec{k}\cdot\rho}\Delta(\vec{R}+\rho,r'')\mathcal{F}^\dagger_\omega(\vec{r}'',R)=1 \qquad (6.202)$$

The integral on the left hand side of (6.202) can be written as

$$\begin{aligned}
&\int d^3\rho_1\int d^3\rho_2 e^{-i\vec{k}\cdot(\vec{\rho}_1+\vec{\rho}_2)}\Delta(\vec{R}+\vec{\rho}_1+\vec{\rho}_2,\vec{R}+\vec{\rho}_2)\mathcal{F}^\dagger_\omega(\vec{R}+\vec{\rho}_2,\vec{R})\\
&=\lim_{\vec{k}'\to\vec{k}}\int d^3\rho_1\int d^3\rho_2 e^{-i\vec{k}'\cdot\vec{\rho}_1}e^{-i\vec{k}\cdot\vec{\rho}_2}\Delta((\vec{R}+\vec{\rho}_2+\frac{\vec{\rho}_1}{2})+\frac{\vec{\rho}_1}{2},(\vec{R}+\vec{\rho}_2+\frac{\vec{\rho}_1}{2})-\frac{\vec{\rho}_1}{2})\mathcal{F}^\dagger_\omega(\vec{R}+\vec{\rho}_2,\vec{R})\\
&=\lim_{\vec{k}'\to\vec{k}}\Delta(\vec{R}+i\frac{\partial}{\partial\vec{k}}+\frac{i}{2}\frac{\partial}{\partial\vec{k}'},\vec{k}')\mathcal{F}^\dagger_\omega(\vec{R},\vec{k}) \qquad (6.203)
\end{aligned}$$

If $\vec{A}(\vec{R})$ and $\Delta(\vec{R},\vec{k})$ are slowly varying functions of $\vec{R}$, then we can neglect all $\frac{\partial}{\partial\vec{k}}$ and $\frac{\partial}{\partial\vec{k}'}$ which are at most of the order of ξ. We can also follow the same procedure for (6.193). The resulting Gorkov equations in this limit will be

$$\{i\omega_n-\frac{1}{2}[\vec{k}-\frac{e}{c}\vec{A}(\vec{R})]^2+\mu\}\mathcal{G}_\omega(\vec{R},\vec{k})+\Delta(\vec{R},\vec{k})\mathcal{F}^\dagger_\omega(\vec{R},\vec{k}) = 1 \qquad (6.204)$$
$$\{-i\omega_n-\frac{1}{2}[\vec{k}+\frac{e}{c}\vec{A}(\vec{R})]^2+\mu\}\mathcal{F}^\dagger_\omega(\vec{R},\vec{k})-\Delta^*(\vec{R},\vec{k})\mathcal{G}_\omega(\vec{R},\vec{k}) = 0 \qquad (6.205)$$

These are now algebraic equations instead of integral equations. This approximation is usually referred to as *quasi-classical approximation.* The reason is that the equations involve position $\vec{R}$ and momentum $\vec{k}$ at the same time, similar to classical equations. The self-consistency equation also takes the form

$$\Delta^*(\vec{R},\vec{k}) = \frac{1}{\beta}\sum_n \int d^3k' \tilde{V}(\vec{k}-\vec{k}')\mathcal{F}^\dagger_\omega(\vec{R},\vec{k}') \tag{6.206}$$

where $\tilde{V}(\vec{k})$ is the Fourier transform of $V(\vec{r})$. The solutions to (6.204) and (6.205) are

$$\mathcal{G}_\omega(\vec{R},\vec{k}) = \frac{-i\omega_n - \frac{1}{2}[\vec{k}+\frac{e}{c}\vec{A}(\vec{R})]^2 + \mu}{\{i\omega_n - \frac{1}{2}[\vec{k}-\frac{e}{c}\vec{A}(\vec{R})]^2+\mu\}\{-i\omega_n - \frac{1}{2}[\vec{k}+\frac{e}{c}\vec{A}(\vec{R})]^2+\mu\} + \Delta^2(\vec{k})}$$

$$\mathcal{F}^\dagger_\omega(\vec{R},\vec{k}) = \frac{\Delta^*(\vec{k})}{\{i\omega_n - \frac{1}{2}[\vec{k}-\frac{e}{c}\vec{A}(\vec{R})]^2+\mu\}\{-i\omega_n - \frac{1}{2}[\vec{k}+\frac{e}{c}\vec{A}(\vec{R})]^2+\mu\} + \Delta^2(\vec{k})}$$

In the absence of magnetic field these solutions will be simplified to

$$\mathcal{G}_\omega(\vec{k}) = \frac{-i\omega_n - \epsilon_{\vec{k}}}{\omega^2 + E^2_{\vec{k}}}$$

$$\mathcal{F}^\dagger_\omega(\vec{k}) = \frac{\Delta^*(\vec{k})}{\omega^2 + E^2_{\vec{k}}} \tag{6.207}$$

with

$$\epsilon_{\vec{k}} = \frac{1}{2}k^2 - \mu \qquad \textit{and} \qquad E_{\vec{k}} = \sqrt{\epsilon^2_{\vec{k}} + \Delta^2(\vec{k})} \tag{6.208}$$

The self-consistency equation (6.206) also will be

$$\Delta^*(\vec{R},\vec{k}) = \int d^3k' \tilde{V}(\vec{k}-\vec{k}')\Delta^*(\vec{k}')\frac{1}{\beta}\sum_n \frac{1}{\omega^2 + E^2_{\vec{k}'}} \tag{6.209}$$

Summing over Matsubara frequencies, the self-consistency equation becomes

$$\Delta(\vec{k}) = -\int d^3k' \tilde{V}(\vec{k}-k')\frac{\Delta(\vec{k}')}{2E_{\vec{k}'}}\tanh(\frac{E_{\vec{k}'}}{2T}) \tag{6.210}$$

which is the well known BCS gap equation.

In the presence of magnetic field, simplifications can be achieved if we introduce new Green's functions $\tilde{\mathcal{G}}$ and $\tilde{\mathcal{F}}$ by

$$\begin{aligned}\tilde{\mathcal{G}}(\vec{r}\tau,\vec{r}'\tau') &= \mathcal{G}(\vec{r}\tau,\vec{r}'\tau')e^{-i(\chi(\vec{r})-\chi(\vec{r}'))} \\ \tilde{\mathcal{F}}^{\dagger}(\vec{r}\tau,\vec{r}'\tau') &= \mathcal{F}^{\dagger}(\vec{r}\tau,\vec{r}'\tau')e^{i(\chi(\vec{r})+\chi(\vec{r}'))}\end{aligned} \tag{6.211}$$

and also a new pairing potential

$$\tilde{\Delta}(\vec{r},\vec{r}') = \Delta(\vec{r},\vec{r}')e^{-i(\chi(\vec{r})+\chi(\vec{r}'))} \tag{6.212}$$

where $\chi(\vec{r})$ is the phase of the operator $\psi(\vec{r})$ at some fixed gauge. The Gorkov equations (6.204) and (6.205) for $\tilde{\mathcal{G}}$ and $\tilde{\mathcal{F}}$ become

$$\{i\omega_n - \frac{1}{2}[\vec{k}+\vec{v}_s(\vec{R})]^2+\mu\}\tilde{\mathcal{G}}_\omega(\vec{R},\vec{k}) + \tilde{\Delta}(\vec{R},\vec{k})\tilde{\mathcal{F}}^{\dagger}_\omega(\vec{R},\vec{k}) = 1 \tag{6.213}$$

$$\{-i\omega_n - \frac{1}{2}[\vec{k}-\vec{v}_s(\vec{R})]^2+\mu\}\tilde{\mathcal{F}}^{\dagger}_\omega(\vec{R},\vec{k}) - \tilde{\Delta}^*(\vec{R},\vec{k})\tilde{\mathcal{G}}_\omega(\vec{R},\vec{k}) = 0 \tag{6.214}$$

where $\vec{v}_s$ is the superfluid velocity defined by

$$\vec{v}_s(\vec{r}) = \nabla\chi(\vec{r}) - \frac{e}{c}\vec{A}(\vec{r}) \tag{6.215}$$

This is the same definition as in (5.148) if we notice that $\chi = \phi/2$. Shifting the chemical potential μ by $v_s^2/2$, we have

$$\frac{1}{2}(\vec{k}\pm\vec{v}_s)^2 - \mu = \epsilon_{\vec{k}} \pm \vec{k}\cdot\vec{v}_s \tag{6.216}$$

Gorkov equations will then be simplified to

$$\begin{pmatrix} i\omega_n - \epsilon_{\vec{k}} - \vec{k}\cdot\vec{v}_s & \tilde{\Delta} \\ \tilde{\Delta}^* & i\omega_n + \epsilon_{\vec{k}} - \vec{k}\cdot\vec{v}_s \end{pmatrix}\begin{pmatrix}\tilde{\mathcal{G}}\\ \tilde{\mathcal{F}}\end{pmatrix} = \begin{pmatrix}1\\0\end{pmatrix} \tag{6.217}$$

and their solutions will be

$$\begin{aligned}\tilde{\mathcal{G}}_\omega(\vec{R},\vec{k}) &= \frac{i\omega_n - \vec{k}\cdot\vec{v}_s(\vec{R}) + \epsilon_{\vec{k}}}{[i\omega_n - \vec{k}\cdot v_s(\vec{R})]^2 - E^2_{\vec{k}}(\vec{R})} \\ \tilde{\mathcal{F}}^{\dagger}_\omega(\vec{R},\vec{k}) &= \frac{-\tilde{\Delta}^*(\vec{R},\vec{k})}{[i\omega_n - \vec{k}\cdot\vec{v}_s(\vec{R})]^2 - E^2_{\vec{k}}(\vec{R})}\end{aligned} \tag{6.218}$$

Notice that the only difference between these and (6.207) is a Doppler shift (by $\vec{k} \cdot \vec{v}_s$) in the Matsubara frequencies. We again sum over the Matsubara frequencies in the gap equation to get

$$\tilde{\Delta}(\vec{R},\vec{k}) = -\int d^3k' \tilde{V}(\vec{k}-\vec{k}') \frac{\tilde{\Delta}(\vec{R},\vec{k}')}{2E_{\vec{k}'}(\vec{R})} \{ f[\vec{k}' \cdot v_s(\vec{R}) - E_{\vec{k}'}(\vec{R})] - f[\vec{k}' \cdot \vec{v}_s(\vec{R}) + E_{\vec{k}'}(\vec{R})] \} \tag{6.219}$$

where

$$f(E) = \frac{1}{e^{\beta E}+1} \tag{6.220}$$

is the Fermi distribution function and β is the inverse temperature $1/T$. Note that as $\vec{v}_s \to 0$, this reduces to (6.210).

6.1.2 Calculation of Current in a Superconductor

The current density, in terms of the Green functions, can be written as

$$\begin{aligned} \vec{j}(r) &= \frac{ie}{2} \lim_{\vec{r}\to\vec{r}'} \sum_\sigma (\nabla_{\vec{r}'} - \nabla_{\vec{r}}) < \psi^\dagger_\sigma(\vec{r}')\psi_\sigma(\vec{r}) > -\frac{e^2}{c}\vec{A}(\vec{r}) \sum_\sigma < \psi^\dagger_\sigma(\vec{r})\psi_\sigma(\vec{r}) > \\ &= \frac{ie}{2} \lim_{\vec{r}\to\vec{r}'} \sum_\sigma (\nabla_{\vec{r}'} - \nabla_{\vec{r}}) \mathcal{G}(\vec{r}0,\vec{r}'0^+) - \frac{e^2}{c}\vec{A}(\vec{r}) \sum_\sigma \mathcal{G}(\vec{r}0,\vec{r}0^+) \\ &= ie \lim_{\vec{r}\to\vec{r}'} (\nabla_{\vec{r}'} - \nabla_{\vec{r}}) \tilde{\mathcal{G}}(\vec{r}0,\vec{r}'0^+) + 2e\vec{v}_s(\vec{r})\tilde{\mathcal{G}}(\vec{r}0,\vec{r}0^+) \end{aligned} \tag{6.221}$$

The current in this form is manifestly gauge invariant. Keeping in mind that the superfluid density is $n_s(\vec{r}) = \sum_\sigma < \psi^\dagger_\sigma(\vec{r})\psi_\sigma(\vec{r}) >= 2\tilde{\mathcal{G}}(\vec{r}0,\vec{r}0^+)$, the current can be written as

$$\vec{j}(\vec{r}) = en_s\vec{v}_s(\vec{r}) + \vec{j}_{qp}(\vec{r}) \tag{6.222}$$

where

$$\vec{j}_{qp}(\vec{r}) = ie \lim_{\vec{r}\to\vec{r}'} (\nabla_{\vec{r}'} - \nabla_{\vec{r}}) \tilde{\mathcal{G}}(\vec{r}0,\vec{r}'0^+) \tag{6.223}$$

$\vec{j}_{qp}$ turns out to be the current due to quasiparticle excitations in the superconductor. Fourier transforming, using the same techniques discussed in the last subsection, we get

$$\vec{j}_{qp}(\vec{R}) = ie \int \frac{d^3k}{(2\pi)^3} (\nabla_{\vec{R}} - 2i\vec{k}) \frac{1}{\beta} \sum_n \tilde{\mathcal{G}}_\omega(\vec{R}, \vec{k}) \tag{6.224}$$

Again under quasi-classical approximation, one can neglect $\nabla_{\vec{R}}$ and write

$$\begin{aligned} \vec{j}_{qp}(\vec{R}) &= \frac{2e}{\beta} \sum_n \int \frac{d^3k}{(2\pi)^3} \vec{k} \tilde{\mathcal{G}}_\omega(\vec{R}, \vec{k}) \\ &= e \int \frac{d^3k}{(2\pi)^3} \vec{k} \{ (1 + \frac{\epsilon_{\vec{k}}}{E_{\vec{k}}}) f[E_{\vec{k}} + \vec{k} \cdot \vec{v}_s(\vec{R})] - (1 - \frac{\epsilon_{\vec{k}}}{E_{\vec{k}}}) f[E_{\vec{k}} - \vec{k} \cdot \vec{v}_s(\vec{R})] \} \end{aligned} \tag{6.225}$$

In the last step, we have performed a Matsubara sum. Combining the two terms the current can be written as

$$\vec{j}_{qp}(\vec{R}) = -2e \int \frac{d^3k}{(2\pi)^3} \vec{k} f[E_{\vec{k}} - \vec{k} \cdot \vec{v}_s(\vec{R})] \tag{6.226}$$

or

$$\vec{j}_{qp}(\vec{R}) = -4eN_F \left\langle \vec{v}_F \int_0^\infty d\xi f \left(\sqrt{\xi^2 + |\Delta|^2} - \vec{v}_F \cdot \vec{v}_s \right) \right\rangle_{FS} \tag{6.227}$$

where N_F is the density of states at the Fermi surface and $\langle ... \rangle_{FS}$ represents averaging over the Fermi surface. Note that Δ, in general, can depend on the point on the Fermi surface. Equation (6.227) has a natural interpretation. The argument of the Fermi distribution function f is the Doppler shifted quasiparticle energy at the particular point on the Fermi surface. Thus (6.227) is actually a Fermi surface average of the current due to the quasiparticles excited via thermal excitation plus the Doppler shift. This can be viewed as a normal fluid in the opposite direction of the superfluid that tends to reduce the supercurrent density. At zero temperature, the Fermi function is a step function which is zero unless its argument is negative. Therefore (6.227) is zero unless

$$\vec{v}_F \cdot \vec{v}_s > |\Delta| \tag{6.228}$$

Eq. (6.228) actually defines a critical value $v_c = |\Delta|_{\min}/v_F$ for the superfluid velocity v_s, beyond which the superconducting gap vanishes at some regions of the Fermi surface. Increasing v_s beyond v_c increases the number of quasiparticle excitations and eventually destroys the superconductivity. Therefore, there is an interval of v_s over which we can have superconductivity with a gap that vanishes in some region of the Fermi surface. This is usually known as *gapless superconductivity.* For an s-wave superconductor, (6.228) gives a finite critical value for the superfluid velocity. For a d-wave superconductor (or any superconductor with nodes in the superconducting gap) on the other hand, the gap vanishes at the nodes even at zero v_s. In other words, quasiparticles exist at node lines even for infinitesimal v_s and zero temperature. This phenomenon is highly anisotropic because the nodes exist only at four symmetric points on the Fermi surface. The effect of these nodal quasiparticles in the Meissner state was studied by Yip and Sauls [104] and others [153]. Here, we focus on the effect in the vortex state; which has been studied in [132, 146]. We again derive a generalized London equation and solve it numerically for a vortex lattice to calculate physical quantities.

6.2 Generalized London Equation

As we mentioned earlier, the fourfold anisotropic nature of the gap nodes is expected to influence the magnetic properties of a d-wave superconductor. This influence will be via two distinct effects: a *nonlinear* effect due to quasiparticle generation because of Doppler shift in the quasi-particle spectrum, and *nonlocal* effect due to divergence of the coherence length along the nodal directions. In this section we study these effects in two separate subsections. In what follows we assume that these two effects can be studied independently and their effects are additive. In other words, we assume that any interconnection between these two effects produces higher order corrections to our generalized

London equation. In general the excitation of quasiparticles at the gap nodes can affect the coherence length and therefore the nonlocality of the system. Similarly nonlocalities can change the form of Eq. (6.227). This effect which is neglected in our calculations has been studied extensively in the context of superfluid ^{3}He [154].

6.2.1 Nonlinear Corrections

Let us first neglect any nonlocal effect and focus on the quasiparticles generated at the gap nodes. As we mentioned at the end of the last section, excitation of quasiparticles at the gap nodes produces a current density flowing in the direction opposite to the superfluid velocity - sometimes called back-flow. The total current is given by (6.222). We again define the superfluid velocity by

$$\vec{v}_s = \frac{1}{2}(\nabla\phi - \frac{2e}{c}\vec{A}). \tag{6.229}$$

with ϕ being the phase of the order parameter. In this definition, $\vec{v}_s$ is in the direction of the superfluid, i.e. in the opposite direction of motion of the Cooper pairs (which is used in [104, 146] as the definition for the direction of $\vec{v}_s$). The contribution of the quasiparticles generated at the nodes to the total current is given by (6.227) which we rewrite it as

$$\vec{j}_{qp} = -4eN_F \int_{FS} ds\vec{v}_F(s) \int_0^\infty d\xi f(\sqrt{\xi^2 + \Delta(s)^2} - \vec{v}_F(s)\cdot\vec{v}_s) \tag{6.230}$$

where s parameterizes a point on the Fermi surface. $\Delta(s)$ is the superconducting gap which in general can have s-wave, d-wave, or other symmetries. At zero temperature (6.230) leads to

$$\vec{j}_{qp} = -4eN_F \int ds\vec{v}_F(s)\theta(\vec{v}_F\cdot\vec{v}_s - |\Delta|)\sqrt{(\vec{v}_F\cdot\vec{v}_s)^2 - \Delta^2} \tag{6.231}$$

At higher temperatures however, this gives the first term in the Sommerfeld expansion; which is a good approximation as long as $T < T^\star = T_c(H/H_0)$, where H_0 is of order of the

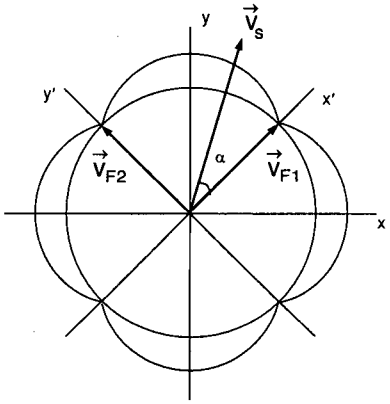

Figure 6.13: Circular Fermi surface with a $d_{x^2-y^2}$ gap. Quasiparticles will be excited at nodes marked by $\vec{v}_{F1}$ and $\vec{v}_{F2}$ opposite to $\vec{v}_s$.

thermodynamic critical field, H_c [104]. The presence of the θ-function in (6.231), results in excitations only at the nodes which are in the direction of $\vec{v}_s$. Fig. 6.13 illustrates a circular Fermi surface with a d-wave gap. The quasiparticles are excited at the nodes marked by $\vec{v}_{F1}$ and $\vec{v}_{F2}$ in the direction of $\vec{v}_s$. For a small enough v_s, the excitations stay very close to the gap nodes. Therefore, one can linearize the gap function near the nodes writing $\Delta(\theta) \simeq \gamma\Delta_0\theta$, with Δ_0 the maximum gap and γ defined by

$$\gamma = \frac{1}{\Delta_0}[\frac{d}{d\theta}\Delta(\theta)]_{\text{node}} \tag{6.232}$$

The most commonly used form for a d-wave gap is $\Delta(\theta) = \Delta_0 \cos(2\theta)$. In that case, (6.232) leads to $\gamma = 2$. The component of $\vec{j}_{qp}$ along the x'-direction which is diagonal to the x and y (a and b) directions (as illustrated in Fig. 6.13) is then

$$\begin{aligned} j_{qpx'} &= -4eN_F v_F \int_{-\theta_c}^{\theta_c} \frac{d\theta}{2\pi} \sqrt{(v_F v_s \cos\alpha)^2 - |\gamma\Delta_0\theta|^2} \\ &= -en_s \frac{v_s^2}{v_0} \cos\alpha |\cos\alpha| = -en_s \frac{v_{sx'}|v_{sx'}|}{v_0} \end{aligned} \tag{6.233}$$

α is the angle between v_s and x'-axis, $n_s = N_F v_F^2$ is the superfluid density, $v_0 = \gamma\Delta_0/v_F$ is some characteristic velocity and θ_c is a cut off imposed by the θ-function in (6.231).

Similarly the y'-component is

$$j_{qpy'} = -en_s \frac{v_{sy'}|v_{sy'}|}{v_0} \tag{6.234}$$

and the total current thereby becomes

$$\vec{j} = en_s[\vec{v}_s - (v_{sx'}|v_{sx'}|\hat{x}' + v_{sy'}|v_{sy'}|\hat{y}')/v_0]. \tag{6.235}$$

The nonanalytic nature of the effect is evident from this equation. It is now possible to write a free energy in such a way that (6.235) can be obtained by minimization with respect to $\vec{A}$. Keeping in mind that $\vec{j} = (c/4\pi)\nabla \times \vec{B} = (c/4\pi)\nabla \times \nabla \times \vec{A}$ and $\partial/\partial\vec{v}_s = -\frac{c}{e}\partial/\partial\vec{A}$, the corresponding free energy density can be written as

$$f = n_s\left[\frac{1}{2}v_s^2 - \frac{1}{3v_0}(|v_{sx'}|^3 + |v_{sy'}|^3)\right] + \frac{B^2}{8\pi} \tag{6.236}$$

In general, it is possible to solve (6.235) for $\vec{v}_s$ in terms of $\vec{j} = (c/4\pi)\nabla \times \vec{B}$, substitute it into (6.236) and write down a London free energy only in terms of $\vec{B}$ and its derivatives. However, instead of solving (6.235) exactly, we find $\vec{v}_s$ perturbatively assuming that the nonlinear part is much smaller than the linear part. This way we get a polynomial correction to the London equation which is convenient for numerical purposes. To first order in perturbation theory we have

$$\vec{v}_s = \frac{c}{4\pi en_s}\left[\nabla \times \vec{B} + \frac{c}{4\pi en_s v_0}\left((\nabla \times \vec{B})_{x'}|\nabla \times \vec{B}|_{x'}\hat{x}' + (\nabla \times \vec{B})_{y'}|\nabla \times \vec{B}|_{y'}\hat{y}')\right)\right] \tag{6.237}$$

Substituting this into (6.236) and keeping the lowest order terms, the London free energy density becomes

$$f_L = \frac{1}{8\pi}\Big[B^2 + \lambda_0^2(\nabla \times \vec{B})^2 + (\frac{2\pi}{3\gamma})\frac{\xi_0\lambda_0^2}{B_0}(|(\nabla \times \vec{B})_{x'}|^3 + |(\nabla \times \vec{B})_{y'}|^3)\Big] \tag{6.238}$$

where $\lambda_0 = \sqrt{c^2/4\pi e^2 n_s}$ is the zeroth order penetration depth, $\xi_0 = v_F/\pi\Delta_0$ is the coherence length, $B_0 \equiv \phi_0/2\pi\lambda_0^2$ is a characteristic field of the order of H_{c1} and $\phi_0 = \pi c/e$

is the flux quantum. For magnetic fields in the z-direction, (6.238) becomes

$$f_L = \frac{1}{8\pi}\Big[B^2 + \lambda_0^2(\nabla B)^2 + (\frac{2\pi}{3\gamma})\frac{\xi_0\lambda_0^2}{B_0}(|\partial_{x'}B|^3 + |\partial_{y'}B|^3)\Big] = f_L^0 + f_{\rm nl} \tag{6.239}$$

with f_L^0 and f_{nl} representing the ordinary London free energy density and the leading nonlinear correction to the free energy density respectively. The corresponding London equation is given by

$$-\lambda_0^2\nabla^2 B + B - (\frac{2\pi}{\gamma})\frac{\xi_0\lambda_0^2}{B_0}(\partial_{x'}^2 B|\partial_{x'}B| + \partial_{y'}^2 B|\partial_{y'}B|) = 0 \tag{6.240}$$

A similar London equation is also derived by Zutic and Valls who investigated the effect in the Meissner state [153].

In order to find the magnetic field distribution in a vortex lattice, one has to insert a source term $\Sigma_j\rho(\vec{r} - \vec{r}_j)$ on the right hand side of (6.240) with $\vec{r}_j$ being the position of the vortices in the lattice. The function $\rho(\vec{r})$ takes into account the vanishing of the order parameter at the center of the vortex cores. Numerically, it is more convenient to work in Fourier space rather than real space. Fourier transforming (6.240) with a proper source term on the right hand side yields

$$B_{\vec{k}} + \lambda_0^2 k^2 B_{\vec{k}} - G_{\rm nl}(\vec{k}, B_{\vec{k}}) = \bar{B}F(\vec{k}) \tag{6.241}$$

where $\vec{k}$ is a reciprocal lattice wave vector, $G_{\rm nl}$ is the Fourier transform of the nonlinear term and $\bar{B}$ is the average magnetic field. The cut off function $F(\vec{k})$ comes from the Fourier transformation of the source term and removes the divergences by cutting off the momentum sums. We are going to use Gaussian cutoff (5.168) in our numerical calculation in the next section.

6.2.2 Nonlocal Corrections

In our derivation of the corrections to the London equation in the previous subsection, we derived a local relation between current density $\vec{j}$ and superfluid velocity $\vec{v}_s$ (or vector

potential $\vec{A}$). This was a result of the *local approximation* we used in our derivation. In fact, this relation is always nonlocal over the length scale of the coherence length ξ_0; which is of the order of the finite spatial extent of the Cooper pair [130]. Magnetic field in a superconductor varies in the length scale given by London penetration depth λ_0 and therefore nonlocal corrections to physical quantities, such as the effective penetration depth, will be of order κ^{-2}, where $\kappa \equiv \lambda_0/\xi_0$ is the GL ratio. For strongly type II materials ($\kappa \gg 1$) such corrections are negligible. Since cuprate superconductors fall well within this class (κ is of 50 for most) local electrodynamics is usually used. However, a closer examination suggests that this might not be justified in all situations, if, as it is widely believed, these materials exhibit nodes in the gap. In such a case in place of the usual coherence length $\xi_0 = v_F/\pi\Delta_0$ one is forced to define an angle dependent quantity, $\xi_0(\hat{p}) = v_F/\pi\Delta_{\hat{p}}$, which diverges along the nodes. Clearly, in the vicinity of nodes the condition $\lambda_0/\xi_0(\hat{p}) \gg 1$ is no longer satisfied and, in fact, the extreme nonlocal limit is achieved. Nonlocal corrections therefore cannot be dismissed in unconventional superconductors. The effect of these corrections on the temperature dependence of penetration depth at low T was studies by Kosztin and Leggett [111]. Here, we discuss about the effect on the vortex lattice properties. What we follow here is based on a work published in Ref. [132]. From the above arguments, it is clear that corrections due to the nonlocal effects at the gap nodes will be highly anisotropic and will in general break the rotational symmetry of the flow field around the vortex, contributing an anisotropic component to the inter-vortex interaction in the mixed state.

Let us now find these nonlocal corrections to the London model neglecting all the nonlinear effects discussed in the previous subsection. In the next subsection, we will combine these two effects into a single London equation to be used in numerical evaluations. Nonlocal relation between $\vec{j}$ and $\vec{A}$ is conveniently written in the Fourier space as

[130]

$$\vec{j}_k = -(c/4\pi)\hat{Q}(\vec{k})A_k. \tag{6.242}$$

Here $\hat{Q}(\vec{k})$ is the electromagnetic response tensor which can be computed, within the weak coupling theory, by generalizing the standard linear response treatment of Gorkov equations [155] to an anisotropic gap. We find

$$Q_{ij}(\vec{k}) = \frac{4\pi T}{\lambda_0^2} \sum_{n>0} \left\langle \frac{\Delta_{\hat{p}}^2 \hat{v}_{Fi} \hat{v}_{Fj}}{\sqrt{\omega_n^2 + \Delta_{\hat{p}}^2}(\omega_n^2 + \Delta_{\hat{p}}^2 + \gamma_{\vec{k}}^2)} \right\rangle, \tag{6.243}$$

where $\gamma_{\vec{k}} = \vec{v}_F \cdot \vec{k}/2$, $\lambda_0 = \sqrt{c^2/4\pi e^2 v_F^2 N_F}$ is the London penetration depth as before, ω_n are the Matsubara frequencies and the angular brackets again mean the Fermi surface averaging. Derivation of (6.243) involves a calculation of the perturbative correction to the Green's functions to linear order in $\vec{A}$ using Gorkov's equations. The result is then used to calculate the supercurrent $\vec{j}$ [155]. Eq. (6.243) is valid for arbitrary Fermi surface and gap function. For isotropic gap one recovers an expression derived by Kogan *et al.* from the Eilenberger theory [156]. One may simplify solving the London equation again by writing it in terms of magnetic field only. Eliminating $\vec{j}$ from (6.242) using the Ampère's law $\vec{j} = (c/4\pi)\nabla \times \vec{B}$, one obtains

$$\vec{B}_k - \vec{k} \times [\hat{Q}^{-1}(\vec{k})(\vec{k} \times \vec{B}_k)] = 0. \tag{6.244}$$

To study vortex lattice using this formalism, it is necessary to insert a cutoff function $F(k)$ on the right-hand side of the Eq. (6.244). In our numerical calculations in the next section we again use Gaussian cutoff function (5.168). For many purposes it is also convenient to write down the corresponding London free energy, such that $\delta\mathcal{F}_L/\delta\vec{B}_k = 0$ gives the above London equation:

$$\mathcal{F}_L = \sum_{\vec{k}} [\vec{B}_k^2 + (\vec{k} \times \vec{B}_k)\hat{Q}^{-1}(\vec{k})(\vec{k} \times \vec{B}_k)]/8\pi. \tag{6.245}$$

At long wavelengths $\hat{Q}(\vec{k})$ can be evaluated by expanding expression (6.243) in powers of $\gamma_{\vec{k}}^2$. The zeroth order term

$$Q_{ij}^{(0)} \equiv \delta_{ij}\lambda^{-2} = \frac{4\pi T}{\lambda_0^2}\sum_{n>0}\left\langle \frac{\Delta_{\hat{p}}^2 \hat{v}_{Fi}\hat{v}_{Fj}}{(\omega_n^2+\Delta_{\hat{p}}^2)^{3/2}}\right\rangle, \tag{6.246}$$

clearly recovers the ordinary London free energy. Here, $\lambda = \lambda(T)$ is the temperature dependent penetration depth which, at low temperatures, has the well known T-linear behavior [157, 33]; for a $d_{x^2-y^2}$ superconductor with $\Delta_{\hat{p}} = \Delta_d(\hat{p}_x^2 - \hat{p}_y^2)$ and a cylindrical Fermi surface (from now on we shall focus on this simple case) $\lambda^{-2} \approx \lambda_0^{-2}(1-2\ln 2T/\Delta_d)$. The leading nonlocal term is quadratic in k:

$$Q_{ij}^{(2)} = -\frac{4\pi T}{\lambda_0^2}\sum_{n>0}\left\langle \frac{\Delta_{\hat{p}}^2 \hat{v}_{Fi}\hat{v}_{Fj}}{(\omega_n^2+\Delta_{\hat{p}}^2)^{5/2}}\gamma_{\vec{k}}^2\right\rangle. \tag{6.247}$$

The expression $Q_{ij} = \delta_{ij}\lambda^{-2} + Q_{ij}^{(2)}$ is easily inverted to leading order in k to get $Q_{ij}^{-1} \approx \lambda^2[\delta_{ij} - \lambda^2 Q_{ij}^{(2)}]$. Substituting this into (6.245) and specializing to fields along the z-direction we have

$$\mathcal{F}_L = \sum_{\vec{k}} B_{\vec{k}}^2[1 + \lambda^2 k^2 + \lambda^2\xi^2(c_1 k^4 + c_2 k_x^2 k_y^2)]/8\pi. \tag{6.248}$$

Here $\xi = v_F/\pi\Delta_d$ and Δ_d is assumed to be a temperature dependent solution to the appropriate gap equation. Dimensionless coefficients c_1 and c_2 are given by

$$c_\mu = \frac{\lambda^2}{\lambda_0^2}\pi^3\Delta_d^2 T\sum_{n>0}\frac{1}{2\pi}\int_0^{2\pi} d\theta \frac{\Delta_{\hat{p}}^2 w_\mu}{(\omega_n^2+\Delta_{\hat{p}}^2)^{5/2}}, \tag{6.249}$$

where $w_1 = \hat{v}_{Fx}^2\hat{v}_{Fy}^2$, $w_2 = (\hat{v}_{Fx}^2 - \hat{v}_{Fy}^2)^2 - 4\hat{v}_{Fx}^2\hat{v}_{Fy}^2$ and the Fermi surface has been explicitly parameterized by the angle θ between $\hat{p}$ and x-axis; $\hat{v}_F = (\cos\theta, \sin\theta)$ and $\Delta_{\hat{p}} = \Delta_d \cos 2\theta$. Coefficients c_1 and c_2 depend on temperature through a dimensionless parameter $t \equiv T/\Delta_d$. From (6.249) one can deduce their leading behavior in the two limiting cases: for $t \ll 1$ we find

$$c_1 = \frac{\pi^2}{8}\frac{\lambda^2}{\lambda_0^2}\frac{1}{t} \quad , \quad c_2 = -4c_1, \tag{6.250}$$

and for $t \gg 1$ (i.e., near T_c)

$$c_1 = \alpha \frac{\lambda^2}{\lambda_0^2} \frac{1}{t^4} \quad , \quad c_2 = 8c_1, \tag{6.251}$$

where $\alpha = \zeta(5)(1 - 2^{-5})/8\pi^2 = 0.01272$. In the above λ also depends on t, but this will be unimportant for the following qualitative discussion.

The free energy (6.248) formally coincides with (5.188), deduced previously in the last chapter with phenomenological considerations. The present model however, allows us to evaluate the coefficient of the symmetry breaking term c_2 (or ϵ in (5.188)). At high temperatures, c_2 is found to be positive; in agreement with our previous result. As we showed in the last chapter, such a term leads to a centered rectangular vortex lattice structure with principal axes oriented along x or y axes of the ionic lattice (see Fig. 6.14a). The magnitude of distortion from a perfect triangular lattice is controlled by the magnitude of c_2 and grows with increasing magnetic field. Eq. (6.251) shows that at fixed field this distortion will initially grow with decreasing temperature. At low temperatures (6.250) predicts $c_2 < 0$. This will lead to the same centered rectangular lattice but rotated by 45° (Fig. 6.14b). Numerical evaluation of (6.249) shows that c_2 passes through zero at $t^* \simeq 0.19$. At this temperature the free energy (6.248) is isotropic and the lattice will be triangular at all fields. The change of sign of c_2 reflects the competition between the two terms of different symmetry in w_2. At $t \ll 1$ only the region around the node is important where $(\hat{v}_{Fx}^2 - \hat{v}_{Fy}^2)^2$ vanishes, while at $t \gg 1$ the average involves the entire Fermi surface to which both terms in w_2 contribute. This change of sign is a unique consequence of nodes in the gap function and would not occur in conventional superconductors.

Another consequence of nodes is the fact that, as can be seen from (6.250), both c_1 and c_2 diverge as $1/t$ for $t \to 0$. This divergence signals that the response tensor $\hat{Q}(\vec{k})$ is a non-analytic function of $\vec{k}$ at $T = 0$, and the expansion in powers of $\gamma_{\vec{k}}^2$ breaks down.

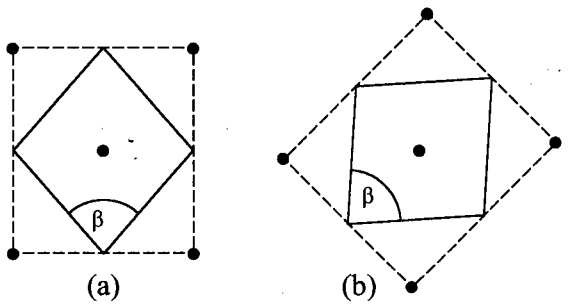

Figure 6.14: Two high symmetry orientations of centered rectangular unit cell.

Formally this is caused by the fact that at $T = 0$, at the nodal point, the expression (6.243) for $Q_{ij}(\vec{k})$ contains a term proportional to $1/\gamma_{\vec{k}}^2$. At $T = 0$ the frequency sum in (6.243) becomes an integral which can be evaluated exactly with the result:

$$Q_{ij}(\vec{k}) = \frac{1}{\lambda_0^2}\left\langle \hat{v}_{Fi}\hat{v}_{Fj}\frac{2\text{arc sinh } y}{y\sqrt{1+y^2}}\right\rangle, \tag{6.252}$$

where $y = \gamma_{\vec{k}}/\Delta_{\hat{p}}$. For small k the dominant contribution to the angular average comes from the close vicinity of nodes and can be evaluated by linearizing $\Delta_{\hat{p}}$ around the nodes. One finds that the leading nonlocal contribution is *linear* in k rather than quadratic. For $Q_{ij} = \delta_{ij}\lambda_0^{-2} + Q_{ij}^{(1)}$, we have $Q_{xx}^{(1)} = Q_{yy}^{(1)} = -\mu(k_M\xi_0)$ and $Q_{xy}^{(1)} = Q_{yx}^{(1)} = -\mu(k_m\xi_0)\text{sgn}(\hat{k}_x\hat{k}_y)$, where $k_M = \max(|k_x|, |k_y|)$ and $k_m = \min(|k_x|, |k_y|)$. Prefactor $\mu = \pi^2/8\sqrt{2} = 0.8723$ is exact in the sense that all corrections to Q_{ij} are $O(k^2)$. The resulting free energy at $T = 0$ is

$$\mathcal{F}_L = \sum_{\vec{k}} B_{\vec{k}}^2[1 + \lambda_0^2k^2 + \mu\lambda_0^2\xi_0k_M(k_M^2 - k_m^2)]/8\pi. \tag{6.253}$$

The nonlocal term is clearly non-analytic in k. Its functional form is universal in the sense that it is independent of the Fermi surface structure (as long as it has the same symmetry as the order parameter) and the prefactor μ only depends on the angular slope of the gap function and Fermi velocity at the node.

The present calculation can be easily generalized to treat the effects of Fermi surface anisotropy. As mentioned above tetragonal anisotropy will not modify the $T \to 0$ universal behavior but may lead to quantitative changes at higher temperatures. Orthorhombic anisotropy, on the other hand, will modify even the $T \to 0$ limit. We expect that it will, to leading order, merely rescale the coordinate axes, leading to the same structures as described above stretched by the axes, leading to the same structures as described above stretched by the appropriate factor [140]. It may further remove the degeneracy between two equivalent lattices related by 90° rotation. Also neglected in our calculation is the effect of electronic disorder, which will remove the non-analyticity of $\hat{Q}(\vec{k})$ at longest wavelengths, just as small finite temperature would. Since the lattice structure is most sensitive to $\hat{Q}(\vec{k})$ at finite $k \sim 1/l$ (l is the vortex spacing), we expect our predictions to be robust with respect to weak disorder.

6.2.3 Combining Nonlinear and Nonlocal Corrections

Having established theories for nonlinear and nonlocal effects independently, we now would like to combine them in one London equation to be used in numerical calculations. Nonlocal effect can be added to the generalized London equation (6.241), simply by replacing the second term with its nonlocal counterpart

$$B_{\vec{k}} + \mathcal{L}_{ij}(\vec{k}) k_i k_j B_{\vec{k}} - G_{\rm nl}(\vec{k}, B_{\vec{k}}) = \bar{B} F(\vec{k}). \tag{6.254}$$

Sums over i and j are implicit here. $\mathcal{L}_{ij}(\vec{k})$ is related to the electromagnetic response tensor $\hat{Q}(\vec{k})$ by

$$\mathcal{L}_{ij}(\vec{k}) = Q_{ij}(\vec{k}) / \det \hat{Q}(\vec{k}). \tag{6.255}$$

The electromagnetic response tensor $\hat{Q}(\vec{k})$ is given by (6.243) for $T \neq 0$, and by (6.252) at $T = 0$.

In the local case, we have $\mathcal{L}_{ij}(\vec{k}) = \lambda_0^2 \delta_{ij}$ which leads back to (6.241). Taking $G_{\rm nl}$ to the right hand side of (6.254), $B_{\vec{k}}$ can be obtained by

$$B_{\vec{k}} = \frac{\bar{B}F(\vec{k}) + G_{\rm nl}(\vec{k}, B_{\vec{k}})}{1 + \mathcal{L}_{ij}(\vec{k})k_i k_j}. \tag{6.256}$$

We will use this equation, in the next section, to find $B_{\vec{k}}$ iteratively for a specific lattice geometry. Having $B_{\vec{k}}$, the free energy can be easily calculated using

$$\mathcal{F} = \mathcal{F}_{\rm nl} + \sum_{\vec{k}} [1 + \mathcal{L}_{ij}(\vec{k})k_i k_j] B_{\vec{k}}^2 \tag{6.257}$$

where $\mathcal{F}_{\rm nl}$ is the free energy due to the nonlinear term in Eq. (6.239)

$$\mathcal{F}_{\rm nl} = (\frac{2\pi}{3\gamma}) \frac{\xi_0 \lambda_0^2}{B_0} \int d^2r \left(|\partial_{x'} B|^3 + |\partial_{y'} B|^3 \right) \tag{6.258}$$

6.3 Numerical Calculations

Unlike Ginsburg-Landau, the London free energy cannot completely determine the vortex lattice by a simple minimization. Instead, one has to impose a set of source terms located at the position of the vortices on an assumed lattice. The functional form of the source terms does not come from the London theory and requires more fundamental treatments; as we discussed in Sec.(5.2.2). Information about the functional form of the source term is included in (6.256) via $F(k)$, and information about the positions of the vortices is included in the reciprocal lattice vectors $\vec{k}$. The free energy must then be minimized with respect to the positions of the vortices in order to find the equilibrium lattice configuration. In general, a 2D lattice can be determined by four parameters. However, it turns out that a centered rectangular lattice is energetically more favorable than an oblique lattice. On the other hand, the vortex lattice spacing is fixed by the average magnetic field $\bar{B}$ ($\bar{B} \approx H$ away from H_{c1}). Thus we are left with two variational parameters, i.e. the lattice orientation with respect to a and b directions and the apex

angle β - the angle between the two basic vectors of the lattice. We therefore find the vortex lattice geometry by minimizing $\mathcal{F}$ in with respect to the apex angle β for different orientations of the lattice.

In our numerical calculation, we first neglect the nonlinear effects and consider only the nonlocal corrections. At the end, we will add the effect of the nonlinear corrections to the results. We shall see that the nonlinear corrections are subdominant to the nonlocal ones. Therefore the results we obtain, ignoring the nonlinear effects, are actually very close to the reality. In our calculations, we first find B_k using (6.256) but ignoring $G_{\rm nl}$ (i.e. ignoring the nonlinear corrections). Substituting (6.256) into (6.257), and also ignoring $\mathcal{F}_{\rm nl}$, we can calculate the free energy. At $T = 0$, we can alternatively use (6.253) to calculate the free energy. Numerical evaluation, shows that the free energy

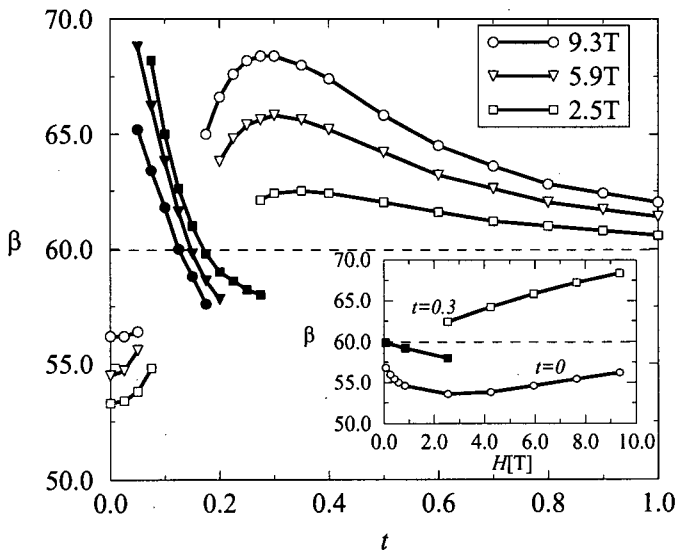

Figure 6.15: Equilibrium angle β as a function of reduced temperature $t = T/\Delta_d$ for various fields. Open symbols mark lattice with orientation along x or y direction while solid symbols mark the lattice rotated by 45°. We use $\lambda_0 = 1400$Åand $\kappa = 68$. Inset: β as a function of field at fixed T.

(6.253) gives rise to a centered rectangular vortex lattice, aligned with x or y axes, but

now with the apex angle $\beta < 60°$; unlike (5.188) which gives a $\beta > 60°$. In order to map out the complete equilibrium H-T phase diagram we have carried out a numerical computation of the vortex lattice structure using the full expression for the response tensor $\hat{Q}(k)$, as given by Eqs. (6.243) and (6.252). We find that the free energy has two local minima for centered rectangular lattices aligned with two high symmetry directions (see Fig. 6.14), as expected from the tetragonal symmetry of the problem. Which of the two becomes the global minimum depends on temperature and field. The results are summarized in Fig. 6.15. For high temperatures, the exact result agrees well with the one obtained from the long wavelength free energy (6.248). The deformation of the lattice from perfect triangular, grows with decreasing temperature, reaches maximum, and then falls. Maximum distortion occurs around $t \simeq 0.3$, attaining $\beta \simeq 70°$ at 10T. Extrapolating this field dependence (see inset to Fig. 6.15), the lattice should become square lattice around $H \approx 30$T, but this field is outside the domain of validity of the London model. At lower temperatures the distortion decreases but instead of going all the way back to triangular at t^*, the lattice undergoes a first order phase transition to another centered rectangular lattice rotated by 45° and with $\beta < 60°$. Further decrease of temperature causes the angle to grow again. We note that the precise temperature at which it crosses 60° depends on field, but for all fields it is close to $t^* = 0.19$, as predicted by the long wavelength approximation. At yet lower temperature we predict another first order transition to a centered rectangular lattice along x (or y) with $\beta < 60°$. It has to be noted that the free energy difference between the two minima is very small in the region where the 45° rotated lattice wins. It is thus likely that real system, in which vortex pinning to various defects occurs, will prefer to remain in the metastable state at these intermediate temperatures. Instead of two consecutive first order transitions the experiment would detect only a smooth crossover from a lattice with $\beta > 60°$ to the one with $\beta < 60°$. Alternatively domains with various orientations may develop.

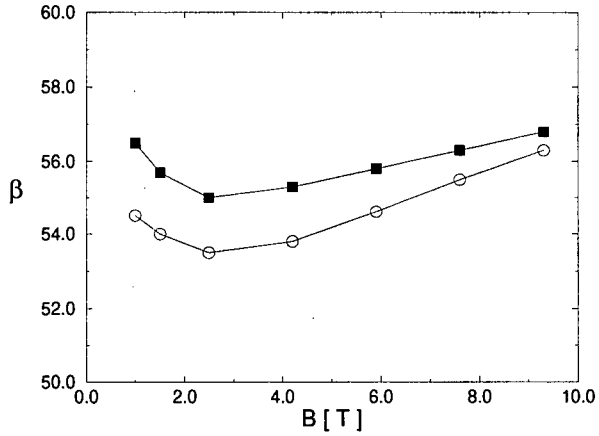

Figure 6.16: Apex angle β as a function of magnetic field B at $T = 0$. Circles represent the result of the calculation using only the nonlocal corrections. Squares correspond to the calculations considering both nonlinear and nonlocal corrections.

At this point, we can add the nonlinear corrections to our numerical calculations. The general strategy is to use (6.256) to calculate $B_{\vec{k}}$ iteratively. At each step $G_{\rm nl}$ has to be calculated numerically. The non-analytic form of $G_{\rm nl}$, prevents us from using usual convolution integrals in our Fourier transformation. Instead, we first calculate $G_{\rm nl}$ on a lattice in a unit cell of the vortex lattice in position space. Then we use Fast Fourier Transformation (FFT) to calculate the Fourier transformed $G_{\rm nl}$ at the reciprocal lattice wave vectors $\vec{k}$. In our numerical calculation, we use $\lambda_0 = 1400$Å, $\kappa = \lambda_0/\xi_0 = 68$ as before and also $\gamma = 2$.

At $T = 0$, the stable orientation of the lattice is again aligned with a and b axes. Fig. 6.16 shows the results of our numerical calculations for β as a function of magnetic field. The upper curve (squares) is the result of combined calculation, considering both nonlocal and nonlinear corrections, i.e. using (6.256) and (6.257). The lower curve (circles) on the other hand, corresponds to taking into account only the nonlocal corrections (this curve is the same as the $t = 0$ curve in the inset of Fig. 6.15). As is clear from Fig. 6.16, the

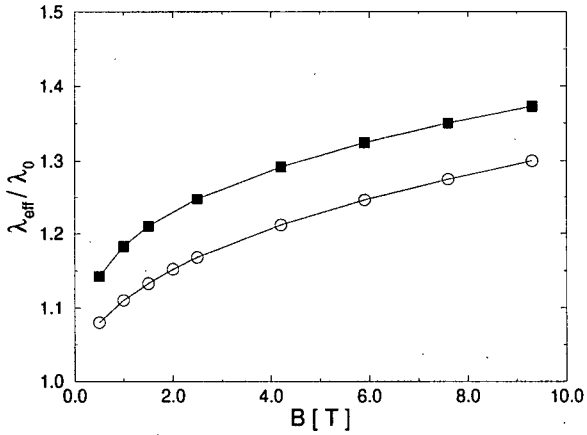

Figure 6.17: The effective penetration depth as a function of the magnetic field. Circles represent the result of the calculations considering only the nonlocal effects whereas squares are the result of combined calculation considering both nonlocal and nonlinear effects.

difference between the two cases is small and about one or two degrees. Therefore, the phase diagram given in Fig. 6.15 retains its validity qualitatively, even after adding the nonlinear correction to the generalized London free energy.

We also calculate the effective penetration depth λ_{eff} for different magnetic fields in almost the same way as it is calculated from μSR data [125]. In these experiments, the μSR precession signal obtained from experiment is fit to a signal obtained by Fourier transforming a theoretical magnetic field distribution function $n(B)$ defined by

$$n(B') = \frac{1}{\Omega} \int d^2r \delta[B' - B(\vec{r})] \tag{6.259}$$

with Ω denoting the area of a unit cell. The magnetic field $B(\vec{r})$ in (6.259) is calculated on a hexagonal vortex lattice with the same average magnetic field as the experimental field and using the ordinary London model with some cutoff function. The λ which provides the best fit to data is considered as λ_{eff}. Here, we calculate λ_{eff} in a different way (but similar in spirit), using the fact that in the ordinary London model, for a general vortex

lattice and for a large enough field,

$$\overline{(B-\bar{B})^2} \equiv \overline{\Delta B^2} = \bar{B}^2 \sum_{\vec{k}\neq 0} \frac{e^{-\xi^2 k^2}}{(1+\lambda^2 k^2)^2} \simeq \lambda^{-4}\bar{B}^2 \sum_{\vec{k}\neq 0} \frac{e^{-\xi^2 k^2}}{k^4} = \Gamma(\xi)\lambda^{-4} \tag{6.260}$$

were $\Gamma(\xi)$ is a function that depends on the structure of the vortex lattice. Associating all the field dependence of $\overline{\Delta B^2}$ in our calculation with the field dependence of an effective penetration depth λ_{eff}, we can define λ_{eff} by

$$\frac{\lambda_{\text{eff}}}{\lambda_0} = \left(\frac{\overline{\Delta B_0^2}}{\overline{\Delta B^2}}\right)^{\frac{1}{4}} \tag{6.261}$$

where $\overline{\Delta B_0^2}$ is the mean squared value of the magnetic field $(B_0(\vec{r}) - \bar{B})$ evaluated using the ordinary London model on a hexagonal lattice with the same average field $\bar{B}$ and with the penetration depth λ_0.

Fig. 6.17 shows the result of our numerical calculation for λ_{eff} using (6.261). The lower curve corresponds to the calculations including only the nonlocal correction. The upper curve corresponds to the result of the calculations using both nonlinear and nonlocal terms. The effect of the nonlinear term to the field dependence of λ_{eff} is almost nothing but an overall shift. Fig. 6.18 exhibits magnetic field distribution $n(B)$ at the average magnetic field $\bar{B} = 5.9T$. The solid line in Fig. 6.18 represents the magnetic field distribution calculated from the nonlinear-nonlocal London equation. The double peak feature is a sign of existing two different saddle points in a unit cell of the lattice which is a result of having a $\beta \neq 60°$. This line-shape is then compared with another line-shape (dashed line) obtained from an ordinary London calculation but with a larger value of λ_0. Similar line shapes with some additional broadening can also be produced from μSR data. The broadening is due to lattice disorder, interaction of muons with nuclear dipolar fields and finite lifetime of muons. The resolution of the magnetic field as a result of this broadening is $\delta B \sim 10^{-3}T$. The difference between the solid line and dashed line in Fig. 6.18 as well as the double peak feature of the solid line is therefore not observable by

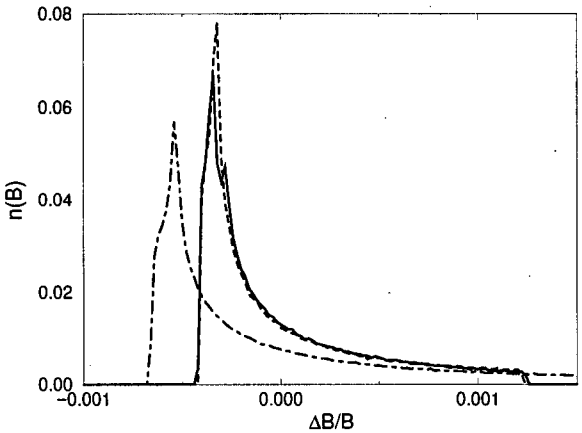

Figure 6.18: **Solid line:** Magnetic field distribution obtained from the nonlinear-nonlocal London equation with $\bar{B} = 5.9T$ and $\lambda_0 = 1400$ Å. **Dot-dashed line:** field distribution obtained from an ordinary London equation on a hexagonal lattice with the same $\bar{B}$ and λ_0. **Dashed line:** Result of the same ordinary London calculation but with $\lambda_0 = 1850$ Å.

μSR experiments because of these broadening effects. Thus as far as these line-shapes are concerned, it is difficult to distinguish a nonlinear-nonlocal effect from a simple shift in the magnetic penetration depth in the ordinary London model. Fig. 6.19 compares the effect of including both nonlinear and nonlocal corrections to the London equation with the effect of including only the nonlocal term. Comparing the two line-shapes, it is apparent that the effect of the nonlinear term is small compared to the nonlocal term as was emphasized before.

6.4 Conclusion

Ordinary London theory is not adequate to describe all the different properties of a vortex lattice in high T_c superconductors; especially the properties resulting from the presence of the superconducting gap nodes or other anisotropies on the Fermi surface. However,

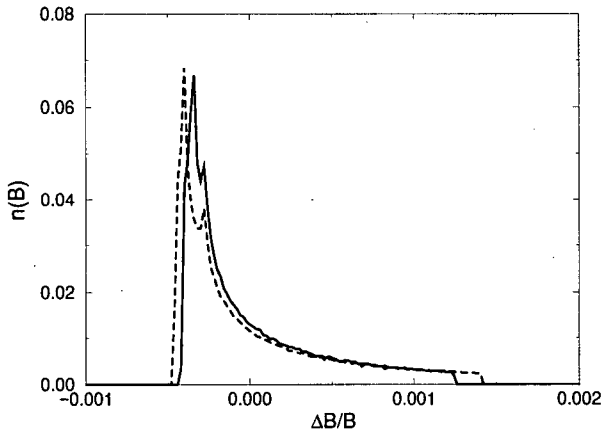

Figure 6.19: **Solid line:** Magnetic field distribution obtained from the nonlinear-nonlocal London equation. **Dashed line:** Magnetic field distribution obtained from a London equation including only the additional nonlocal term using the same parameters.

as we established throughout this thesis, a generalized London model with appropriate higher order corrections which take into account these anisotropic effects, can still provide a fairly simple way to calculate different properties of a vortex lattice. The corrections we found to the London equation were classified into *nonlocal* and *nonlinear* ones. In both analytic and non-analytic (low T) cases, nonlocal corrections play the dominant role in determining the vortex lattice properties.

Equilibrium vortex lattice geometry exhibits novel field and temperature dependence owing to the fourfold anisotropic effects expressed by the corrections to the London equation (Fig. 5.11, Fig. 6.15 and Fig. 6.16). Numerical calculation of the lattice geometry is rather insensitive to the details of the vortex cores. The reason is that the details of the magnetic field inside the vortex cores mainly affect the magnetic self-energies of the vortices. In magnetic fields far below H_{c2} on the other hand, the vortex lattice geometry is mostly determined by the magnetic interaction energy between vortices which is not sensitive to the precise shape of the core. Therefore, our replacement of the vortex

core by a simple Gaussian source term should be adequate for the vortex lattice structure calculations.

The effective penetration depth λ_{eff} also exhibits field dependence at low temperatures as illustrated in Fig. 6.17. Some important points need to be emphasized here:

(i) The field dependence of λ_{eff} is not linear as is evident from Fig. 6.17. Variation of λ_{eff} with magnetic field is faster at lower fields. At low magnetic fields, the relative variation of the effective penetration depth in our calculation is about 7% for an increase of 1T in the magnetic field which is close to 7.3% variation obtained from μSR data for an optimally doped and 9.5% variation for a detwinned underdoped YBCO single crystal using the same cutoff function as (5.168) for fitting calculations [125, 127]. Most recent μSR results [158] extrapolated to $T = 0$, has provided a measurement of λ_{eff} as a function of magnetic field up to 7.5T. An excellent agreement between this result and our nonlinear-nonlocal theory is presented in Fig. 6.20.

(ii) More importantly, this field dependence of λ_{eff} has a predominantly nonlocal origin rather than a nonlinear one; contrary to what is generally believed. The contribution of the nonlinear term to the total (minimized) free energy is almost one order of magnitude smaller than the nonlocal term. What is more important however, is the field dependence and β dependence of these terms not their orders of magnitude at fixed β and B. As we mentioned earlier, we consider β as a variational parameter to be fixed by minimizing the London free energy. As can be inferred from Fig. 6.16 and Fig. 6.17, the field dependence and β dependence of the nonlinear term in the free energy is also smaller than the nonlocal term. It is worth noting that in the Meissner state, a linear nonlocal term can never produce field dependence in the penetration depth (as it is usually defined in that state) and therefore a nonlinear term is necessary for such an effect [104]. In the vortex state on the other hand, a nonlocal term can result in a field dependent effective penetration depth, if we define it the way it is defined in μSR experiments. We should

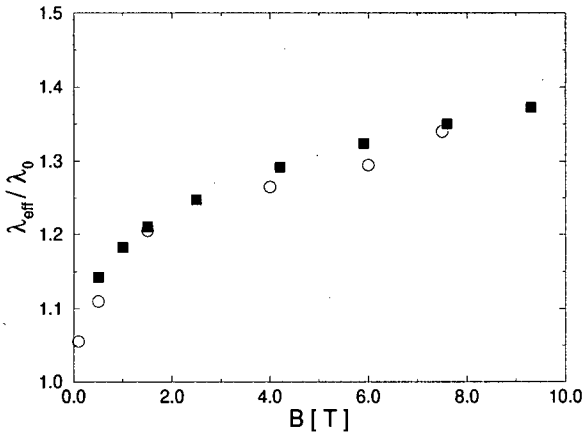

Figure 6.20: Comparison between our nonlinear-nonlocal theory and a recent μSR result at $T = 0$. Squares represent our calculation of the effective penetration depth using nonlinear-nonlocal model (cf. Fig. 6.17). Circles correspond to the recent μSR data [158]. Our λ_0 (= 1400 Å) is a fitting parameter which might be different from the measured value.

emphasize here that in this way of definition, $\lambda_{\text{eff}}^{-2}$ does not directly give the superfluid density as it does in the Meissner state..

To understand this better, let's neglect the nonlinear term and assume a linear but nonlocal London equation. The total magnetic field, in this case, will be the superposition of the fields around individual vortices. The magnetic field around an isolated vortex is given by

$$B(\vec{r}) = \Phi_0 \int \frac{d^2k}{(2\pi)^2} \frac{F(k)e^{i\vec{k}.\vec{r}}}{1 + \mathcal{L}_{ij}(\vec{k})k_i k_j} \tag{6.262}$$

where Φ_0 is the flux quantum and $F(k)$ is the cutoff function resulting from the source term. $\mathcal{L}_{ij}(\vec{k})$ is defined in (6.255). The field decays with some constant (field independent) decay rate λ; which is the Meissner state penetration depth (see Fig. 6.21). Increasing the magnetic field does not affect the profile of the magnetic field and therefore λ. Rather it squeezed the vortices together. For small values of k, $\mathcal{L}_{ij}(\vec{k}) \approx \lambda_o^2 \delta_{ij}$. Since small k

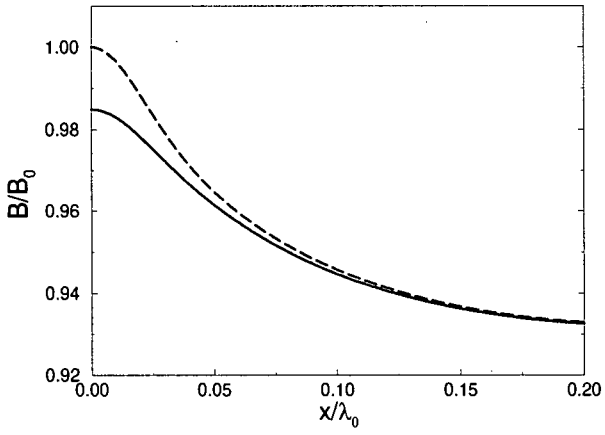

Figure 6.21: Magnetic field as a function of the distance from the center of the vortex (a-direction) for an isolated vortex. The solid line corresponds to the nonlocal London equation whereas the dashed line represents an ordinary London calculation with the same value of λ_0. $B_0 = B(r = 0)$ for the ordinary London vortex.

corresponds to large r, one expects an isotropic field, similar to the local London case, far away from the vortex core. For large values of k on the other hand, $\mathcal{L}_{ij}(\vec{k})$ has strong k-dependence with four-fold anisotropy. Thus the closer to the vortex core, the more deviation form an isotropic ordinary London single vortex is expected, as is clearly shown in Fig. 6.21. At low magnetic fields, the vortices are far apart and their magnetic fields overlap in regions far away from their cores. The properties of the vortex lattice should then be similar to the ordinary london hexagonal lattice. As the magnetic field is increased, the vortices come closer to each other. Although the profile of the magnetic field around each vortex remains unchanged, the overlap regions will be closer to the vortex cores and will be more affected by the nonlocal term. Therefore, it is conceivable that at large magnetic fields, the vortex lattice properties such as the magnetic field distribution will be affected by the nonlocal term in the London equation. The magnetic field near the vortex core is always reduced by the nonlocal term as is clear in Fig. 6.21.

This is because $\mathcal{L}_{ij}(\vec{k}) - \lambda_0^2\delta_{ij}$ is a positive definite tensor for all k and therefore the denominator of the integrand in (6.262) is always larger than the corresponding ordinary London one. As a result, the magnitude of $\overline{\Delta B^2}$ is smaller for the nonlocal case and therefore λ_{eff} defined by (6.261) tends to be larger. This explains why $\lambda_{\text{eff}}/\lambda_0$ is always greater than one in Fig. 6.17. Fig. 6.18 exhibits the resemblance between a change in the magnetic field distribution due to the nonlocal term and due to a shift in the ordinary London penetration depth. The slight difference between the solid and dashed lines in Fig. 6.18 would be unobservable in μSR experiments as a result of the broadening effects. Since no field dependence due to the nonlocal term is expected in the Meissner state, λ_{eff} as defined here and also in μSR experiments is expected to be conceptually different from what is usually defined as penetration depth in the Meissner state, although they are closely related.

(iii) The magnitude and field dependence of λ_{eff} is not so sensitive to the apex angle β. In other words, a few degrees change in the variational parameter β does not modify the magnetic field distribution as much as a variation in the average magnetic field does.

(iv) Calculation of λ_{eff} is rather sensitive to the form of the vortex source term. The importance of the source term in the calculation of $\overline{\Delta B^2}$ has already been emphasized by Yaouanc *et al.*[159]. In Ref.[125], λ_{eff} is obtained by fitting to the μSR data using both a Gaussian cutoff ((5.168)) and also the cutoff function proposed by Hao *et al.*[160, 159]. The difference between the two cases is significant and about 30% for the magnitude of λ_{eff} and even more (for detwinned sample) for the relative variation with respect to the magnetic field. This can explain the importance of the source term in calculations of the effective penetration depth.

μSR experiments [125, 128] on $NbSe_2$, which is believed to be a conventional superconductor, also show a field dependence in the effective penetration depth; although it

is much weaker than what is observed in high T_c compounds. Since there is no node in the superconducting gap of these materials, the theory presented in this thesis cannot explain this field dependence. However, since the size of the vortex core in these materials is large and comparable to the vortex lattice spacing for the magnetic fields of experimental interest, it is conceivable that a significant effect can come from the cores as is pointed out in Ref. [159]. Thus, a more careful consideration of the vortex core might be necessary in order to have a better quantitative explanation of the experimental results.

Bibliography

[1] J.G. Bednorz, K.A. Muller, Z. Phys. **64**, 189 (1986).

[2] P.W. Anderson, Science **235**, 1196 (1987).

[3] F.C. Zhang and T.M. Rice, Phys. Rev. B **37**, 3759 (1988).

[4] E. Manousakis, Reviews of Modern Physics **63**, 1 (1991).

[5] P. C. Hohenberg, Phys. Rev. **158**, 383 (1967); N. D. Mermin and H. Wagner, Phys. Rev. Lett. **17**, 1133 (1966).

[6] S. Chakravarty, B.I. Halperin, and D.R. Nelson, Phys. Rev. B **39**, 2344 (1989).

[7] D.S. Marshall, D.S. Dessau, A.G. Loeser, C.-H. Park, A.Y. Matsuura, J.N.Eckstein, I. Bosovic, P. Fournier, A. Kapitulnik W.E. Spicer and Z.-X. Shen Phys. Rev. Lett. **76**, 4841 (1996).

[8] T.E.Mason, G.Aeppli, and H.A.Mook, Phys. Rev. Lett. **68**, 1414 (1992); S.-W.Cheong *et al.*, Phys. Rev. Lett. **67**, 1791 (1991).

[9] Y. Fukuzumi, K. Mizuhashi, K. Takenaka and S. Ushida, Phys. Rev. Lett. **76**, 684 (1996).

[10] Y. Ando, G.S. Boebinger, A. Passner, T. Kimura and K. Kishio, Phys. Rev. Lett. **75**, 4662 (1995).

[11] C. Berthier, Y. Berthier, P. Butaud, W.G. Clark, J.A. Gillet M. Horvatić, P. Ségransan and J.Y. Henry, Appl. Magn. Reson. **3**, 449 (1992).

[12] An excelent survey is the recent preprint by: T. Timusk and B. Statt, cond-mat/9905219.

[13] Pengcheng Dai, H.A. Mook, and F. Doğan, Phys. Rev. Lett. **80**, 1738 (1998).

[14] For a review see C. Berthier, M.H. Julien, M. Horvatić, and Y. Berthier, J. Phys. I France **6**, 2205 (1996);

[15] Another excelent review is: C.P. Slichter, in *Strongly Correlated Electron Systems*, edited by K.S. Bedell *et al.* (Addison-Wesely, Reading, MA, 1994).

[16] M. Takigawa, P.C. Hammel, R.H. Hefner, Z. Fisk J.L. Smith and R.B. Schwarz, Phys. Rev. Lett. **63**, 1865 (1989).

[17] M. Horvatić, Y. Bertheir, P. Butaud, Y. Kitaoka, P. Ségransan, C. Berthier, H. Katayama-Yoshida, Y. Ohabe and T. Takahashi, Physica C **159**, 689 (1989).

[18] H. Alloul, T. Ohno and P. Mendels, Phys. Rev. Lett. **63**, 1700 (1989).

[19] B.S. Shastry, Phys. Rev. Lett. **63** 1288 (1989).

[20] F. Mila and T.M. Rice, Physica **157C**, 581 (1989).

[21] T. Moriya, J. Phys. Soc. Jpn. **18**, 515 (1963).

[22] C.H. Pennington, D.J. Durand, C.P. Slichter, J.P. Rice, E.D. Bukowski and D.M. Ginsberg, Phys. Rev. B **39**, 274 (1993).

[23] A. J. Millis, H. Monien and D. Pines, Phys. Rev. B **42**, 167 (1990).

P. Burlet, J. Bossy, J.Y. Henry, and G. Lapertot, Physica C **185-189**, 86, (1991)

[24] M.T. Beal-Monod, C. Bourbonnais and V.J. Emery, Phys. Rev. B **34**, 7716 (1986).

[25] C. Bourbonnais and L.G. Caron, Europhys. Lett. **5**, 209, (1988).

[26] D.J. Scalapino, in *High Temperature Superconductivity Proceedings*, edited by K.S. Bedell, D. Coffey, D.E. Meltzer, and J.R. Schrieffer (Addison-Wesley, New York, 1990).

[27] N. Bulut and D.J. Scalapino, Phys. Rev. B **45**, 2371 (1992).

[28] T. Moriya, Y. Takahashi, K. Ueda, J. Phys. Soc. Jap. **59**, 2905 (1990); Physica C **185**, 114 (1991); J. Phys. Chem. Sol. **53**, 1515 (1992); J. Magn. Magn. Mater. **104**, 456 (1992).

[29] G.E. Volovik and L.P. Gorkov, JETP Lett. **39**, 674 - 677 (1984); Sov. Phys. JETP **61**, 843 - 854 (1985).

[30] M. Sigrist and K. Ueda, Rev. Mod. Phys. **63**, 239 (1991)

[31] P. Monthoux, A. Balatsky, D. Pines, Phys. Rev. B **46**, 14803 (1992).

[32] D. Pines, in " High T_c Superconductivity and the C_{60} Family ", ed. T.D.Lee, H.C.Ren (Gordon and Breach, 1995).

[33] W. N. Hardy, D. A. Bonn, D. C. Morgan, R. Liang and K. Zhang, Phys. Rev. Lett. **70**, 3999 (1993).

[34] For a review see D. J. Van Harlingen, Rev. Mod. Phys. **67**, 515 (1995).

[35] P. Monthoux, D. Pines, Phys. Rev. B **47**, 6069 (1993).

[36] P. Monthoux, D. Pines, Phys. Rev. B **49**, 4261 (1994).

[37] P.W. Anderson, Phys. Rev. Lett. **64**, 1839 (1990).

[38] P.W. Anderson, Phys. Rev. Lett. **65**, 2306 (1990).

[39] R.L. Willett, Adv. Phys. **46**, 447 (1997).

[40] B. Halperin, P.A. Lee and N. Read, Phys. Rev. B **47**, 7312 (1993).

[41] J. Engelbrecht and M. Randeria, Phys. Rev. Lett. **65**, 1032 (1990).

[42] H. Fukuyama and O. Narikiyo, J. Phys. Soc. Japan. **60**, 1032 (1991); H. Fukuyama, Y. Hasegawa, O. Narikiyo, J. Phys. Soc. Japan **60**, 2013 (1991) .

[43] P.C.E. Stamp, J. de Physique I, **3**, 625 (1993).

[44] R. Shankar, Rev. Mod. Phys. **66**, 129 (1994).

[45] A.A. Abrikosov and I.M. Khalatnikov, Zh. Eksp. Teor. Fiz. **33**, 1154 (1958) [Sov. Phys. JETP **6**, 888 (1958)].

[46] A.B. Migdal, Sov. Phys. JETP **7**, 996 (1958).

[47] J.R. Schrieffer, J. Low Temp. Phys. **99**, 397 (1995).

[48] B.L. Altshuler, L.B. Ioffe, A.J. Millis, Phys. Rev. B **52**, 5563 (1995).

[49] A.V.Chubukov, Phys. Rev. B **52**, R3840 (1995).

[50] A.V. Chubukov, D.K. Morr, P. Monthoux, Phys. Rev. B **56**, 7789 (1997).

[51] A.V. Chubukov, Philos. Mag. B **74** 563 (1996).

[52] M. C. Schabel *et al.*, Phys. Rev. B **57**, 6090 (1998); *ibid* **57**, 6107 (1998).

[53] L.D. Landau, Sov. Phys. JETP **3**, 920 (1957).

[54] L.D. Landau, Sov. Phys. JETP **5**, 101 (1957).

[55] A.J. Leggett, Rev. Mod. Phys. **47**, 331 (1975).

[56] G. Baym and C. Pethick, *Landau Fermi-Liquid Theory: Concepts and Applications*, (Wiley 1991).

[57] D. Pines and P. Nozieres, *The Theory of Quantum Liquids* V. I, (Benjamin, New York, 1966).

[58] R.D. Mattuck, *A Guide to Feynman Diagrams in the Many-Body Problem* (Dover 1992).

[59] D. Pines, *The Many-Body Problem* (Benjamin, New York, 1961).

[60] J.W. Negele and H. Orland, *Quantum Many-Particle Systems* (Addison Wesely 1987).

[61] L.P. Kadanoff, and G. Baym, Phys. Rev. **124**, 287 (1961).

[62] G. Baym, Phys. Rev. **127**, 1391 (1962).

[63] P.C.E. Stamp, J. Phys. F **15**, 1827 (1985).

[64] Y.M. Vilk *et al.*, Phys. Rev. B bf 49, 13267 (1994); A.-M. Dare', L. Chen, A.-M.S. Tremblay, Phys. Rev. B **49**, 4106 (1994); A.-M. Dare', Y.M. Vilk and A.-M.S. Tremblay, Phys. Rev. B **53**, 14236 (1996); Y.M. Vilk and A.-M.S. Tremblay, J. Phys I, France **7** 1309 (1997), and references therein.

[65] G.Y. Chitov and D. Sénéchal, Phys. Rev. B **57**, 1444 (1998).

[66] A.A. Abrikosov, L.P. Gorkov and I.E. Dzyaloshinski, *Methods of Quantum Field Theory in Statistical Physics* (Dover 1975).

[67] G. Beydaghyan, Master's Thesis, University of British Columbia (1993).

[68] G.D. Mahan, *Many-Particle Physics* (Plenum 1990).

[69] J.M. Luttinger, Phys. Rev. **119**, 1153 (1960).

[70] V. Emery in *Highly Conducting One-Dimensional Solids*, Edited by J.T. Devreese, R.P. Evrard, V.E. Van Doren (Plenum 1979).

[71] M. Fabrizio, A. Parola and E. Tossati Phys. Rev. B **44**, 1033 (1991).

[72] H. Fukuyama and M. Ogata, J. Phys. Soc. Japan **63**, 3923 (1994).

[73] J. Polchinski, Nucl. Phys. B **422**, 617 (1994).

[74] A. Virosztek and J. Ruvalds, Phys. Rev. B **42**, 4064 (1990).

[75] C.M. Varma et al., Phys. Rev. Lett. **63**, 1996 (1989).

[76] A. Stern, B.I. Halperin, Phys. Rev. **B52**, 5890 (1995).

[77] M.H.S. Amin, P.C.E. Stamp, in progress.

[78] J. Gonzalez, F. Guinea and M.A.H. Vozmediano, Phys. Rev. Lett. **79**, 3514 (1997).

[79] S.-C. Zhang, Science, **275**, 1089 (1997).

[80] J.M. Tranquada, B.J. Sternleib, J.D. Axe, Y. Nakamura, S. Uchida, Nature 375, 561 (1995), J.M. Tranquada, *et al.* Phys. Rev. B **54**, 7489 (1996).

[81] L. Balents, M.P.A. Fisher, C. Nayak, Int. J. Mod. Phys. B **12** 1033 (1998).

[82] S. Doniach and S. Engelsberg, Phys. Rev. Lett. **17** 750 (1966).

[83] N.F. Berk and J.R. Scherriefer, Phys. Rev. Lett. **17** 433 (1966).

[84] M.J. Rice Phys. Rev. **159**, 153 (1967); **162**, 189 (1967); **163**, 206 (1967).

[85] J.A. Hertz, K. Levin, M.T Beal-Monod, Phys. Solid State Com. **18**, 803 (1976).

[86] F.M. Hayden *et al.*, Phys. Rev. Lett. **76**, 1344 (1996).

[87] A.V. Chubukov, D. Pines and B.P. Stojkovic, J. Phys. Cond. Matt. **8**, 10017 (1996).

[88] J. Yu, S. Massidda, A.J. Freeman, Phys. Lett. A **122**, 198 (1987); Q. Si, Y. Zha, K. Levin, J.P. Lu, Phys. Rev. B **47**, 9055 (1993)

[89] R. Hlubina, T.M. Rice, Phys. Rev. B **51**, 9253 (1995); *ibid* **52** 13043 (1995).

[90] B.P. Stojkovic, D. Pines, Phys. Rev. Lett. **55**, 8576 (1997).

[91] A. Sokol, D. Pines, Phys. Rev. Lett. **71**, 2813 (1993).

[92] V. Barzykin and D. Pines, Phys. rev. B **52** 13585 (1995).

[93] A.V. Chubukov, D.K. Morr, Phys. Rep. **288**, 355 (1997).

[94] D.K. Morr, A.V. Chubukov, Phys. Rev. B **56**, 9134 (1997).

[95] P.W. Anderson, Adv. Phys. **46**, 3 (1997).

[96] P.W. Anderson, *The theory of superconductivity in the high T_c cuprates* (Princeton, 1997).

[97] A.J. Millis, Phys. Rev. B **45**, 13047 (1992).

[98] M.H.S. Amin and P.C.E. Stamp, Phys. Rev. Lett. **77**, 3017 (1996).

[99] G. Shirane *et al.*, Phys. Rev. Lett. **63**, 330 (1989); T. Mason *et al.*, Phys. Rev. Lett. **77**, 1604 (1996); G. Aeppli *et al.*, Science **278**, 1432 (1997); S.M. Hayden *et al.*, Phys. Rev. Lett. **76**, 1344 (1996); K. Yamada *et al.*, Phys. Rev. B **57**, 6165 (1998).

[100] J.M. Tranquada *et al.*, Phys. Rev. B **46**, 5561 (1992).

[101] I. Grosu, M. Crisan, Phys. Rev. B **49**, 1296 (1994). Our results do not agree with this paper. The form of equations (1) and (5) of Grosu and Crisan seem to be appropriate to a nearly ferromagnetic system - their expansion are being made near $\vec{q} = 0$ (rather than $\vec{q} \sim \vec{Q}$).

[102] See in this connection W.F. Brinkman, in Proc. 24th Nobel Symposium (Stockholm, Nobel Foundation) 1973.

[103] Y.M. Vilk, A.-M.S. Tremblay, Europhys. Lett. **33**, 159 (1996).

[104] S. K. Yip and J. A. Sauls, Phys. Rev. Lett.**69**, 2264 (1992), D. Xu, S. K. Yip and J. A. Sauls, Phys. Rev. B **51**, 16233 (1995).

[105] A. Maeda, Y. Iino, T. Hanaguri, N. Motohira, K. Kishio and T. Fukase, Phys. Rev. Lett.**74**, 1202 (1995); A. Maeda, T. Hanaguri, Y. Iino, S. Masuoka, Y. Kokata, Jun-ichi Shimoyama, K. Kioshio, H. Asaoka, Y. Matsushita, M. Hasegawa and H. Takei, J. Phys. Soc. Jpn. **65** 3638 (1996).

[106] C.P. Bidinosti, W.N. Hardy, D.A. Bonn, Ruixing Liang, Phys. Rev. Lett. **83**, 3277 (1999).

[107] G. E. Volovik, J. Phys. C: Solid State Phys. **21**, L221 (1988); G E. Volovik, Sov. Phys. JETP **58**, 469 (1993).

[108] K. A. Moler, D. J. Baar, J. S. Urbach, R. Liang, W. N. Hardy and A. Kapitulnik, Phys. Rev. Lett.**73**, 2744 (1994).

[109] A. P. Ramirez, Phys. Lett. A **211**, 59 (1996).

[110] R. A. Fisher, J. E. Gordon, S. F. Reklis, D. A. Wright, J. P. Emerson, B. F. Woodfield, E. M. McCarro III and N. E. Phillips Physica C **252**, 237 (1995).

[111] I. Kosztin and A. J. Leggett, Phys. Rev. Lett. **79**, 135 (1997).

[112] S. Kamal *et al.*, Phys. Rev. Lett. **73**, 1845 (1994).

[113] A. A. Abrikosov, Zh. Eksp. Teor. Fiz. **32**, 1442 (1957) [Sov. Phys. JETP **5**, 1174 (1957)].

[114] V. L. Ginsburg and L. D. Landau, J. Exptl. Theoret. Phys. (USSR) **20**, 1064 (1950).

[115] For review see: *Anisotropy Effects in Superconductors*, ed. by H. Weber (Plenum, New York, 1977).

[116] G. Blatter *et al.*, Rev. Mod. Phys. **66**, 1125 (1994).

[117] B. Keimer, J. W. Lynn, R. W. Erwin, F. Dogan , W. Y. Shih and I. A. Aksay, J. Appl. Phys. **76**, 6788 (1994); B. Keimer, W. Y. Shih, R. W. Erwin, J. W. Lynn, F. Dogan and I. A. Aksay, Phys. Rev. Lett. **73**, 3459 (1994).

[118] I. Maggio-Aprile, Ch. Renner, A. Erb, E. Walker and O. Fisher, Phys. Rev. Lett. **75**, 2754 (1995).

[119] K. Takanaka and K. Kuboya, Phys. Rev. Lett. **75**, 323 (1995).

[120] A. J. Berlinsky, A. L. Fetter, M. Franz, C. Kallin and P. I. Soininen, Phys. Rev. Lett. **75**, 2200 (1995)

[121] M. Franz, C. Kallin, P. I. Soininen, A. J. Berlinsky and A. L. Fetter, Phys. Rev. B **53**, 5795 (1996)

[122] J. H. Xu, Y. Ren and C.-S. Ting, Phys. Rev. B **53**, R2991 (1996);

[123] R. Heeb, A. Van Otterlo, M. Sigrist and G. Blatter, Phys. Rev. B **54** 9385 (1996).

[124] M. B. Walker and T. Timusk, Phys. Rev. B **52**, 97 (1995).

[125] J. E. Sonier, PhD thesis, University of British Columbia.

[126] J. E. Sonier, R. F. Kiefl, J. H. Brewer, D. A. Bonn, S. R. Dungiger, W. N. Hardy, R. Liang, W. A. MacFarlane, T. M. Reseman, D. R. Noakes and C. E. Stronach, Phys. Rev. B **55**, 11789 (1996).

[127] J. E. Sonier, R. F. Kiefl, J. H. Brewer, D. A. Bonn,W. N. Hard y, R. Liang, W. A. MacFarlane, R. I. Miller, T. M. Reseman, D. R. Noakes, C. E. Stronach and M. F. White, Phys. Rev. Lett. **79**, 2875 (1997).

[128] J. E. Sonier, R. F. Kiefl, J. H. Brewer, J. Chakhalian, S. R. Dungiger, W. A. MacFarlane, R. I. Miller, A. Wong, G. M. Luke and J. W. Brill, Phys. Rev. Lett. **79**, 1742 (1997).

[129] Y. Wang, Ph.D. Thesis, Indiana University, 1996; A. H. MacDonald and Y. Wang, to be published.

[130] M. Tinkham, *Introduction to Superconductivity* (Krieger, Malabar, 1975);

[131] V. G. Kogan, M. Bullock, B. Harmon, P. Miranvić, Lj. Dobrosavljević-Grujić, P. L. Gammel and D. J. Bishop, Phys. Rev. B **55**, R8693 (1997).

[132] M. Franz, I. Affleck and M. H. S. Amin, Phys. Rev. Lett. **79**, 1555 (1997).

[133] F. London and H. London, Proc. Roy. Soc. (London), **A149**, 71 (1935); Physica **2**, 241 (1935).

[134] M. R. Eskildsen, *et al.*, Phys. Rev. Lett. **78**, 1968 (1997).

[135] B.I. Halperin, T.C. Lubensky and S.-K. Ma, Phys. Rev. Lett. **32**, 292 (1974); . Dasgupta and B.I. Halperin, Phys. Rev. Lett. **47**, 1556 (1981).

[136] See e.g. P. G. de Gennes, *Superconductivity of Metals and Alloys* (W.A. Benjamin, Inc. 1966); A. L. Fetter and P. C. Hohenberg, in *Superconductivity*, ed. R. D. Parks (Marcel Dekker, New York, 1969) vol. II.

[137] J. R. Clem, J. Low. Temp. Phys. **18**, 427 (1975).

[138] E. H. Brandt, Phys. Rev. Lett. **78**, 2208 (1997).

[139] E. H. Brandt, J. Low. Temp. Phys. **24**, 709 (1977) and **73**, 355,(1988); E. H. Brandt, Phys. Rev. B **37**, 2349 (1988).

[140] I. Affleck, M. Franz and M. H. S. Amin, Phys. Rev. B **55**, R704 (1996).

[141] R. Joynt, Phys. Rev. B**41**, 4271 (1990).

[142] G. E. Volovik, Pis'ma Zh. Eksp. Teor. Fiz. **58**, 457 (1993) [JETP Lett. **58**, 469 (1993)].

[143] P. C. Hohenberg and N.R. Werthamer, Phys. Rev. **153**, 493 (1966).

[144] M. Ichioka, N. Enomoto, N. Hayashi, K. Machida, Phys. Rev. B **53**, 2233 (1996).

[145] D. L. Feder and C. Kallin, Phys. Rev. Lett. **79**, 2871 (1997).

[146] M. H. S. Amin, I. Affleck, M. Franz, Phys. Rev. B **58**, 5848 (1998).

[147] M. Ichioka, N. Hayashi, N. Enomoto, and K. Machida, Phys. Rev. B **53**, 15316 (1996).

[148] G. J. Dolan, F. Holtzberg, C. Field, T. R. Dinger, Phys. Rev. Lett. **62**, 2184 (1989).

[149] T. Timusk, (private communication).

[150] J. E. Sonier, R. F. Kiefl, J. H. Brewer, D. A. Bonn, J. F. Caro lan, K. H. Chow, P. Dosanjh, W. N. Hardy, R. Liang, W. A. MacFarlane, P. Mendels, G. D. Moris, T. M. Reseman and J. W. Schneider, Phys. Rev. Lett. **72**, 744 (1994).

[151] L. P. Gorkov, J. Exptl. Theoret. Phys. (USSR), **36**, 1918 (1959); [Sov. Phys. JETP **9**, 1364 (1959)].

[152] A. M. Zagoskin, *Quanyum Theory of Many-Body Systems* (Springer 1998).

[153] I. Zutic and O. T. Valls, Phys. Rev. B **54**, 15500 (1996); Phys. Rev. B **56** 11279 (1997); J. Comp. Phys. **136**, 337 (1997).

[154] D. Vollhardt and P. Wolfe, *The superfluid Phases of Helium 3* (Taylor and Francis 1990).

[155] E. M. Lifshits and L. P. Pitaevskii, *Statistical physics II* (Pergamon Press, New York 1980) pp. 208-216.

[156] V. G. Kogan *et al.*, Phys. Rev. B **54**, 12386 (1996).

[157] D. J. Scalapino, Phys. Rep. **250**, 329 (1995).

[158] J.E. Sonier *et al.*, Preprint (cond-mat/9906452)

[159] A. Yaouanc, P. Dalmas de Réotier and E. H. Brandt , Phys. Rev. B **55**, 11107 (1997).

[160] Z. Hao, J. R. Clem, M. W. McElfresh, L. Civale, A. P. Malozemoff and F. Holtzberg, Phys. Rev. B **43**, 2844 (1991).